AZAD, MICHAEL M., Ph.D. A Comparison Study of Superabsorbent Polymer with Microwave - Assisted Polymerization and Free Radical Solution Polymerization: Synthesis, Kinetics, and Applications. (2018)
Directed by Dr. Dan J. Herr. 194 pp.

This purpose of this research is to compare the formation kinetics of two approaches to synthesizing crosslinked polyacrylic acid (x-PAA) superabsorbent polymers (SAP). Specifically, it tests the applicability of the reported general rate expression for free radical solution polymerization to the synthesis of x-PAA SAPs via Microwave-Assisted Polymerization (MAP) and Free Radical Solution Polymerization (FRSP). This study of FRSP and MAP formation kinetics of x-PAA superabsorbent materials provides predictive models and new foundational insights into the rate-limiting steps for these three-dimensional polymerization reactions. These foundational models, based on the observed results from the designed kinetic studies, may help to guide and enable the design of new networked polymers with enhanced functional properties.

The published complex mechanism of PAA polymerization, which was assumed to explain the kinetics of superabsorbent polymerization, does not seem to be valid in FRSP and MAP synthesis of PAA SAPs. In fact, for these kinetic studies, the data supported none of the initial hypotheses for all the data in a given reaction. For the FRSP, only a sequential kinetic model, i.e., zero-order followed by the first order in monomer model explains the observed data. For the MAP PAA SAP syntheses, several sequential kinetic models may explain the observed data. A first-order model supports the first-half-reaction, and a zero-order model explains the second-half-reaction. So overall, the key findings show that one cannot conclude with 99% confidence (2σ) the existence of a

single zero or first-order kinetic process over the entire reaction for each type polymerization, i.e., MAP or FRSP. However, there are regions of sequential zero-order and/or first-order kinetics that explain the dominant mechanistic modes for both types of polymerizations.

The MAP reaction, due to its rapid nature, enables a much more uniform distribution of inert material, such as clay, that can be achieved with the FRSP process. Percolation theory provides a way to understand why these interconnected channels help to enhance the movement of a liquid through the PAA SAP's gel network. This theory could explain why a clay containing polymer made with the MAP process exhibits higher and more consistent permeability than a corresponding system synthesized via the FRSP reaction.

A COMPARISON STUDY OF SUPERABSORBENT POLYMER WITH MICROWAVE - ASSISTED POLYMERIZATION AND FREE RADICAL SOLUTION POLYMERIZATION: SYNTHESIS, KINETICS, AND APPLICATIONS

by

Michael M. Azad

A Dissertation Submitted to
the Faculty of The Graduate School at
The University of North Carolina at Greensboro
in Partial Fulfillment
of the Requirements for the Degree
Doctor of Philosophy

Greensboro
2018

Approved by

_____
Committee Chair

APPROVAL PAGE

This dissertation written by Michael M. Azad has been approved by the following committee of the Faculty of The Graduate School at the University of North Carolina at Greensboro.

Committee Chair Dr. Daniel Herr

Committee Members Dr. James Ryan

Dr. Jianjun Wei

Dr. Lifeng Zhang

_____

Date of Acceptance by Committee

_____

Date of Final Oral Examination

TABLE OF CONTENTS

Page

LIST OF TABLES

Page

LIST OF FIGURES

Page

CHAPTER I

A COMPARISON STUDY OF SUPERABSORBENT POLYMER WITH MICROWAVE - ASSISTED POLYMERIZATION AND FREE RADICAL SOLUTION POLYMERIZATION: SYNTHESIS, KINETICS, AND APPLICATIONS

Introduction

The research in the area of superabsorbent polymer is mainly done within the polymer industry. The aim in the industry is to make the product but not necessarily to understand how they got from point A to point B. The main process in the industry is free radical solution polymerization, and the monomer of choice is acrylic acid because this is an economical way of producing the polymer, but not necessarly the best way. The aim of this dissertation is to compare the customary free radical solution polymerization (FRSP) with the microwave-assisted polymerization (MAP), look at their advantages and disadvantages, and above all, their kinetics and the science behind their performance. Chapter II will decribe the way these polymerization techniques work, how we developed our polymerization techniques, polymer's properties, and advantages and disadvantages of each polymerization technique.

Chapter III deals with the polymer permeability. Superabsorbent polymer absorbs and retains large quanty of liquid, but lacks permeability. To improve permeability an

inert chemical is added to the polymer, and its effect on the permeability and other properties have been studied in both polymerization techniques.

Both papers in chapers II and III have been published in the Journal of Applied Polymer.

Chapter IV examines the prevalent belief in the reason behind permeability improvement. It looks at the reason behind a robust permeability improvement in the MAP vs FRSP. It looks at the homogeneous distribution of clay in the MAP, its role as a spacer which separates particles and also increases surface area which in turn improves permeability. This belief is tested by using microscopy to measure the pore sizes and determine the surface areas. The percolation channels may explain the reason behind the permeability improvement.

Chapter V tackles the concept of kinetics in both polymerization techniques and compares our understanding of the kinetics versus the conventional belief in the industry. The concept of complex kinetic which has been discussed in the literature is being challenged and the idea of the sequential zero and first order kinetics is presented and discussed. Due to the nature of the medias in different stages of the polymerization, going from homogeneous aqueous solution to another homogeneous gel type media, the sequential kinetic theory explains our data much better that the complex kinetic can.

CHAPTER II

MICROWAVE-ASSISTED POLYMERIZATION: SUPERABSORBENT POLYMER WITH IMPROVED PROPERTIES

‡Michael M. Azad and ‡Marinella G. Sandros
Department of Nanoscience, University of North Carolina at Greensboro, Greensboro, NC 27401, USA
Marinella G. Sandros (Email: m_sandro@uncg.edu)

Abstract

Microwave-assisted polymerization is utilized as a promising technique to synthesize superabsorbent polymer (SAP). A small amount of thermal initiator was used to initiate the reaction and polymer's properties were evaluated at acid levels of 31-50% and degrees of neutralization of 68-75 mol %. Polymers were characterized with SEM, and properties such as capacity and absorbency under load were measured in 0.9% sodium chloride solution. In addition, extractables and residual acrylic acid contents were measured to determine reaction's efficiency. In conclusion, the synthesis of superabsorbent polymer via microwave heating reduces the time and cost of production while improving the physical properties of the polymer.

Introduction

Superabsorbent polymers are generally produced with partially neutralized acrylic acid, which imparts charge density to the polymer backbone. A small amount of crosslinker makes the polymer water- insoluble. This polymer absorbs over 100 times its own weight in aqueous liquid and retains it under moderate to high pressure.[1-3] Superabsorbent polymers are mainly used in the hygiene industry,[4] but it has also found commercial applications[5] in other areas such as agriculture, packaging, cable, firefighting, and medical industries.[6-15] Free radical solution polymerization is the current process of choice in the industry,[8] but rising production cost and a constant quest to improve a polymer's properties has necessitated the search for an improved method.

The Free radical solution polymerization method utilizes acid content of 31-35% and it requires a lot of energy, money, and time[16,17] to rid itself of the water which was needed to dissipate heat in the polymerization step.[8] Cheng et al.[18] reported the synthesis of a novel superabsorbent polymer using microwaves and Kretschmann et al.[19] used microwaves to prepare a polymer based on poly (acrylic acid) in a short period of time. Microwave-assisted synthesis, in comparison to the conventional heating, improves reaction speed, reproducibility and scalability. Electric charges present in solutions are irradiated with the microwave that end up converting electromagnetic energy into heat, resulting in improved reaction rate. Bogdal et al.[20] defines microwave heating as a non-contact energy transfer (instead of heat transfer) with a rapid start-up and stop capabilities or as Giachi et al.[21] puts it, the microwave-assisted polymerization has turned from a scientific curiosity to a reliable polymerization technique. Also, enhanced copolymer

formation and shorter polymerization time was reported by Menon et al.[22] for the production of biodegradable polymers with microwave-assisted polymerization.

As Fredric L. Buchholz and Nicholas A. Peppas described in their book "Superabsorbent Polymers, Science and Technology",[8] monomer concentration will affect the "properties of the polymer, the kinetics, and the economics of the polymerization process".[8] In this manuscript, the potential of microwave-assisted polymerization was used for the production of superabsorbent polymers by varying acrylic acid contents and testing crucial properties such as capacity, absorbency under load, extractable and residual acrylic acid under those conditions.

Materials

Glacial Acrylic acid was purchased from BASF; potassium hydroxide, sodium chloride, hydrogen peroxide, ascorbic acid, hydrochloric acid, 85% O-phosphoric acid, HPLC grade methanol, ultra-pure water, and ammonium persulfate from Aldrich; and ethoxylated trimethylolpropane triacrylate (ETMPTA) from Sartomer. All the chemicals were used without purification.

Equipment

Retsch ZM1000 for milling, RO-TAP model RX-29 equipped with USA Standard Test Sieve for sieving, Heraeus Instrument Labofuge 400 for centrifuge retention capacity, Thermo Scientific Lindberg Blue M lab oven for drying of the polymer, HPLC from Water with UV detector, Nucleosil column (C8, 120 Å 5 µm, 250 x 4.6mm),

mobile phase (0.2ml 85% O-Phosphoric acid, 5.0ml HPLC grade methanol, 0.9948L ultra-pure water), Brinkmann 816 titration system for extractables, and Microwave from CEM was utilized for polymerization.

Centrifuge Retention Capacity (CRC) Measurement

Superabsorbent polymer (SAP) sieved to 300-600 microns was added in the amount of 0.160 grams to a teabag with dimensions: 63.5 mm x 76 mm. The teabag was fashioned from heat-sealable teabag paper from Dexter Alstrom (see Fig. 1). The SAP-containing bag and a blank bag with no polymer were sealed and soaked in a container with 2 liters of 0.9% sodium chloride solution (see Fig. 2). After 30 minutes, these were removed from the saline solution and centrifuged at 1,600 rpm for 3 minutes to eliminate the interstitial / unbound liquid, and then they were weighed. The centrifuge retention capacity was calculated as:

CRC (g/g) = (Weight of centrifuged teabag with swollen polymer
– weight of centrifuged blank bag -weight of dry polymer)
÷ (Weight of dry polymer)

Figure 1. Weighing Teabag.

Figure 2. Teabags in Soaking Solution.

Absorbency Under Load (AUL) Measurement

Superabsorbent polymer sieved to 300-600 microns was added in the amount of 0.160 grams to a test cylinder with a flat screen mesh at the bottom. The SAP granules were distributed evenly, and an acrylic spacer was inserted followed by the appropriate piston to supply the required weight / pressure. The total dry weight of the assembly was measured and recorded. A glass frit was added to a soaking dish filled with 0.9% sodium chloride solution to the top level of the glass frit. Filter paper was added to the frit, and then the AUL assembly was placed onto the filter paper (see figures 3-5). After 60 minutes, the AUL unit was removed and weighted. The following equation was used to calculate AUL:

AUL (g/g) = (Weight of AUL unit with superabsorbent polymer after one hour of liquid absorption

– weight of AUL unit with dry superabsorbent polymer)

÷ (Actual superabsorbent polymer weight)

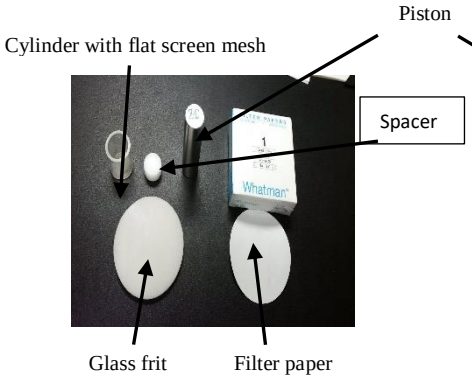

Figure 3. AUL Unit Components.

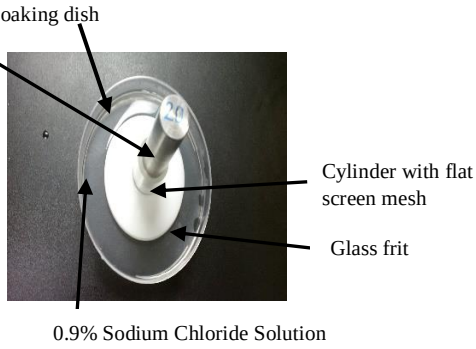

Figure 4. AUL unit in Soaking Dish.

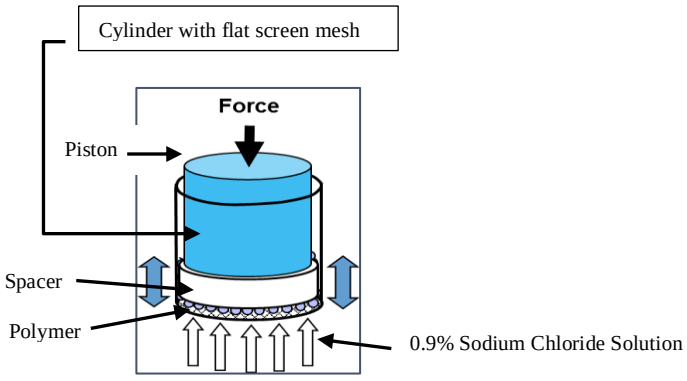

Figure 5. AUL Unit.

Extractable Measurement

Into a 250-ml glass Erlenmeyer flask, one gram of superabsorbent polymer was added to 200 ml of 0.90% sodium chloride solution while stirring at 250 rpm. After 1 hour, the resulting mixture was filtered by the use of a vacuum pump and a GF micro-filter. Fifty grams of the filtered solution was placed into a 150-ml beaker. For a blank, 50 grams of 0.90% sodium chloride solution was added into another 150-ml beaker. The calculation for percent extractables consists of a three-step, pre-set endpoint titration,

which is done at pH 10.3, 10, and 2.7. Both 0.90% sodium chloride solution and sample were titrated, and the following equation was used to calculate percent extracables:

Sample value % - Blank value % = % Extractable polymer

Monomer Solution

Monomer solution (620 grams acrylic acid + 675 grams potassium hydride + 628 grams deionized water for 31% acid content) was prepared by adding potassium hydroxide to the deionized water while it was cooled in an ice bath (temperature was kept around 30 °C). In a separate beaker, crosslinker, ethoxylated trimethylolpropane triacrylate, was added to the acrylic acid and then this mixture was combined with the potassium hydroxide solution under constant stirring. The monomer solution for free radical solution polymerization was cooled to 10 °C and then was purged with nitrogen for five minutes to remove dissolved oxygen. However, the monomer solution for microwave-assisted polymerization was kept at 30 °C and was not purged.

Microwave-Assisted Polymerization

Monomer solution was transferred to the polymerization vessel which contained the required amount of ammonium persulfate (see Fig. 6) and placed in the microwave cavity, which was equipped with a condenser. Gradient programing was used to do the polymerization under constant stirring in the microwave cavity. Wattage was 100 and pressure was set to zero bars. Programming consisted first of: 2 cycles of heating for 2 minutes and cooling for twenty seconds. This was followed by heating one minute and

cooling for another 20 seconds**.** Polymer was allowed to cool for 2 minutes and then was extracted from the polymerization tube. The sample was extruded, dried, milled, and sieved.

Free Radical Solution Polymerization

Monomer solution was transferred to the polymerization vessel which the required amount of Hydrogen peroxide, ascorbic acid and ammonium persulfate (see Fig. 7) was used to initiate the polymerization. Since this is an open system, temperature control was not possible. Polymer was extruded, dried, milled, and sieved.

Results and Discussion

Superabsorbent polymer was produced based on Schematic 1. To render it water-insoluble, 0.01 wt.% ethoxylated trimethylolpropane triacrylate (ETMPTA) was added to the monomer solution as a crosslinker. The degree of neutralization (DN) was in the range of 68-75 mol% and microwave-assisted polymerization was compared to free radical solution polymerization at acrylic acid levels of 31, 35, 40, 45 and 50%. The first two levels, 31 and 35%, are currently in the range being used in the production of superabsorbent polymer in the industry by employing free radical solution polymerization. The 40, 45, and 50% acid contents are beyond the grasp of the current polymerization method, but one can produce a superabsorbent polymer at these levels by using microwave-assisted polymerization method. In general, swelling of the superabsorbent polymer is the result of the osmotic pressure differences between network

and solvent, electrostatic attraction based on ion-dipole interaction, and repulsion of the charged groups on the polymer. In fact, swelling of the polymer continues until the expanding forces are in equilibrium with the restraining forces (stretching of the network chains and restriction of crosslinks). The degree of crosslinking and charges on the polymer are two primary factors that will determine the strength of the polymer and also the amount of liquid it will absorb.

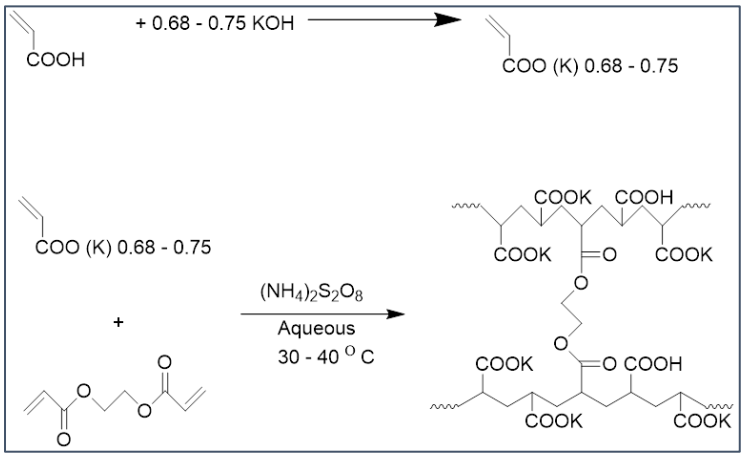

Schematic 1. A Generic Schematic Representation of the Polymerization of Acrylic Acid by Microwave Polymerization (redrawn from a description by F. L. Buchholz).

Conventional free radical solution polymerization uses redox coupling (e.g. ascorbic acid and hydrogen peroxide) to initiate the polymerization and the addition of radical/thermal initiator, such as sodium or ammonium persulfate, is necessary to reduce residual acrylic acid in the final product. However, only small amounts of thermal initiator were needed to do the microwave polymerization (5-10 ppm ammonium persulfate). Higher amounts of initiator resulted in a higher percentage of extractables. Minimizing these small, linear polymer chains will translate into a product with better

properties. Conventional free radical solution polymerization requires a large amount of initiators to start and propagate the chain. However, higher amounts of initiators will also produce higher percentages of extractables. As the level of initiator increases, they have tendency to bump in to each other, which will result in chain termination and obviously, shorter chains. Additionally, larger amounts of initiator increase the polymer nucleation points, which will also result in more, shorter chains. Longer polymer chains have two advantages over shorter ones: 1) physical entanglement becomes more likely which hinders migration of any free chains outside of the polymer matrix; 2) statistically, a longer chain is more likely to have incorporated crosslinker molecules and thereby be attached covalently to the polymer matrix.

In microwave-assisted process, the polymerization could be done without an initiator, but polymer becomes too sticky, and processing of this type of polymers is not very practical in the larger scale. Five to ten ppm of ammonium persulfate was used as a radical/thermal initiator, and redox coupling became unnecessary. Conversely, conventional free radical solution polymerization uses 300-400 ppm of redox coupling and 75-150 ppm of radical/thermal initiators. In microwave-assisted polymerization, extractables stayed under 5% in all formulations and residual acrylic acid levels were around 1200 ppm for non-surface coated polymer. Lower percentage of extractables could be attributed to the lower amounts of initiator used in the microwave-assisted polymerization. Surface coating is employed as a means to impart gel strength to the polymer without sacrificing significant amounts of absorption capacity. Most superabsorbent polymers in the market today have extractables levels of >10% and

residual acrylic acid content of <1000 ppm for the finished product. Extractables tend to leach out of the polymer network once the polymer is swollen, thus affecting superabsorbent properties both by loss of superabsorbent mass, and by the osmotic competition of extractables against the insoluble polymer matrix. Additionally, the lower residual acrylic acid which results from microwave-assisted polymerization is desirable for safety reasons.

Microwave polymerization makes oxygen purging of the monomer solution unnecessary. It is just possible that the nature of heating in the microwave-assisted polymerization (energy transfer instead of heat transfer) is minimizing the effect of oxygen on the propagating monomer chains. In conventional free radical solution polymerization, purging of the monomer solution with nitrogen is necessary to speed up the reaction by eliminating dissolved oxygen.[23,24] Molecular oxygen, with its bi-radical structure and high reactivity towards electron rich groups, participates in chemical reactions and to some degree determines the ultimate outcome of these reactions. Oxygen will significantly reduce the polymerization rate and will ultimately affect the polymer's properties.

Another necessary, but time-consuming step is the cooling of the monomer solution. In the industry, a tremendous amount of time and money is being wasted to cool the monomer solution to 10 °C, which again could be eliminated by switching to microwave-assisted polymerization.

In this work, sodium hydroxide was replaced with potassium hydroxide to resolve the solubility issues of sodium hydroxide at higher acid content. After polymerization, the

polymer was extruded and dried in the conventional lab oven at 165 °C, for an hour. Dried polymer was milled and sieved. Particle size of the final product was in the range of 106-810 microns. The acrylic acid content of the current free radical solution polymerization is in the range of 31-35%. Water acts as a heat sink in the polymerization step, but in the drying step, one has to waste lots of energy to eliminate it. Acid content of microwave-assisted polymerization was increased to 50%. Financial implication of the extra 10-15% acid addition in the polymerization step is huge and this could add millions of dollars to the bottom line. Properties of the polymers with 50% acid were similar to those with 31% acid (Figure 6) and the time that it took to do the polymerization did not changed as the acid level increased. Superior network formation during the polymerization step could be one reason for this improvement. Conversely, with free radical solution polymerization, degradation of the polymer's properties becomes obvious as the acid content passes 35% (Figure 7) and the polymerization becomes very explosive at acid levels of 40, 45 and 50%. It was very hard to get the reproducibility from one run to the next at these levels, and the reported properties are based on small polymer amounts, which were collected from several polymerization runs. Although, polymer produced with lower acid content has better properties, the economic realities have forced the companies to increase the acid contents past 31%.

As stated before, partial neutralization adds charge density to the polymer network, which is necessary for better liquid absorption. In the microwave-assisted polymerization, optimal properties were obtained with 73 mol% neutralization.

One of the most fascinating outcomes of the microwave-assisted polymerization was its absorbency under load (AUL). Pre-products (product without surface coating) produced with free radical solution polymerization are very weak and cannot be used in a diaper or other applications as they are. To impart robustness to this polymer, a long and expensive surface crosslinking step is necessary. Base polymers produced with conventional solution polymerization had AUL values under 10g/g (Figure 7), but it increased to more than 14g/g for the polymers produced with microwave-assisted polymerization (Figure 6). As one could imagine, the surface crosslinking step will be much shorter for this type of polymer.

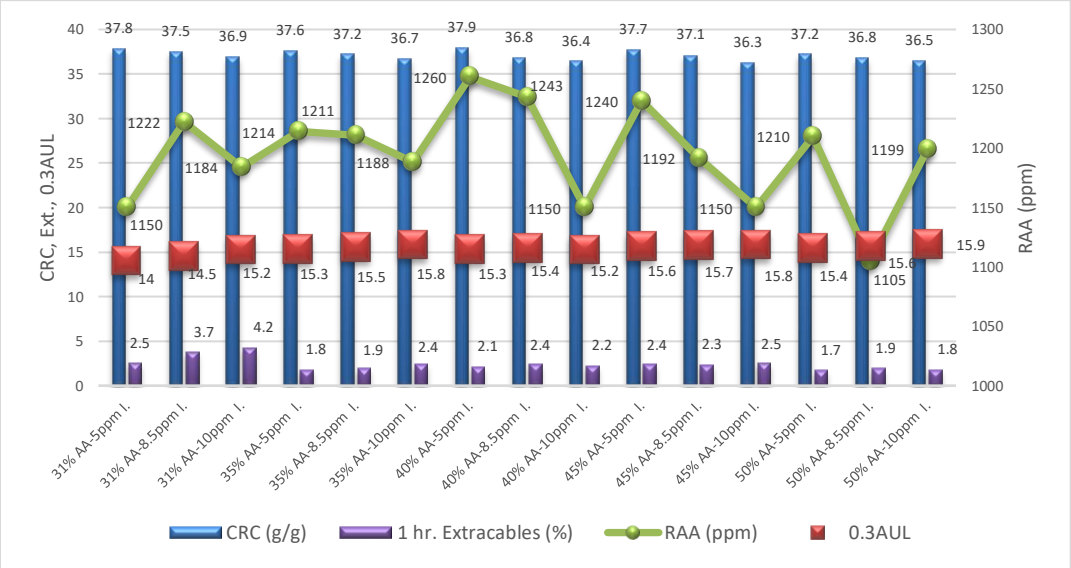

Figure 6. Measured Polymer Properties at Different Acid Contents (Microwave Polymerization).

I. = Initiator

In microwave-assisted polymerization, residual acrylic acid (RAA) stayed under 1300 ppm for all the acid levels, while extracables were less than 5% (Figure 6).

In free radical solution polymerization, higher amounts of initiator (over 300 ppm) are needed to initiate the polymerization. These polymers had extractable values higher than 10% (Figure 7). Residual acrylic acid (RAA) values were under 1300 ppm and this is the direct result of using a large amount of ammonium persulfate (75 ppm) in the polymerization step. As the amount of ammonium persulfate level was increased from 75 ppm to 125 ppm, RAA levels decreased in all five acid content levels.

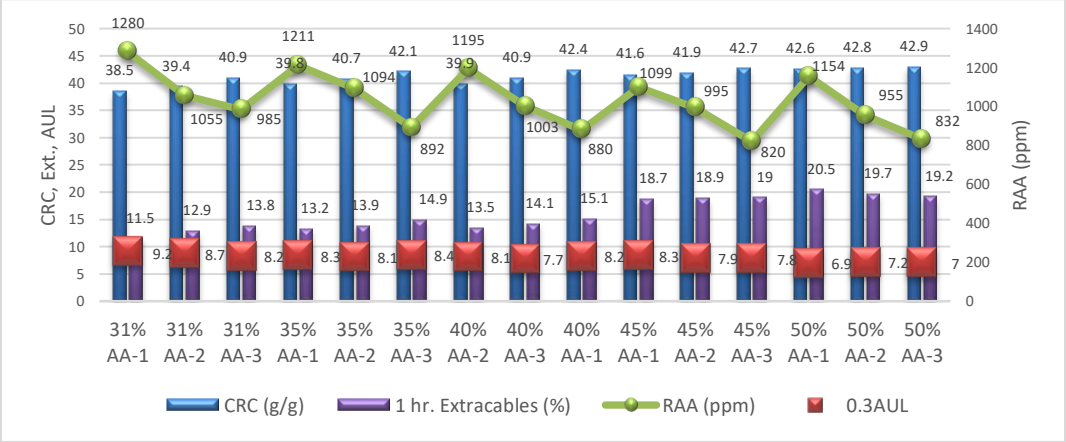

Figure 7. Measured Polymer Properties at Different Acid Contents (Free Radical Solution Polymerization).
AA-1: H_2O_2=150ppm, $C_6H_8O_6$=150ppm, $(NH_4)_2S_2O_8$=75ppm
AA-2: H_2O_2=175ppm, $C_6H_8O_6$=175ppm, $(NH_4)_2S_2O_8$=100ppm
AA-3: H_2O_2=225ppm, $C_6H_8O_6$=225ppm, $(NH_4)_2S_2O_8$=125ppm

SEM images of the free radical solution polymerization show relatively homogeneous polymer with straight edges, while heterogeneity (increased surface area) is apparent for the one made with microwave-assisted polymerization (Figures 8-9). Increased surface area usually manifest itself in liquid absorption speed. This had a direct effect on the length of time which it took for the polymer to absorb a particular amount of

liquid. Two grams of polymer made with microwave-assisted polymerization absorbed 50 ml of 0.9% sodium chloride solution in less than 30 seconds, while it took more 50 seconds for the one made with free radical solution polymerization to accomplish the same task. At a given particle size, polymer with higher surface area has the tendency to absorb liquid at a much faster rate than that with a smaller one. The same rule applies for the polymer with a porous structure. Peaks and valleys are more pronounced in the surfaces of some particles produced with microwave-assisted polymerization and it is not surprising that increased surface area produced faster absorption.

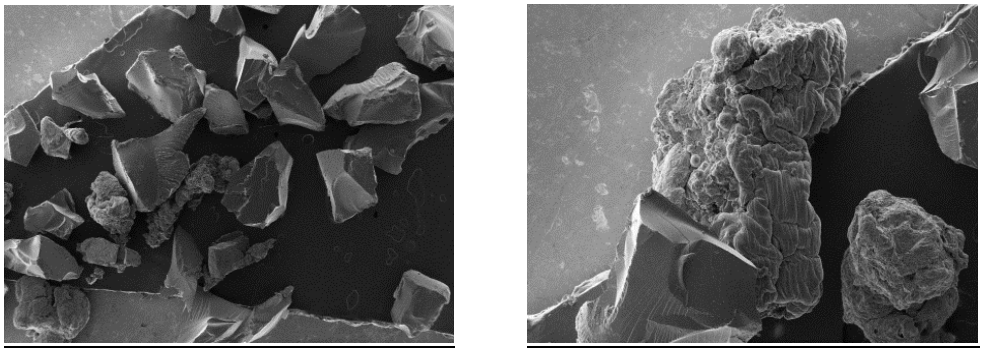

(X 50) (X 100)

Figure 8. SEM Images of Polymer Particles from Microwave Polymerization.

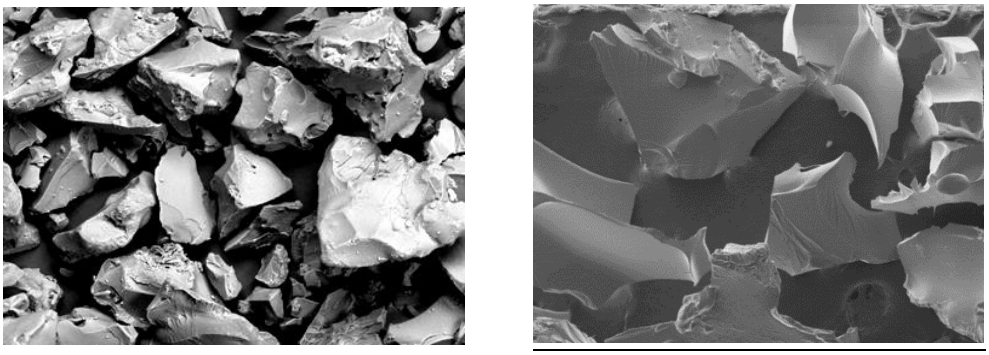

(X 50) (X 100)

Figure 9. SEM Images of Polymer Particles from Free Radical Polymerization.

In the microwave-assisted polymerization, as the acid level increased from 31 to 50%, polymers became less glassy and opaquer in their appearance (Figures 10-12). Immediately following polymerization, the percentage of water in the polymer with 31% acid was measured at 21%, while those made with 50% acid stayed at 9% which had very little effect on the CRCs.

To the contrary, a drop in CRC in the range of 1-1.5 g/g was observed as the amount of initiator increased from 5 to 10 ppm in each acid level. At the constant initiator level, the CRC remained nearly unchanged as the acid content was increased from 31 to 50%. The trend was not the same for the polymers made with free radical solution polymerization. CRC increased by about 0.3-2.5 g/g as the amount of initiator increased, while the acid contents (31 to 50%) raised the capacity by 1.3 to 4.1 g/g. Percentage of water was 23% and 11% for acid levels of 31 and 50% respectively. The total amount of initiator used in free radical solution polymerization was much higher in all three levels (375 ppm vs 5 ppm, 450 ppm vs 8.5 ppm, and 575 ppm vs 10 ppm).

Figure 10. Images of Polymer Made Using 31% Acrylic Acid.

5 ppm Initiator 8.5 ppm Initiator 10 ppm Initiator

Figure 11. Images of Polymer Made Using 35% Acrylic Acid.

5 ppm Initiator 8.5 ppm Initiator 10 ppm Initiator

Figure 12. Images of Polymer Made Using 50% Acrylic Acid.

Reproducibility of the polymers made with microwave-assisted polymerization was surprisingly good. Since the polymerization process is so rapid, reproducibility was one of the major concerns. Table 1 summarizes some of the results (performed in triplicate in each case) with favorable standard deviations.

Table 1. Reproducibility Study of Polymer at 31, 35, and 40% Acid Content

Sample	Acid contents and Initiator levels	CRC (g/g)	0.3 AUL	RAA (ppm)	1 hr. Extractables (%)
1	31% AA-5ppm Initiator				
	Ave.	**37.9**	**14.3**	**1180**	**2.3**
	STDEV	**0.2**	**0.3**	**23.3**	**0.2**
2	35% AA-5ppm Initiator				
	Ave.	**37.5**	**15.6**	**1191**	**2**
	STDEV	**0.3**	**0.2**	**18.6**	**0.2**
3	50% AA-5ppm Initiator				
	Ave.	**37.2**	**15.6**	**1175**	**2**
	STDEV	**0.4**	**0.3**	**8.2**	**0.2**

Conclusion

Microwave-assisted polymerization could potentially reduce production costs by increasing solid content, reducing polymerization time, and eliminating the purging step. Based on the results, acid content can be increased to 50% without affecting the polymer's properties. In addition, 0.3 AUL of the base polymers were about 5 g/g higher than those of the conventional products, while extractables stayed under 5% (>10% for the current polymers). Initiation temperature was kept at 30 °C.

In the next phase of this work, nano-clay and co-monomer will be added into the monomer solution and the properties of the surface coated polymers will be investigated.

Acknowledgment

The authors would like to acknowledge the assistance of Mr. Stephen Vance and Ms. Effat Zeidan with experimental setups.

References

1. A. Pourjavadi, M. Ayyari, M. Amini-Fazl, Eur. Polym. J. 2008, 44, 1209.
2. J. Chen, K. J. Park, J. Control. Release 2000, 65, 73.
3. J. P. Cook, G. W. Goodall, O.V. Khutoryanskaya, V. V. Khutoryanskiy, Macromol. Rapid Commun. 2012, 33, 332-336.
4. A. Das, V. Kothari, S. Makhija, K. Avyaya, J. Appl. Polym. Sci. 2007, 107, 1466.
5. Z. Cheng, J. Li, J. Yan, L. Kang, X. Ru, M. Liu, J. Appl. Polym. Sci. 2013, 39621, 3674-3681.
6. M. Teodorescu, A. Lungu, P. O. Stanescu, Indus. Eng. Chem. Res. 2009, 48, 6527.
7. M. R. Guilherme, A. V. Reis, A. T. Paulino, T. A. Moia, L. H. C. Mattoso, E. B. Tambourgi, J. Appl. Polym. Sci. 2010, 117, 3146.
8. F. L. Buchholz, N. A. Peppas, In Modern Superabsorbent Polymers Science and Technology; ACS Symposium Series 573; Washington DC, 1994; pp 2-36.
9. N. G. Kandile, A. S. Nasr, Carbohydr. Polym. 2009, 78, 753.
10. M. Sadeghi, H. J. Hosseinzadeh, J. Bioact. Compat. Polym. 2008, 23, 381.
11. Y. Liu, Y. Cui, G. Yin, H. Ma, *Iran Polym. J*. 2009, 18, 339-348.
12. K. Kabiri, S. Faraji-Dana, M. J. Zohuriaan-Mehr, *Polym. Adv. Technol*. 2005, 16, 659-666.
13. X. X. Zou, In *Superabsorbents*; Chemical Industry, 2nd ed; Beijing, 2002; pp 2.
14. S. A. Dubrovskii, N. V. Afanas'eva, M. A. Lagutina, K. S. Kazanskii, *Polym Bull*. 1990, 24, 107-113.
15. K. M. Raju, M. P. Raju, Y. M. Mohan, *J. Appl. Polym. Sci.* 2002, 85, 1795-1801.
16. L. Yang, X. Ma, N. Guo, Carbohydr. Polym. 2011, 85, 413.
17. T. Yoshimura, I. Uchikoshi, Y. Yoshiura, R. Fujioka, Carbohydr. Polym. 2005, 61, 322.
18. Z. Cheng, J. Li, J. Yan, L. Kang, X. Ru, M. Liu, J. Appl. Polym. Sci. 2013, 39621, 3674-3681.
19. O. Kretschmann, S. Schmitz, H. Ritter, Macromol. Rapid Commun. 2007, 28, 1265–1269
20. D. Bogdał, P. Penczek, J. Pielichowski, A. Prociak, Adv. Polym. Sci. 2003, 163, 193-263.
21. G. Giachi, M. Frediani, L. Rosi, P. Frediani, Microwave Heating; Croatia, 2011; pp 181-206.
22. S. Menon, M. V. Deepthi, R. R. N. Sailaja, G. S. Ananthapamanabha, Indian J. of Advances in Chemical Sci. 2014, 2, 76-83.
23. V. Singh, D. N. Tripathi, A. Tiwari, R. Sanghi, J. Appl. Polym. Sci. 2004, 95, 820.
24. Z. Tong, W. Peng, Z. Zhiqian, Z. Baoxiu, J. Appl. Polym. Sci. 2004, 95, 264.

Graphical Abstract

MICROWAVE ASSISTED POLYMERIZATION: SUPERABSORBENT POLYMER WITH IMPROVED PROPERTIES

‡Michael M. Azad and ‡Marinella G. Sandros
Department of Nanoscience, University of North Carolina at Greensboro, Greensboro, NC 27401, USA
Marinella G. Sandros (Email: m_sandro@uncg.edu)

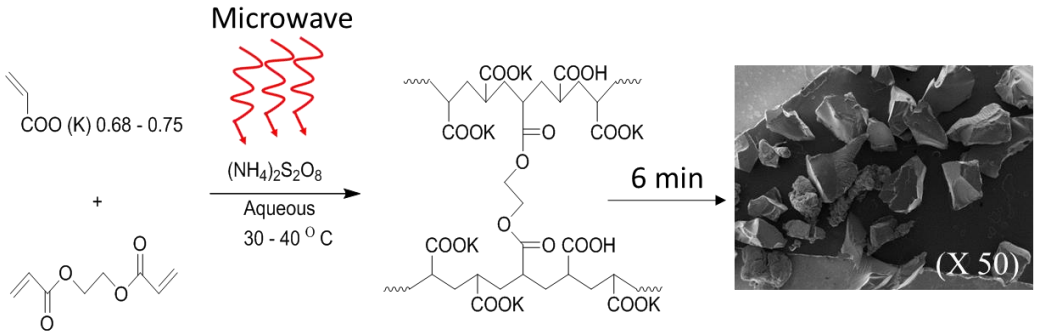

Schematic 2. General Polymerization of Acrylic Acid (Microwave or Free Radical Polymerization) and Surface Coating of the Polymer (redrawn from a description by F. L. Buchholz).

CHAPTER III

MICROWAVE-ASSISTED POLYMERIZATION: INERT ADDITION AND SURFACE COATING OF SUPERABSORBENT POLYMER WITH IMPROVED PHYSICAL PROPERTIES

‡Michael M. Azad[1,2] and ‡Marinella G. Sandros[1]
[1]Department of Nanoscience, University of North Carolina at Greensboro, Greensboro, NC 27401, USA
[2]Evonik Industries, 2401 Doyle Street, Greensboro, NC 27404
Marinella G. Sandros (Email: m_sandro@uncg.edu)

Abstract

Two different polymerization techniques, microwave-assisted polymerization and free radical solution polymerization, were utilized in the syntheses of superabsorbent polymers with varying amounts of acrylic acid (31-50%). Degrees of neutralization were in the range of 68 - 75 mol%, and clay level was varied at 0 - 5%. The base polymer produced with microwave-assisted polymerization had higher absorbency under low load (0.3 psi) than those with the free radical solution polymerization. To improve its absorbency under higher loads (0.6 and 0.9 psi), the surface coating step was implemented by employing the use of ethylene glycol diglycidyl ether (EGDGE) as a surface crosslinking agent. Properties such as capacity, permeability, and absorbency under different loads were tested in 0.9% sodium chloride solution for the base and the surface

coated polymers. In addition, extractables and residual acrylic acid were measured to determine the reaction's efficiency. In conclusion, surface coating improved polymer properties, and the incorporation of clay imparted permeability to the polymer.

KEYWORDS: superabsorbent polymer; absorbency under load; centrifuge retention capacity; extractables; crosslinking; swelling; Surface crosslinking

Introduction

Superabsorbent polymer is most commonly produced with lightly crosslinked and partially neutralized acrylate or methacrylate monomers [1]. Any monomer with a polymerizable double bond could be used [1] in the making of superabsorbent polymer. Acrylic acid [1] has gained popularity because of its favorable cost structure, and free radical solution polymerization is the preferred process in industrial settings.

Compared to a surface coated superabsorbent polymer, a lightly crosslinked superabsorbent *base* polymer has higher centrifuge retention capacity (CRC) but lacks measurable gel strength. Centrifuge retention capacity is based on the amount of aqueous liquid that a polymer can absorb and bind chemically, and the amount of crosslinker in the monomer solution will determine that capacity. In addition, since sodium polyacrylate is a water-soluble polymer, a crosslinker is needed to make it water-insoluble. Although superabsorbent polymer absorbs hundreds of times of its own weight in deionized water [1-2], its capacity is in the range of 30-50 g/g for 0.9% sodium chloride (used to simulate urine in laboratories) [1]. The first generation of superabsorbent polymer in the hygiene

industries was *base* polymer. While this was an upgrade to the existing diaper, lower gel strength prevented the utilization of its total capacity due to gel blocking, a phenomenon which prevents liquid movement in the diaper core due to the constriction and eventual blocking of liquid transport channels as the gel swells. Since superabsorbent polymer has found application in different industries [1, 3-28], higher absorbency under load (AUL) [1] is necessary to withstand the applied pressure in these types of applications. AUL improvement is accomplished with a surface reaction step that crosslinks the exterior of the superabsorbent polymer particles/ granules.

In general, 'surface crosslinking,' as it is referred to, accounts for a fair portion of the total cost of superabsorbent polymer production, due to the long and complicated surface coating step [2]. This step has been used to improve polymers' absorbency under load [1], among other properties. It strengthens the *base* polymer by creating a shell around the core, but the trade-off is decreased absorption capacity [1-2]. Introduction of a photo-induced surface crosslinking agent by S. Jackusch et al. [2] is a step in the right direction, as it improves polymer's permeability and shortens the time it takes to perform the surface crosslinking step. However, the presented data is only for the polymers with lower CRC (CRC <30 g/g), and the combined properties (CRC, AUL, and Permeability) of these polymers are still lower than the one produced with a thermally reactive coating [2].

Base polymer produced with free radical solution polymerization has lower AUL (AUL <10 g/g) and higher CRC than that produced via microwave-assisted polymerization, and a long surface crosslinking step has to be implemented to strengthen

the polymer. However, a better way of improving the properties could be accomplished by employing a *base* polymer with higher AUL, and therefore shortening the time that it takes to do the surface crosslinking step. Microwave-assisted polymerization is capable of producing such a polymer (AUL >14 g/g). Giachi et al. describe the advantage of microwave-assisted polymerization in producing a homogeneous polymer with far superior properties which could play a central role in optimizing the production processes. In addition, the time it takes to do the heating is substantially less [1].

Since AUL is an indicator of the amount of liquid that a polymer can absorb (under specific amounts of pressure) and CRC determines its retention capacity, permeability of a swollen bed of superabsorbent polymer translates over to a polymer's ability to distribute the absorbed liquid in a diaper core. Therefore, the liquid distribution in a diaper core is as critical as is its CRC or AUL [2]. For a polymer with higher CRC (CRC >30 g/g), the surface coating process improves its absorbency under load but has very little effect on the permeability of a swollen gel bed. Polymer without permeability of its gel bed cannot wick the liquid away from the point of 'insult' [1] in a hygiene article (e.g., diaper) and therefore underutilizes the full potential [2] of the superabsorbent polymer in the intended application. Addition of clay to the polymer is one way of improving the permeability. In free radical solution polymerization, clay addition to the monomer is riddled with pitfalls. Since the initiation process is relatively slow, clay tends to separate from the monomer solution and sinks to the bottom. To overcome this problem, it could be added to the extruded gel, but again, the heterogeneity of the clay inherent to this application method becomes an issue. In microwave-assisted

polymerization, due to the fast nature of the initiation step, dispersion of the clay in the monomer solution is uniform and once again avails the possibility for the use of clay in the polymerization step.

In the experiments discussed in this manuscript, microwave-assisted polymerization was employed to produce a *base* polymer with higher gel strength for higher CRC-polymer, and the results are compared to those produced with free radical solution polymerization. Acid content, degree of neutralization (DN), and percentage of clay were varied to produce these polymers. Ethylene glycol diglycidyl ether (EGDGE) was used as a surface crosslinking agent, and the surface crosslinking times were measured and compared for polymers with high and low gel strengths. Properties such as Pressure Absorbency Index (PAI), the sum of four AULs at 0.01 psi (0.7 g/cm^2), 0.3 psi (21 g/cm^2), 0.6 psi (42 g/cm^2), and 0.9 psi (63 g/cm^2), were used to monitor the efficiency of the crosslinking step. Energy-dispersive X-ray spectroscopy (EDX) was used to confirm the presence of the clay, and permeability was measured to monitor its uniform distribution.

Materials

Glacial acrylic acid was purchased from BASF; potassium hydroxide, sodium chloride, hydrogen peroxide, ascorbic acid, hydrochloric acid, Ethylene glycol diglycidyl ether (EDGE) and ammonium persulfate from Aldrich; clay from Southern clay; and ethoxylated trimethylolpropane triacrylate (ETMPTA) from Sartomer. All of these chemicals were used as received.

Equipment

RO-TAP model RX-29 equipped with USA Standard Test Sieve for sieving, Retsch ZM1000 for milling, Heraeus Instrument Labofuge 400 for centrifuge retention capacity, Blue M lab oven for drying of the polymer, HPLC from Water for residual acrylic acid analysis, Brinkman 816 titration system for extractables, and Microwave from CEM was utilized for polymerization.

Microwave-Assisted Polymerization

Potassium hydroxide was added to the de-ionized water, and it was cooled in an ice bath while the temperature was kept around 30 °C. The crosslinker, ethoxylated trimethylolpropane triacrylate, was added to the acrylic acid in a separate beaker. Under constant stirring, contents of this beaker were combined with the potassium hydroxide solution. Monomer solution was then transferred to the polymerization vessel and after adding the required amount of ammonium persulfate, the vessel was placed in the microwave cavity, which was equipped with a condenser. Polymerization was done under constant stirring and with a gradient programing. Pressure was set to zero bars while the wattage was 100. Programming consisted first of: 2 cycles of heating for 2 minutes and cooling for twenty seconds. This was followed by heating one minute and cooling for another 20 seconds**.** Polymer was allowed to cool for 2 minutes and then was extracted from the polymerization tube. The sample was extruded, dried, milled, and sieved.

Free Radical Solution Polymerization

Monomer solution was prepared by adding potassium hydroxide to the de-ionized water while the temperature was kept under 30 °C. The crosslinker, ethoxylated trimethylolpropane triacrylate, was added to the acrylic acid in a separate beaker and then this mixture was combined with the potassium hydroxide solution under constant stirring. Monomer solution was cooled to 10 °C and then was purged with nitrogen for five minutes to remove dissolved oxygen. Hydrogen peroxide, ascorbic acid and ammonium persulfate were used to initiate the polymerization. Polymer was extruded, dried, milled, and sieved.

Surface Crosslinking Procedure

Weigh out 100 grams of superabsorbent base polymer and spray it with 3.3 grams of 0.1% EDGE solution in a Kitchen Aid bowl mixer while the mixer is on medium speed. Take the polymer out of the bowl and dry it at 155 °C for 20 to 45 minutes. Sieve it to 106-850 micron.

Water Content (WC) Measurement

The water content of the superabsorbent polymer particles is measured by the EDANA (European Disposables and Nonwovens Association) recommended test method No. 430.2-02 “Moisture content”.

Centrifuge Retention Capacity (CRC) Measurement

The centrifuge retention capacity of the superabsorbent polymer particles is measured by the EDANA (European Disposables and Nonwovens Association) recommended test method No. 441.2-02 “Centrifuge Retention Capacity”.

Absorbency Under Load (AUL) Measurement

The absorbency under load of the superabsorbent polymer particles is measured by the EDANA (European Disposables and Nonwovens Association) recommended test method No. 442.2-02 “Absorption Under Pressure”, using a weight of 0.7 psi (49 g/cm^2) instead of a weight of 0.3 psi (21 g/cm^2) 0.9 psi (63 g/cm^2) 0.6 psi (42 g/cm^2) 0.01 psi (0.7 g/cm^2).

Extractables Measurement

The percent extractables of the superabsorbent polymer particles is measured by the EDANA (European Disposables and Nonwovens Association) recommended test method No. 470.2-02 “Extractable”.

Residual Acrylic Acid (RAA) Measurement

The residual monomers content in the superabsorbent polymer particles is measured according to EDANA (European Disposables and Nonwovens Association) recommended test method No. 410.2-02 “Residual Monomers”.

The EDANA test methods are obtainable, for example, from the European Disposables and Nonwovens Association, Avenue Eugène Plasky 157, B-1030 Brussels, Belgium.

Permeability Index (PI) [Using Gel Bed Permeability (GBP) Test Measurement]

The method for Free Swell Gel Bed Permeability is described in US patent application no. US 2005/0256757 A1, paragraphs 61 through 75.

Results and Discussion

The monomer solutions were prepared with different concentrations of acrylic acid (31-50%) with both free radical solution polymerization and microwave-assisted polymerization. One of the major problems with free radical solution polymerization is its low acid content. Formulation with acid content greater than 35% is impractical and polymerization is uncontrollable. On the other hand, in microwave-assisted polymerization, since the purpose of microwave heating is to heat the monomer solution and not its surroundings, increased acid content did not affect the polymerization step. Acid content of 50% was picked as an extreme case to differentiate microwave-assisted polymerization from free radical solution polymerization.

Potassium hydroxide was used as a neutralization agent to overcome the solubility issue of sodium hydroxide at higher acid content and the degree of neutralization was evaluated at 60-80 mol%. Neutralization of acrylic acid is a way of imparting charge density to the polymer's backbone [1]. Polymers became stickier to the touch as the

degree of neutralization moved toward 60 mol%. This could be attributed to the acidic nature of the polymer, which affects both processing of the polymer and its properties in a negative way. The properties were also impacted negatively for the polymers with higher degrees of neutralization (80 mol%), but these were processable (being less sticky). In both microwave-assisted polymerization and free radical solution polymerization, the optimum DN was 70 mol% which gave the highest CRC. According to counter-ion condensation theory, as the degree of neutralization increases, the free ions will increase on the polymer backbone, but those free ions, which contribute to the osmotic pressure, will not increase after a certain value, and therefore, its CRC will not be as high as one might expect through linear extrapolation (see Fig. 13).

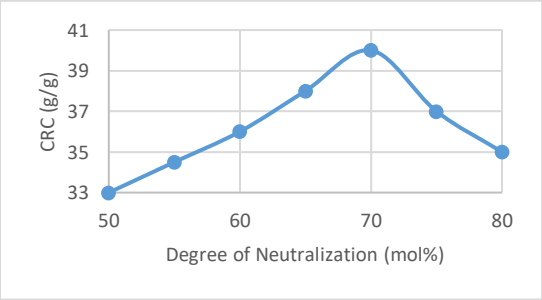

Figure 13. Degree of Neutralization Vs Capacity

CRC of the *base* polymer is determined by the amount of crosslinker in the polymerization step. Any crosslinker with two or more double bonds [1], which are capable of polymerization, could be used as a core crosslinker and ETMPTA was picked for this study.

In the free radical solution polymerization, *base* polymer was produced by utilizing ascorbic acid and hydrogen peroxide as a redox couple, while ammonium persulfate was used as a thermal initiator [1]. Both types of initiation packages are essential in this type of polymerization; redox coupling promotes polymerization and the thermal initiator is used to reduce residual acrylic acid in the final product. In the microwave-assisted polymerization, only 5-10 ppm of thermal initiator (ammonium persulfate) was needed to do the polymerization. Polymer with no initiator was hard to process (sticky to the touch), but as the amount of initiator increased (>10 ppm), the polymerization became unstable and the reproducibility from one run to the next was challenging. The same was true for the combination of redox coupling and thermal initiator use.

Since *base* polymers are prone to gel blocking (liquid movement is impeded), the surface coating step is used to improve its gel strength. Ethylene glycol diglycidyl ether (EDGE) is one of those crosslinking agents. It forms an ester bond in the surface of superabsorbent polymer and strengthens the base polymer [2] by creating a hard shell around its softer core. In addition, the surface coating step provided another opportunity to modify the polymer's properties [1].

Schematic 3 depicts the process of making and then surface coating the superabsorbent polymer.

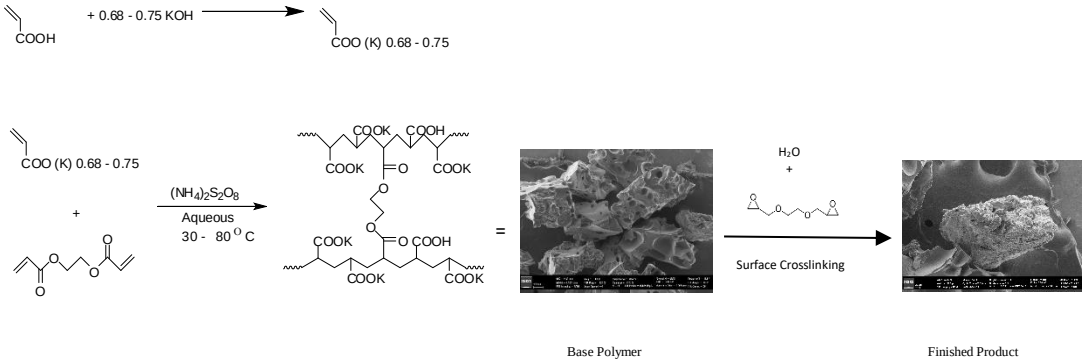

Schematic 3. General Polymerization of Acrylic Acid (Microwave or Free Radical Polymerization) and Surface Coating of the Polymer (redrawn from a description by F. L. Buchholz).

Base polymers produced by free radical solution polymerization (with acid contents of 31-50%) had CRCs in the range of 38-44 g/g, with low 0.3 AUL (~8 g/g), and relatively high extractables (see Table 2). The polymerization at 50% acid content was impossible to control and only a small amount of polymer was collected for characterization purposes. A closer look at the temperature profile (see Fig. 14) shows that temperature increased at a drastic rate and rose beyond 100 °C in less than 5 minutes. This occurs due to the fact that there is inadequate water to act as a heat sink to dissipate the heat of polymerization, and once above 100 °C, violent, explosive conditions are produced by the vaporization of water trapped in the gel.

Table 2. Base Polymers: Measured Properties at Different Acid Contents (Free Radical Solution Polymerization)

Sample		CRC (g/g)	0.3AUL	RAA (ppm)	1 hr. Extractables (%)
1	31% AA-1	37.2	8.1	1251	12.1
2	31% AA-2	39.1	8.4	1232	11.9
3	31% AA-3	41.3	7.9	1165	12.9
4	35% AA-1	39.5	8.4	1181	13.5
5	35% AA-2	41.2	7.7	1111	14.1
6	35% AA-3	41.9	7.5	1089	14.8
7	50% AA-1	42.1	7.9	985	19.9
8	50% AA-2	43.2	7.2	812	18.9
9	50% AA-3	44.4	7.4	865	17.5

AA-1: H_2O_2=150ppm, $C_6H_8O_6$=150ppm, $(NH_4)_2S_2O_8$=75ppm
AA-2: H_2O_2=175ppm, $C_6H_8O_6$=175ppm, $(NH_4)_2S_2O_8$=100ppm
AA-3: H_2O_2=225ppm, $C_6H_8O_6$=225ppm, $(NH_4)_2S_2O_8$=125ppm

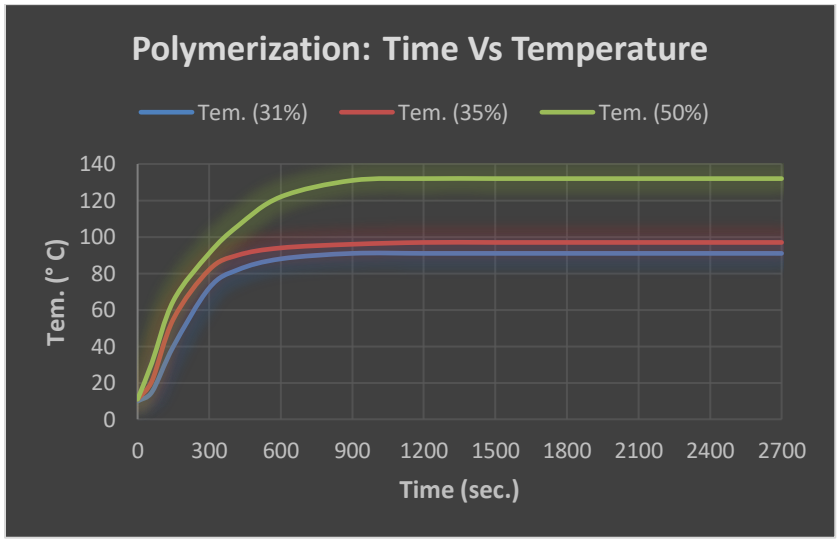

Figure 14. Temperature Profile (Free Radical Solution Polymerization)

Properties of the polymers produced with microwave-assisted polymerization were superior to those with free radical solution polymerization. CRCs stayed in the range of 37-39 g/g, while polymers had higher 0.3 AUL (~15 g/g) and lower extractables

(<5%). Even polymers at 50% acid content had comparable properties (see Table 3). The temperature profile (see Fig. 15) shows polymerization temperature under 100 °C even at 50% acid content. Homogeneity of the polymer in the microwave-assisted polymerization is one reason for getting superior properties. Instead of heating the vessel, the energy is directed toward the monomer solution, and one is able to increase the solid content of the polymer without affecting its properties. Gradient programing helped to control the kinetics in the polymerization step, which resulted in formation of a homogeneous network. Alternating heating and cooling steps helped to keep the uniformity of the network while a condenser provided a relatively controlled environment inside the polymerization vessel. The third factor was optimization of the initiation package.

In microwave-assisted polymerization, a small amount of initiator (5-10 ppm) was used to initiate the polymerization. Low levels of extractables in the polymer could be attributed to the low level of initiator used in the polymerization step. Although initiator is essential in the initiation step, too much of it could be the cause of higher extractables in the superabsorbent polymer. At higher initiator levels, a greater number of smaller polymer chains are produced along with the likelihood for some of these chains not to be crosslinked into the polymer network. These so-called ‘extractables’ are soluble oligomer and polymer chains which can freely migrate from the crosslinked gel once it begins to swell. They have a thickening or viscosifying effect on the liquid around the polymer, and viscous liquid will have a harder time to penetrate into the polymer network. In accordance with Darcy's Law, speed of penetration of a liquid through a porous medium decrease as its viscosity increases.

In the absence of initiator, the polymerization did not proceed to completion. While one needs less than 10 ppm of initiator in microwave-assisted polymerization, the level of initiator needed in free radical solution polymerization is more than 300 ppm.

Also, in contrast to the conventional free radical solution polymerization, purging the monomer solution of oxygen was not needed due to the efficiency of the heating. On the other hand, in free radical solution polymerization, nitrogen purging is necessary to eliminate dissolved oxygen in the monomer solution [29-30]. Due to its electrophilicity, or its affinity for electrons and free radicals, oxygen can prematurely terminate and even inhibit polymerization. Because heating monomer solution is very efficient with microwave-assisted polymerization, thermal initiation can proceed despite the presence of dissolved oxygen.

Table 3. Base Polymers: Measured Properties at Different Acid Contents (Microwave Polymerization)

Sample		CRC (g/g)	0.3 AUL	RAA (ppm)	1 hr. Extractables (%)
1	31% AA-5ppm Initiator	38.9	14.4	1050	2.6
2	31% AA-8.5ppm Initiator	38.1	14.6	922	2.5
3	31% AA-10ppm Initiator	37.5	15.1	855	2.4
4	35% AA-5ppm Initiator	38.4	15.4	985	3.1
5	35% AA-8.5ppm Initiator	37.9	15.2	844	2.4
6	35% AA-10ppm Initiator	36.7	15.9	790	2.6
7	50% AA-5ppm Initiator	38.1	15.1	899	2.1
8	50% AA-8.5ppm Initiator	37.8	15.8	755	1.8
9	50% AA-10ppm Initiator	37.4	15.7	712	2.1

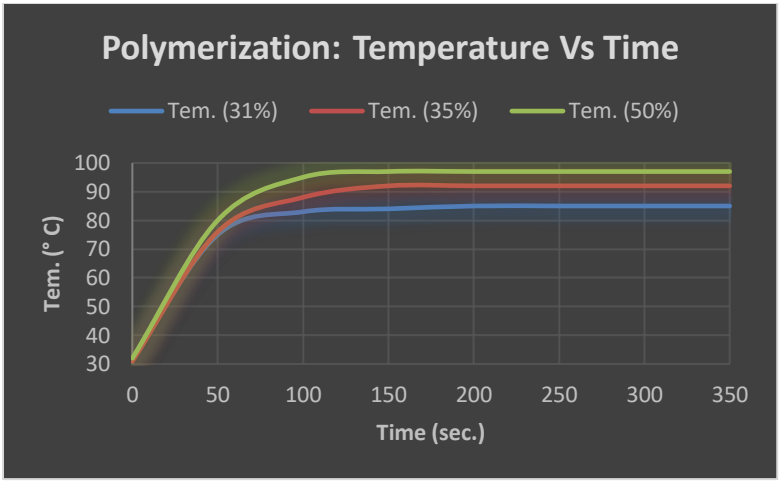

Figure 15. Temperature Profile (Microwave-Assisted Polymerization)

To reinforce its gel strength, *base* polymer was coated with 0.1% of EDGE solution and then was cured in a convention lab oven at 155 °C for 45 minutes. Pressure Absorbency Index (PAI) was used as a method for determining the efficiency of this reaction. PAI is the sum of four AULs [0.01 psi (0.7 g/cm^2), 0.3 psi (21 g/cm^2), 0.6 psi (42 g/cm^2), and 0.9 psi (63 g/cm^2)]. This is an important property as one could judge the gel strength of a polymer at different pressure points and choose an appropriate polymer for the intended application.

In free radical solution polymerization, PAIs were in the range of 112-113 g/g for the polymers with the acid contents of 31 and 35%, but it dropped to 74-76 g/g range as the acid level increased to 50%. These polymers (31 and 35%) had CRCs in the range of 33-34 g/g, 0.9 AULs of 18-20 g/g, extractables of 12-14%, and RAA of 1100-1200 ppm (see Figure 16). Again, both CRCs and 0.9 AULs were lower for those polymers made

with 50% acid. This clearly shows the destructive effect of uncontrollable polymerization on the polymer's properties.

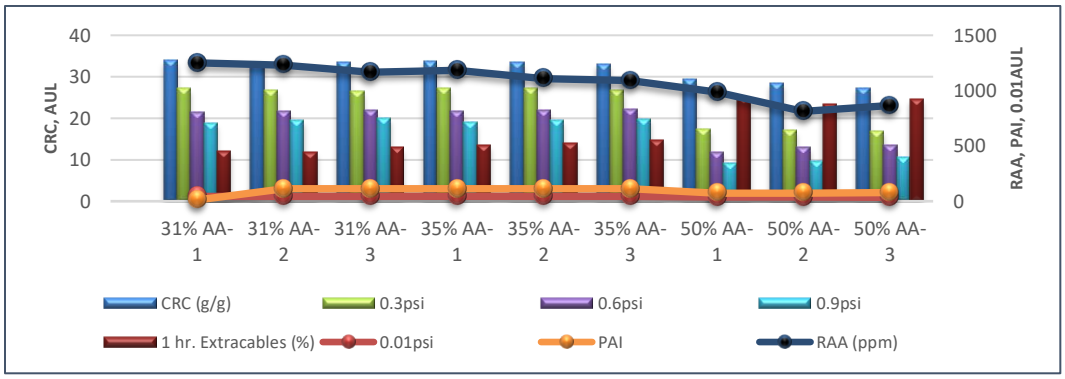

Figure 16. Surface Coated Polymer: Measured Polymer Properties at Different Acid Contents (Free Radical Solution Polymerization).

In the case of microwave-assisted polymerization, base polymers were also surface coated with 0.1% of EDGE solution, and it took only 20 minutes to cure the polymer in a conventional lab oven at 155 °C. PAIs were in the range of 130-134 g/g for all three acid levels, with CRCs of 33-34 g/g, 0.9 AULs of 22-23 g/g, extractables of 1-2%, and RAA of 600-900 ppm (see Figure 17). These polymers were devoid of any swollen gel permeability.

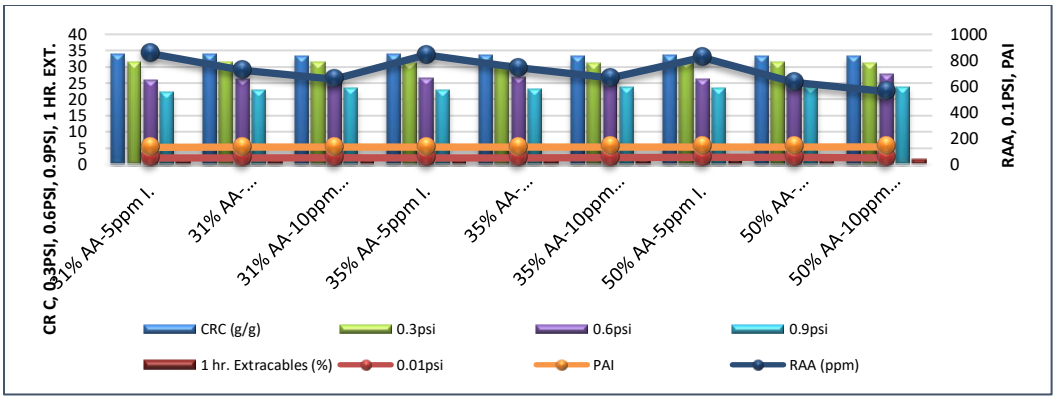

Figure 17. Surface Coated Polymer: Measured Polymer Properties at Different Acid Contents (Microwave-Assisted Polymerization).

As was the case with the *base* polymers, properties of the finished products produced with microwave-assisted polymerization were also superior to those produced with free radical solution polymerization. Shorter surface crosslinking time and superior properties are attributed to a stronger *base* polymer which was produced in the polymerization step.

As absorbency under load improved after surface coating step, the polymer still lacked permeability. Addition of clay to the monomer solution was to increase its permeability. Depending on the process, introduction of clay to the monomer solution could be challenging. In the free radical solution polymerization, since the initiation reaction is not instantaneous, clay sinks to the bottom and separates from the monomer solution. This produces a heterogeneous polymer with inconsistent properties. On the other hand, due to the fast nature of the reaction, microwave polymerization is much more conducive to the clay addition. Therefore, microwave-assisted polymerization not only could become a platform to improve the polymer's properties, but also to reduce the

cost of producing superabsorbent polymer, both in the polymerization and surface crosslinking steps.

In microwave-assisted polymerization, as clay level increased from 1.5 to 5%, the drop on centrifuge retention capacity of the *base* polymers was in the range of 0.5 to 2 g/g. This is not surprising, since clay has lower capacity than superabsorbent polymer and also acts as a crosslinker. On the other hand, the increased acid content (from 31 to 50%) had very little effect on the CRC (see Figure 18).

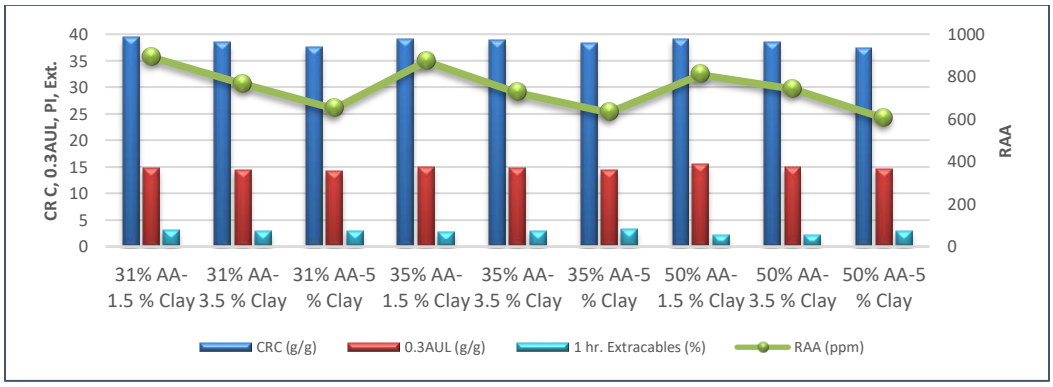

Figure 18. Base Polymers with Clay- Measured Polymer Properties at Different Acid Contents and Clay Levels (Microwave-Assisted Polymerization).

Surface crosslinked polymer had CRCs in the range of 33-34 g/g and 0.9 AULs of 22-24 g/g. As expected, properties did not drop in polymers produced via microwave-assistance. In fact, improvement in certain properties indicated a polymer with increased gel strength. In addition, permeability index increased with the amount of clay, but the acid level had very little effect on the permeability. The rise in the permeability index

(>15 Darcy) with each clay addition in the monomer solution is a good indication that clay is imparting gel permeability to the polymer. In addition, the increased permeability (from 15, in the control to about 40 Darcy in the experimental) was directly proportional to the amount of clay (1.5% to 5% by weight of the polymer) in the monomer solutions for all three acid levels (see Fig. 19). These results indicate that clay is uniformly distributed and is acting as a spacer in the polymer network.

The RAA levels for polymers with clay seem to decrease (by about 100 ppm) in all three acid levels (see Figure 20). Intuitively, heat of polymerization increases with increased acid level, but while one would expect to see lower levels of acrylic acid in this polymer, as well, this was not the case. Another interesting observation was the lower level of RAA in the clay-containing polymers (about 200 ppm less); this could be an indication of an improved polymerization efficiency.

Table 4. Surface Coated Polymers: Measured Properties at Different Acid Contents (Microwave Polymerization).

Sample	Acid contents and clay levels	CRC (g/g)	0.01psi (g/g)	0.3psi (g/g)	0.6psi (g/g)	0.9psi (g/g)	PAI (g/g)
1	31% AA-1.5% Clay	33.5	50.2	31.7	26.1	21.8	129.8
2	31% AA-3.5% Clay	33.7	50.1	31.4	25.8	22	129.3
3	31% AA-5% Clay	33.6	50.2	31.2	26.4	23.1	130.9
4	35% AA-1.5% Clay	34.1	50.9	31.4	26.2	23.1	131.6
5	35% AA-3.5% Clay	33.4	50.3	31.6	26.5	23.4	131.8
6	35% AA-5% Clay	32.9	51.4	32.1	26.1	23.7	133.3
7	50% AA-1.5% Clay	33.6	50.7	31.2	26.5	23.5	131.9
8	50% AA-3.5% Clay	33.1	51.2	31.1	26.7	23.6	132.6
9	50% AA-5% Clay	33	50.1	31	26.4	23.9	131.4

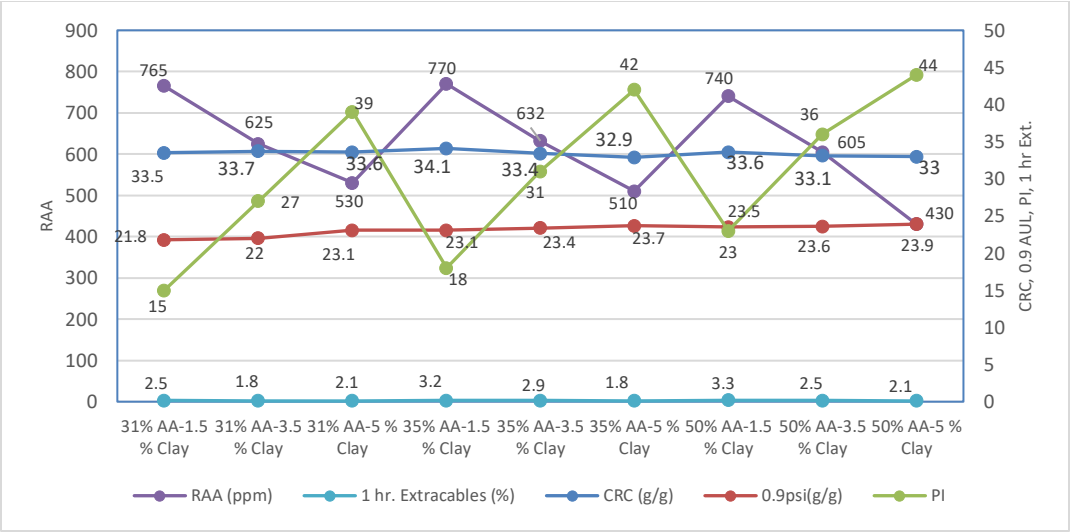

Figure 19. Surface Coated Polymers: Measured Polymer Properties at Different Acid Contents (Microwave Polymerization).

SEM images of the clay-containing particles made with the microwave-assisted polymerization have rougher surfaces than those without (see Figures 20 and 21), and EDX spectra show distinct peaks for aluminum and silicon in the clay-containing particles. In addition, it was composed of carbon and oxygen from acrylic acid and sodium from sodium hydroxide (see Figures 22).

In combination, SEM images, EDX spectra, and permeability data point to the uniformity of the clay distribution in the superabsorbent polymer.

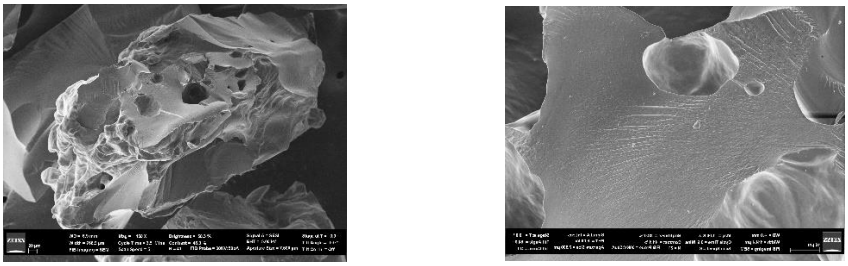

150X 1000X

Figure 20. SEM Images of the Coated Polymer Particles (without Clay) from Microwave-Assisted Polymerization.

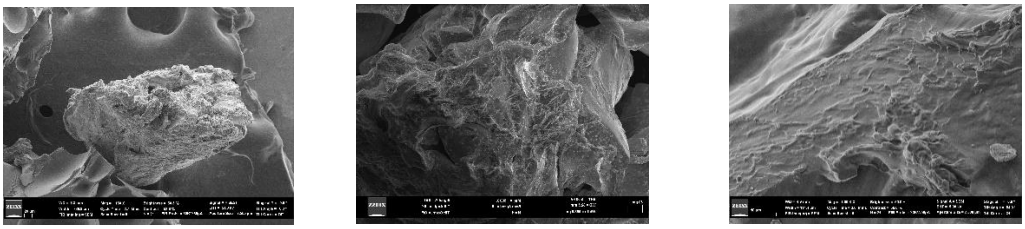

150X 500X 1000X

Figure 21. SEM Images of the Coated Polymer Particles (with Clay) from Microwave-Assisted Polymerization.

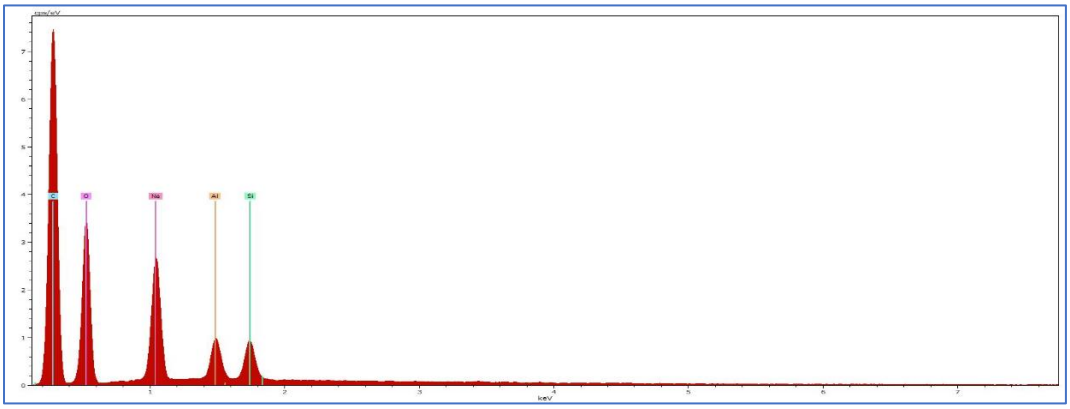

Figure 22. EDX Spectra of the Clay Containing Coated Polymer Particles from Microwave-Assisted Polymerization.

Conclusion

Microwave-assisted polymerization improved properties such as absorbency under load, centrifuge retention capacity, pressure absorbency index, and above all extracables. It also facilitated the addition and uniform distribution of the clay and further imparted improved permeability to the polymer with minimal effect on capacity reduction while improving residual acrylic acid content of the final product. Surface crosslinking with EDDGE was reduced to less than 20 minutes and polymers properties were better than those produced with free radical solution polymerization. Microwave-assisted polymerization is a major technological improvement over free radical solution polymerization and could be scaled-up without too much difficulty.

In the next phase of this work, co-monomer such as maleic and fumaric acid will be added into the formulation for investigation of their impact on properties.

Acknowledgment

The authors would like to acknowledge the assistance of Mr. Stephen Vance and Ms. Effat Zeidan with experimental setups.

References

1. Buchholz FL, Peppas NA (1991) Modern Superabsorbent Polymers Science and Technology. ACS Symposium Series 573, Washington, DC, pp 3-112.
2. Jockusch S, Turro NJ, Mitsukami Y, Moto M, Iwamura T, Lindner T, Di Massimo G (2009) Photoinduced surface crosslinking of superabsorbent polymer particles J. Appl. Polym. Sci. 111: 2163.
3. Cheng Z, Li J, Yan J, Kang L, Ru X, Liu M (2013) Synthesis and properties of a novel superabsorbent polymer composite from microwave irradiated waste material cultured *Auricularia auricula* and poly (acrylic acid-*co*-acrylamide), J. Appl. Polym. Sci. 39621: 3674-3681.
4. Teodorescu M, Lungu A, Stanescu PO (2009) Preparation and properties of novel slow-release NPK agrochemical formulations based on poly (acrylic acid) hydrogels and liquid fertilizers, Indus. Eng. Chem. Res. 48: 6527.
5. Guilherme MR, Reis AV, Paulino AT, Moia TA, Mattoso LHC, Tambourgi EB (2010) Pectin-based polymer hydrogel as a carrier for release of agricultural nutrients and removal of heavy metals from wastewater, J. Appl. Polym. Sci. 117: 3146.
6. Kandile NG, Nasr AS (2009) Environment friendly modified chitosan hydrogels as a matrix for adsorption of metal ions, synthesis and characterization, Carbohydr. Polym. 78: 753.
7. Sadeghi M, Hosseinzadeh HJ (2008) Synthesis of starch-poly (sodium acrylate-coacrylamide) superabsorbent hydrogel with salt and pH-responsiveness properties as a drug delivery system, J. Bioact. Compat. Polym. 23: 381.
8. Liu Y, Cui Y, Yin G, Ma H (2009) Synthesis, characterization, and drug release behavior of novel soy protein/poly (acrylic acid) IPN-hydrogels, Iran Polym. J. 18: 339-348.
9. Kabiri K, Faraji-Dana S, Zohuriaan-Mehr MJ (2005) Novel sulfobetaine-sulfonic acid-contained superswelling hydrogels, Polym. Adv. Technol. 16: 659-666.
10. Zou XX, In *Superabsorbents* (2002) Chemical Industry 2nd edn. Beijing PP 2.
11. Dubrovskii SA, Afanas'eva NV, Lagutina MA, Kazanskii KS (1990) Comprehensive characterization of superabsorbent polymer hydrogels, Polym. Bull. 24: 107-113.
12. Raju KM, Raju MP, Mohan YM (2002) Synthesis and water absorbency of crosslinked superabsorbent polymers, J. Appl. Polym. Sci. 85: 1795-1801.
13. Colombo P (1993) Swelling-controlled release in hydrogel matrices for oral route, Adv. Drug Del. Rev. 11: 37.

14. Gao D, Heimann RB, Lerchner J, Seidel J, Wolf G (2001) Development of a novel moisture sensor based on superabsorbent poly(acrylamide)-montmorillonite composite hydrogels, J. Mater. Sci. 36: 4567.
15. Gao D, Heimann RB, Alexander SDB (1997) Box-Behnken design applied to study the strengthening of aluminate concrete modified by a superabsorbent polymer/clay composite, *Adv Chem Res*, 9: 93-97.
16. Wu L, Liu M, Liang R (2008) Preparation and properties of a double-coated slow-release NPK compound fertilizer with superabsorbent and water retention, *Bioresource Tech*, 99: 547-554.
17. Yamane H, Ideguchi T, Tokuda M, Koga H (1994) A new ground-reducing material based on water absorbent polymer, *Electronics and Communications in Japan*, Part 1, 77: 68-77.
18. Bowman DC, Evans RY, Paul JL (1991) Fertilizer salts reduce hydration of polyacryamide gels and affect physical properties of gel-amended container media, *J Amer Soc Hort Sci*, 115: 382-386.
19. Rudzinski WE, Dave AM, Vaishnav UH, Kumbar SG, Kulkarni AR, Aminabhavi TM (2002) Hydrogels as conclolled release devices in agriculture, *Designed Monomers Polym*, 5: 39-65.
20. Guo M, Liu M, Liang R, Niu A (2006) Granular ureaformaldehyde slow-release fertilizer with superabsorbent and moisture preservation, *J Appl Polym Sci*, 99: 3230-3235.
21. Kenawy E-R (1998) Recent advances in controlled release of agrochemicals, *J Macromol Sci-Rev Macromol Chem Phys*, C38: 365-390.
22. Liang R, Liu M, Wu L (2007) Controlled release NPK compound fertilizer with the function of water retention, *React Func Polym*, 67: 769-779.
23. Guo M, Liu M, Zhan F, Wu L (2005) Preparation and properties of a slow release membrane-encapsulated urea fertilizer with superabsorbent and moisture preservation, *Ind Eng Chem Res*, 44: 4206-4211.
24. Wu L, Liu M (2008) Preparation and properties of chitosan- coated NPK compound fertilizer with controlled-release and water-retention, *Carbohydr Polym*, 72: 240-247.
25 Liu M, Liang R, Zhan F, Liu Z, Niu A (2006) Synthesis of a slow-release and superabsorbent nitrogen fertilizer and its properties, *Polym Adv Technol*, 17, 430-438.
26 Liu M, Liang R, Zhan F, Liu Z, Niu A (2007) Preparation of superabsorbent slow release nitrogen fertilizer by inverse suspension polymerization, *Polym Int*, 56: 729-737.
27. Ahmadpour A, Maskoki A, Rezaie M (2007) *Iran J Polym Sci Tech* (in Persian), Dewatering of yogurt using a permeable membrane and acrylic superabsorbent hydrogel, 20: 551-559.
28. Singh V, Tripathi DN, Tiwari A, Sanghi R (2004) Microwave enhanced synthesis of chitosan-graft-polyacrylamide, J. Appl. Polym. Sci. 95: 820.

29. Tong Z, Peng W, Zhiqian Z, Baoxiu Z (2004) Microwave irradiation copolymerization of superabsorbents from cornstarch and sodium acrylate, J. Appl. Polym. Sci. 95: 264.

Graphical Abstract

MICROWAVE-ASSISTED POLYMERIZATION: INERT ADDITION AND SURFACE COATING OF SUPERABSORBENT POLYMER WITH IMPROVED PHYSICAL PROPERTIES

‡Michael M. Azad[1,2] and ‡Marinella G. Sandros[1]
[1]Department of Nanoscience, University of North Carolina at Greensboro, Greensboro, NC 27401, USA
[2]Evonik Industries, 2401 Doyle Street, Greensboro, NC 27404
Marinella G. Sandros (Email: m_sandro@uncg.edu)

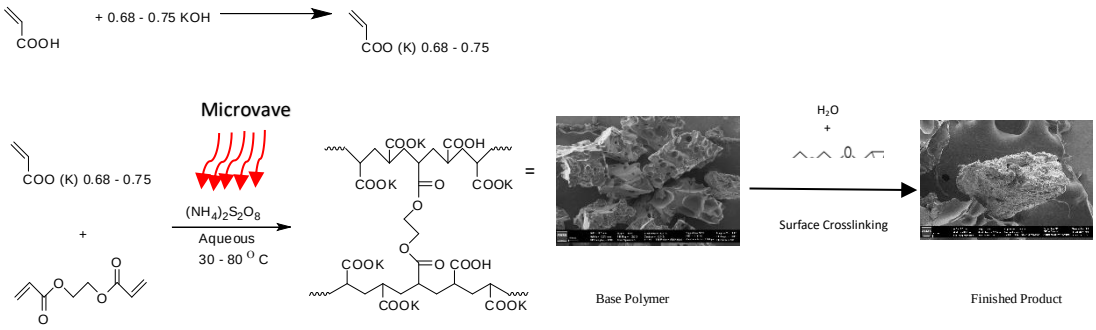

Schematic 4. General Polymerization of Acrylic Acid (Microwave or Free Radical Polymerization) and Surface Coating of the Polymer (redrawn from a description by F. L. Buchholz).

CHAPTER IV

MICROSCOPIC STUDIES OF THE IMPACT OF CLAY ON VOIDS AND PERMEABILITY IN SUPERABSORBENT POLYMERS

Michael M. Azad[1], Jianjun Wei[1], and Daniel J. C. Herr[1]
[1]Department of Nanoscience, University of North Carolina at Greensboro, 2907 East Gate City Boulevard, Greensboro, North Carolina 27401
Correspondence to: D. J. C. Herr (E- mail: djherr@uncg.edu)

Abstract

Microwave-assisted polymerization (MAP) and free radical solution polymerization (FRSP) techniques were utilized to synthesize superabsorbent polymers with different amounts of acrylic acid (31-50% by weight). To gain insight and improve the movement of the liquid through a bulk absorbent articles, such as diaper, and to prevent gel blocking, different amounts of clay powder with particle sizes less than 100 μm, 0 – 5% based on the weight of acrylic acid, were added to the monomer solution and the polymer's permeability was studied. To understand the reason behind the permeability improvement, optical microscopy, with a cooled CCD camera, was used to study the number and sizes of pores in each polymer sample produced with these two different polymerization techniques. The reaction efficiencies were assessed by measuring the percent extractables, i.e., the soluble portion of the polymer, and the residual acrylic acid content. The clay-containing polymers exhibited a larger number of

pores, i.e., 168 pores for MAP versus 44 pores for FRSP, a smaller overall surface area, 216 ± 2.81 μm^2 (1σ) for MAP with clay versus 164 ± 5.99 μm^2 (1σ) for FRSP with clay. The enhanced permeability observed in the MAP system with clay, with larger numbers of smaller pores, may be facilitated by the creation of percolation channels that favor fluid flow between pores, rather than the large and potentially gel-block forming region between pores in the samples without clay. Percolation theory helps to explain the movement of the liquid through the absorbent core and the observed improvement of the permeability index.

KEYWORDS: Superabsorbent polymer; SAP; permeability; clay; microscopy; percolation theory; voids; yield; morphology

Introduction

Acrylic acid or any monomer with a polymerizable double bond[1] could be used in the production of superabsorbent polymers. The absorption and retention of a large quantity of liquid can be maintained under low to moderate pressure.[2]

Retention of a large quantity of liquid is the main property of the superabsorbent polymer, but the movement of liquid in the absorbent core is even more crucial. "Polymer without permeability of its gel bed cannot wick the liquid away from the point of "insult"[1] in a hygiene article, e.g., a diaper, and therefore underutilizes the full potential[2] of the superabsorbent polymer in the intended application."[3]

The addition of clay into the monomer solution is one way of improving the permeability index in a superabsorbent polymer. The current working hypotheses assume that 1) the clay acts a spacer in the polymer network and provides an interconnected channel and/or 2) greater void surface area or volume for the liquid to move throughout the polymer.

The following study was designed to test these hypotheses and to provide a deeper understanding of the reason behind the improved permeability observed in a superabsorbent polymer sample containing clay.

Glossary

CRC (Centrifuge Retention Capacity): Total liquid polymer could absorb.

AUL (Absorbency Under Load): The amount of liquid polymer could absorb under specific pressure (0.01, 0.3, 0.6, 0.7, and 0.9 psi).

RAA (Residual Acrylic Acid): The amount of unreacted acrylic acid in the polymer.

Extracables: Uncrosslinked polymer chains, which are water soluble.

PI (Pressure Absorbency Index): Determines how permeable the polymers are.

Materials

Purchased chemicals included: Glacial acrylic acid from BASF, potassium hydroxide, sodium chloride, hydrogen peroxide (H_2O_2), ascorbic acid ($C_6H_8O_6$), hydrochloric acid, 85% O-phosphoric acid, high performance liquid chromatography (HPLC)-grade methanol, ultrapure water, ethylene glycol diglycidyl ether, and ammonium persulfate [$(NH_4)_2S_2O_4$] from Aldrich, Laptonite clay (Synthetic Hectorite-like clay, diameter = 25 nm and thickness = 1 nm) from Southern clay, and ethoxylated trimethylolpropane triacrylate (ETMPTA) from Sartomer. All chemicals were used as received.

Equipment

The following equipment were used for polymerization and characterization: An HPLC instrument with UV detector from Water, a Dionex IonPac AS20 column, a Nucleosil column (C8, 120 A°, 5 mm, 250 X 4.6 mm, with a mobile phase of 0.2 mL 85% O-phosphoric acid, 5.0mL of HPLC-grade methanol, and 0.9948 L of ultrapure water) for residual acrylic acid analysis, a Retsch ZM1000 for milling, a RO-TAP model RX-29 equipped with USA Standard Test Sieve for sieving, a Heraeus Instrument Labofuge 400 for centrifuge retention capacity (CRC), a Thermoscientific Lindberg Blue M lab oven for the drying of the polymer, a stereo microscope from Olympus (model SXZ 16), a Brinkman 816 titration system for extractables, and a Microwave from CEM for polymerization.

Monomer Solution

Monomer solutions were prepared as reported in our previous work.[3]

Microwave-Assisted Polymerization

Polymerizations were performed as reported in our previous work.[3]

Free-Radical Solution Polymerization

Polymerizations were performed as reported in our previous work.[3]

Surface Crosslinking Procedure

Surface crosslinking was performed as reported in our previous work.[3]

Water Content (WC) Measurement

Test was performed as reported in our previous work.[3]

Centrifuge Retention Capacity (CRC) Measurement

The centrifuge retention capacity of the superabsorbent polymer particles is measured by the EDANA recommended test method No. 441.2-02 “Centrifuge Retention Capacity”.[4]

Absorbency Under Load (AUL) Measurement

The absorbency under load of the superabsorbent polymer particles was measured by the EDANA recommended test method No. 442.2-02 “Absorption Under Pressure”, using a weight of 0.7 psi (49 g/cm^2) instead of a weight of 0.3 psi (21 g/cm^2) 0.9 psi (63 g/cm^2) 0.6 psi (42 g/cm^2) 0.01 psi (0.7 g/cm^2).[5]

Extractables Measurement

The percent extractables of the superabsorbent polymer particles was measured by the EDANA recommended test method No. 470.2-02 “Extractable”.[6]

Residual Acrylic Acid (RAA) Measurement

The residual monomers content in the superabsorbent polymer particles was measured according to EDANA recommended test method No. 410.2-02 “Residual Monomers”.[7]

All EDANA test methods are obtainable from the European Disposables and Nonwovens Association, Avenue Eugène Plasky 157, B-1030 Brussels, Belgium.

Permeability Index (PI) [Using Gel Bed Permeability (GBP) Test Measurement]

The method for Free Swell Gel Bed Permeability is described in US patent application no. US 2005/0256757 A1, paragraphs 61 through 75.[8]

Results and Discussion

Different samples of lightly crosslinked and partially neutralized superabsorbent polymers were produced by employing the FRSP or the MAP synthesis technique, cited above. These polymers exhibit high capacity, but low permeability. To facilitate the movement of the liquid and to impart permeability through the polymer matrix, different concentrations of clay, 0-5 wt.% based on acrylic acid, with particle sizes < 100 nanometers, were added to the monomer solution by employing a high shear mixer. In FRSP, most of the clay sank to the bottom of the polymerization vessel, and there was a distinct separation between the polymer in the top and clay layer in the bottom. The reason for this separation is the relatively long polymerization time to complete the FRSP reaction, which is in the range of 40 minutes. The properties of the representative cross-linked polymer samples are summarized in TABLE 5. The mean for the permeability index is in the range of 3-19.5 Darcy, with standard deviations ranging from 1.4-21.9 Darcy at different acid levels.

On the other hand, the clay was uniformly distributed in the polymers produced with MAP. The uniformity of distribution could be attributed to the shorter reaction times, which are less than 6 minutes for this type of polymerization technique. Since the clay used in this study serves as an inert material with small particle sizes, separation of the clay from the polymer network could be an issue during the milling and sieving steps. Stepwise improvement of the permeability in the MAP with different percentages of clay demonstrates that the higher percentage of the clay yielded higher permeability. Properties of the MAP synthesized polymer samples are summarized in TABLE 6. The

mean estimates for the permeability index ranges from 16.5-48 Darcy, with corresponding standard deviations ranging from 1.4-5.6 Darcy at different acid levels.

Table 5. Measured Polymer Properties at Different Acid Contents (Free Radical Solution Polymerization). Reaction Conditions: T=10C and [H2O2] = [ASA]=[APS]=150 ppm.

Samples	CRC (g/g)	0.9AUL (g/g)	PI (Darcy)	RAA (ppm)	Yield (%)	PAI (g/g)
31%AA-1	22.5	5.4	2	39854	5.4	53.2
	18.2	6.7	4	19635	18.9	63.7
Mean	20.35	6.05	3	29744.5	12.15	58.45
STDEV	3.04	0.92	1.41	14296.99	9.55	7.42
31%AA-2	19.4	6.8	9	24689	6.9	44.4
	16.3	10.1	2	31265	21.1	75.1
Mean	17.85	8.45	5.50	27977.00	14.00	59.75
STDEV	2.19	2.33	4.95	4649.93	10.04	21.71
31%AA-3	34.1	12.3	35	12578	15.4	55.9
	18.6	6.7	4	36458	21.5	63.2
Mean	26.35	9.5	19.5	24518	18.45	59.55
STDEV	10.96	3.96	21.92	16885.71	4.31	5.16
35%AA-1	10.1	6.6	19	9524	24.9	63.4
	29.5	12.3	5	35698	15.9	43.2
Mean	19.8	9.45	12	22611	20.4	53.3
STDEV	13.72	4.03	9.90	18507.81	6.36	14.28
35%AA-2	19.4	5.8	5	34567	18.3	29.7
	15.43	4.9	17	3941	28.1	71.2
Mean	17.42	5.35	11.00	19254.00	23.20	50.45
STDEV	2.81	0.64	8.49	21655.85	6.93	29.34
35%AA-3	15.4	9.5	7	65489	15.8	49.7

	17.8	5.4	3	13256	25.9	63.2
Mean	16.6	7.45	5	39372.5	20.85	56.45
STDEV	1.70	2.90	2.83	36934.31	7.14	9.55
50%AA-1	35.1	4.6	1	65478	2.5	31.7
	12.3	8.5	6	23546	45.3	69.5
Mean	23.70	6.55	3.50	44512.00	23.90	50.60
STDEV	16.12	2.76	3.54	29650.40	30.26	26.73
50%AA-2	29	6.3	27	75243	4.9	39.8
	18.6	9.4	8	12654	35.8	42.3
Mean	23.80	7.85	17.50	43948.50	20.35	41.05
STDEV	7.35	2.19	13.44	44257.11	21.85	1.77
50%AA-3	11.4	10.2	3	39644	7.7	24.5
	25.4	10.2	19	36625	45.4	49.7
Mean	18.4	10.2	11	38134.5	26.55	37.1
STDEV	9.90	0.00	11.31	2134.76	26.66	17.82

AA-1: 1.5% Clay, AA-2: 3.5% Clay, AA-3: 5% Clay

Table 6. Measured Polymer Properties at Different Acid Contents (Microwave-Assisted Polymerization). Reaction Conditions: T=10C and [APS]=5 ppm.

Samples	CRC (g/g)	0.9AUL (g/g)	PI (Darcy)	RAA (g/g)	Yield (%)	PAI (g/g)
31%AA-1	33.5	21.8	15	765	97.5	129.8
	33.7	21.6	18	763	98.2	130.4
Mean	33.6	21.7	16.5	764	97.85	130.1
STDEV	0.14	0.14	2.12	1.41	0.49	0.42
31%AA-2	33.7	22	27	625	98.2	129.3
	33.6	24	29	543	98.4	128.7
Mean	33.65	23	28	584	98.3	129

STDEV	0.07	1.41	1.41	57.98	0.14	0.42
31%AA-3	33.6	23.1	39	530	97.9	130.9
	33.5	23.4	42	596	98.1	129.9
Mean	33.55	23.25	40.5	563	98	130.4
STDEV	0.07	0.21	2.12	46.67	0.14	0.71
35%AA-1	34.1	23.1	18	770	96.8	131.6
	33.9	22.8	21	765	97.2	131.1
Mean	34	22.95	19.5	767.5	97	131.35
STDEV	0.14	0.21	2.12	3.54	0.28	0.35
35%AA-2	33.4	23.4	31	632	97.1	131.8
	33.5	23.9	35	654	97.5	131.5
Mean	33.45	23.65	33	643	97.3	131.65
STDEV	0.07	0.35	2.83	15.56	0.28	0.21
35%AA-3	32.9	23.7	42	510	98.2	133.3
	33.1	24.1	49.6	498	98.5	133.7
Mean	33	23.9	45.8	504	98.35	133.5
STDEV	0.14	0.28	5.37	8.49	0.21	0.28
50%AA-1	33.6	23.5	23	740	96.7	131.9
	33.8	23.4	26	732	97.1	132.1
Mean	33.7	23.45	24.5	736	96.9	132
STDEV	0.14	0.07	2.12	5.66	0.28	0.14
50%AA-2	33.1	23.6	36	605	97.5	132.6
	33	23.7	38	598	97.8	133.2
Mean	33.05	23.65	37	601.5	97.65	132.9
STDEV	0.07	0.07	1.41	4.95	0.21	0.42
50%AA-3	33	23.9	44	430	97.9	134.9
	32.8	24.6	52	415	98.2	134.5

Mean	32.9	24.25	48	422.5	98.05	134.7
STDEV	0.14	0.49	5.66	10.61	0.21	0.28

AA-1: 1.5% Clay, AA-2: 3.5% Clay, AA-3: 5% Clay

As mentioned before, the clay was not uniformly distributed in the polymers produced with FRSP and most of the clay settled to the bottom of the polymerization vessel. In FRSP, the properties were inconsistent and polymer *fines* were enrichment with clay in most of the samples.

Quantifying Percentage of Clay

Two different methods were used to quantify the amount of clay in the polymers.

1) The percentage of *fines* in the polymers with and without clay was quantified using a mass balance. *Fines* are defined as particles of smaller than 106 microns in size. When the polymer is being sized for the final classification, 106-850 microns, using a standard US sieve, particles less than 106 microns are not included in the final product. These particles are usually classified as dust and have undesirable properties, i.e., gel blocking, when they are included in most hygiene and non-hygiene articles. If clay falls off the polymer network, the percentage of *fines* will increase, due to the enrichment of the fines with clay.
2) The percentage of aluminum and silicon ions in the final product was quantified via ion chromatography.

The results for FRSP are summarized in TABLE 7. Based on mass balance measurement, the mean of the *fines* for the FRSP control was 2.4%, which increased to 3.5, 5.2, and 6.8% as the amount of clay increased to 1.5, 3.5, and 5% respectively. Based on these observations, it could be concluded that the majority of the clay does not stay in the polymer network and is lost in the milling step. These findings were confirmed by the use of ion chromatography. The total left-over clay in the products made with 1.5, 3.5, and 5% clay was 0.6, 1.4, and 2.1% respectively.

The results were completely different for those polymers made with microwave-assisted polymerization. These findings are summarized in TABLE 8. In the case of mass balance, mean of the *fines* for the control was 2.4% with a standard deviation of 0.01%. For the MAP process, the means stayed at 2.4%, and the standard deviations were in the range of 0.04-0.06%, as the clay level increased from 0 to 5 wt.%. Based on these observations, one could assume that there was no enrichment of *fines* with clay, and the majority of the clay stays in the polymer network. The results with ion chromatography, which measures percentage of ions in the samples, confirmed these findings.

Table 7. Percent Clay in Fines and Polymers with Mass Balance and Ion Chromatography (Free Radical Solution Polymerization). Reaction Conditions: T=10C, [AA]=31% and [H2O2] =[ASA]=[APS]=150 ppm.

% Clay & Fines with Mass Balance	Control (without Clay) %	1.5% Clay	3.5% Clay	5% Clay
% Fines & Clay - Sample 1	2.49	3.91	5.97	7.44
% Fines & Clay - Sample 2	2.38	2.83	5.88	6.48
% Fines & Clay - Sample 3	2.48	2.98	4.99	6.43

% Fines & Clay - Sample 4	2.37	3.96	5.82	5.35
% Fines & Clay - Sample 5	2.41	3.48	4.81	7.37
% Fines & Clay - Sample 6	2.41	3.88	3.77	7.49
Mean	2.42	3.51	5.21	6.76
STDEV	0.05	0.50	0.86	0.84
% Clay & Fines with Ion Chromatography	Control (with Clay) %	1.5% Clay	3.5% Clay	5% Clay
% Fines & Clay - Sample 1	0.01	1.2	1.2	2.5
% Fines & Clay - Sample 2	0.02	0.05	0.18	1.4
% Fines & Clay - Sample 3	0.00	0.03	3.2	0.07
% Fines & Clay - Sample 4	0.00	1.1	2.3	1.03
% Fines & Clay - Sample 5	0.03	1.3	1.1	4.89
% Fines & Clay - Sample 6	0.02	0.07	0.38	2.4
Mean	0.01	0.63	1.39	2.05
STDEV	0.01	0.63	1.16	1.66

Table 8. Percent Clay in Fines and Polymers with Mass Balance and Ion Chromatography for MAP. Reaction Conditions: T=10C, [AA]=31% and [APS]=5 ppm.

% Clay & Fines with Mass Balance	Control (without Clay) %	1.5% Clay	3.5% Clay	5% Clay
% Fines & Clay - Sample 1	2.4	2.41	2.47	2.44
% Fines & Clay - Sample 2	2.39	2.43	2.48	2.48
% Fines & Clay - Sample 3	2.41	2.38	2.39	2.4
% Fines & Clay - Sample 4	2.38	2.46	2.42	2.35
% Fines & Clay - Sample 5	2.39	2.48	2.41	2.37
% Fines & Clay - Sample 6	2.4	2.38	2.37	2.49

Mean	2.40	2.42	2.42	2.42
STDEV	0.01	0.04	0.04	0.06
% Clay & Fines with Ion Chromatography	Control (with Clay) %	1.5% Clay	3.5% Clay	5% Clay
% Fines & Clay - Sample 1	0	1.48	3.52	5.1
% Fines & Clay - Sample 2	0.01	1.48	3.47	5
% Fines & Clay - Sample 3	0.01	1.47	3.49	4.96
% Fines & Clay - Sample 4	0.02	1.51	3.49	4.95
% Fines & Clay - Sample 5	0.01	1.5	3.48	4.95
% Fines & Clay - Sample 6	0	1.49	3.47	4.99
Mean	0.01	1.49	3.49	4.99
STDEV	0.01	0.01	0.02	0.06

To understand the reason behind the permeability improvement, and to study the pore sizes in the polymer, polymers were immersed in methanol or ethanol for an hour and then sliced with a microtome, and their pore sizes were measured under a microscope. In the FRSP control, i.e., no clay, samples show fewer isolated pores with a larger diameter, but the addition of clay seems to decrease pore sizes somewhat. Since the initiation time in FRSP is long, the mixing of the monomer solution stops well before initiation, and most of the existing bubbles tend to dissipate before initiation. In this case, clay tends to sink to the bottom of the polymerization vessel and only small percentage of clay is incorporated into the polymer network and produce a heterogeneous polymer. See Figure 23 - 24 and micrographs in Figures 25 – 28.

Figure 23. FRSP with Clay - Heterogeneous Polymer

Figure 24. MAP with Clay - Homogeneous Polymer

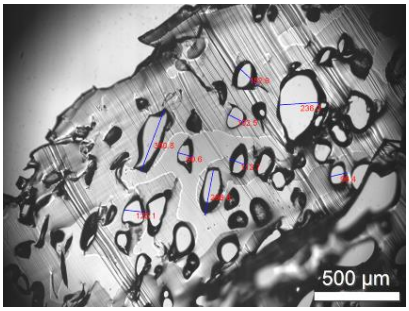

Figure 25. Slice of Gel, FRSP (Control)

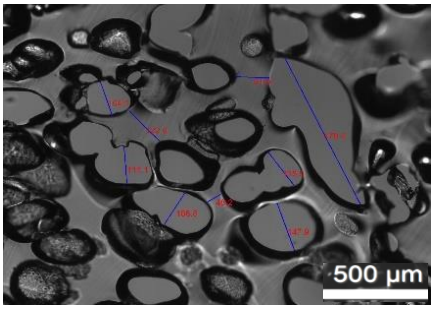

Figure 26. Slice of Gel, FRSP (with Clay)

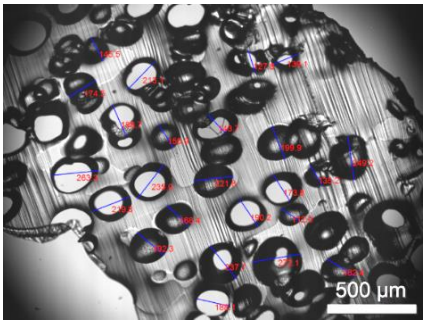

Figure 27. Slice of Gel, MAP (Control)

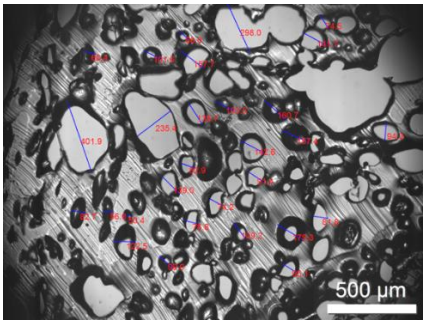

Figure 28. Slice of Gel, MAP (with Clay)

Approximate Average Number of Pores and Pore Sizes (μm) for Different Polymers

In the case of The MAP, the number of pores increased substantially versus those with FRSP, and their average size decreased when clay was added to the monomer solution. As mentioned before for MAP, the polymerization step is fast, and the monomer solution is in constant motion before polymerization. Consequently, the bubbles have very little chance to subside before the polymerization. The addition of clay to the monomer solution may stabilize and/or create a nucleation point for bubble formation and could create a suitable environment for bubbles to form and survive. This is a new hypothesis and needs to be studied further. Also, a homogeneous distribution of the clay in the polymer network, as is the case in the MAP, or lack of it, which is evident in FRSP, could be the reason for the differences in the numbers and sizes of the pores in the polymers produced with two different polymerization techniques. This set of data is summarized in TABLE 9 and Figures 29 - 31. There was a total of 44 pores for the control samples made with the FRSP technique, and the addition of clay did not affect this number. These numbers increased to 78 for the control produced with microwave-assisted polymerization, and it climbed to 168 for the sample with clay in the monomer solution.

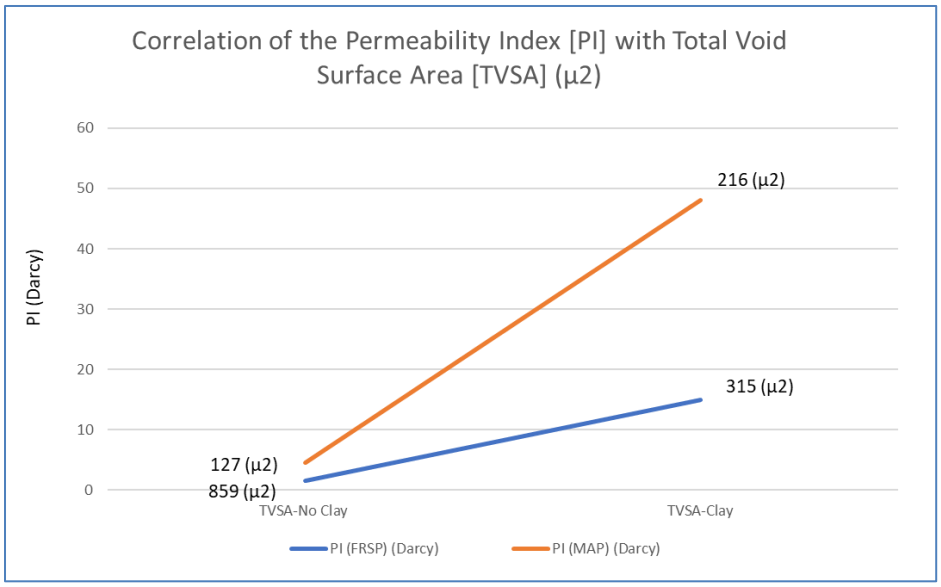

Figure 29. The Correlation of Total Void Surface Area (TVSA), µ2, with the Observed Permeability Index PAA SAPs Synthesized via FRSP and MAP, with and without Clay in the Monomer Solution. Note: FRSP reaction conditions: T=10C, [AA]=31% and [H2O2] = [ASA]=[APS]=150 ppm; MAP reaction conditions: T=10C, [AA]=31% and [APS]=5 ppm.

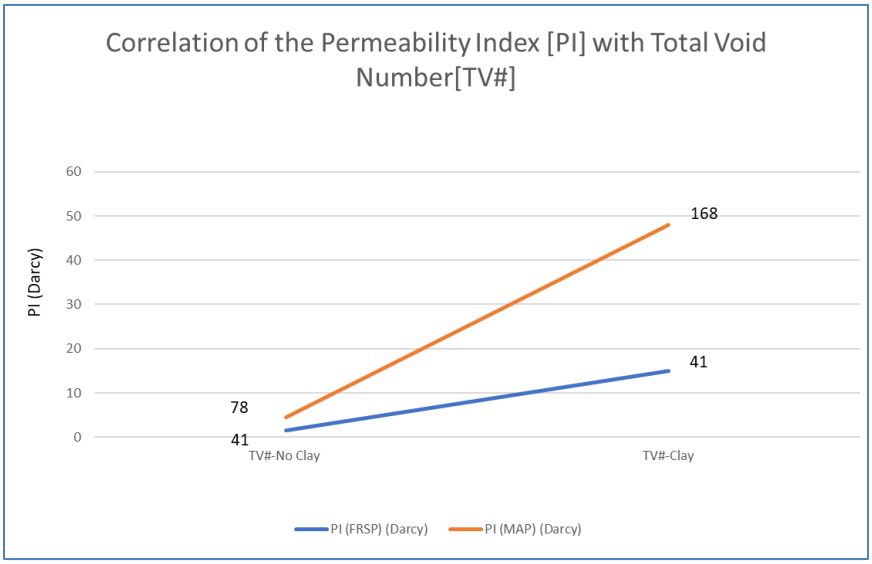

Figure 30. The Correlation of Total Void Number (TV#) with the Observed Permeability Index PAA SAPs Synthesized via FRSP and MAP, with and without Clay in the Monomer Solution. Note: FRSP reaction conditions: T=10C, [AA]=31% and [H2O2]=

[ASA]=[APS]=150 ppm; MAP reaction conditions: T=10C, [AA]=31% and [APS]=5 ppm.

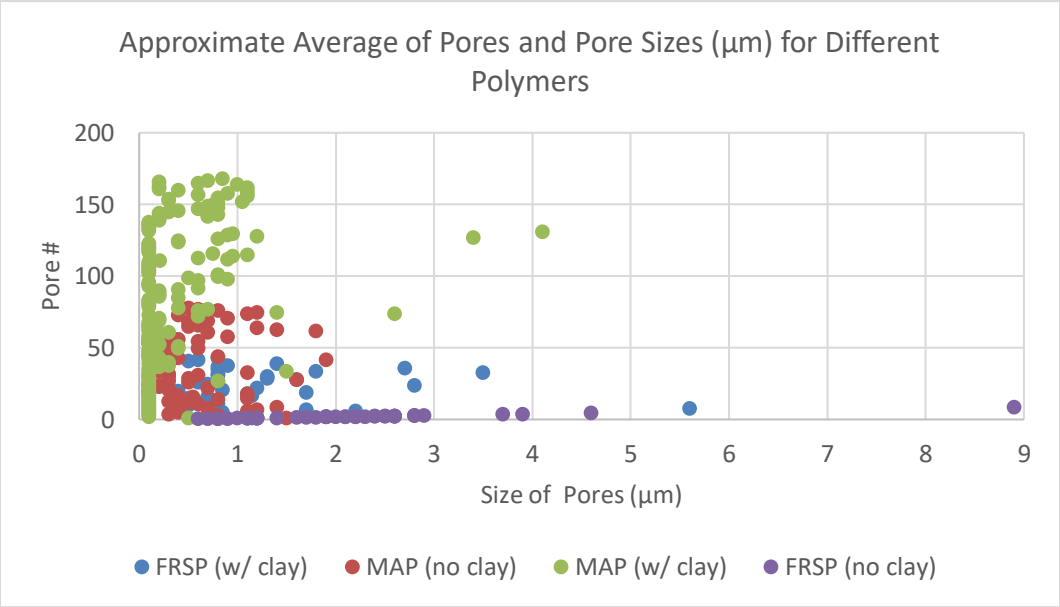

Figure 31. Numbers and Sizes of the Pores with and without Clay in Polymers with Free Radical Solution Polymerization and Microwave-Assisted Polymerization. Note: FRSP reaction conditions: T=10C, [AA]=31% and [H2O2]=[ASA]=[APS]=150 ppm; MAP reaction conditions: T=10C, [AA]=31% and [APS]=5 ppm.

Table 9. Surface Area and Numbers and Sizes of the Pores with and without Clay in Polymers with Free Radical Solution Polymerization and Microwave-Assisted Polymerization. Note: FRSP Reaction Conditions: T=10C, [AA]=31% and [H_2O_2]=[AsA]=[APS]=150 ppm; MAP Reaction Conditions: T=10C, [AA]=31% and [APS]=5 ppm.

					Surface Area= $4*\pi*r^2$			
Pore #	**FRSP (no clay) µm**	**FRSP (w/ clay) µm**	**MAP (no clay) µm**	**MAP (w/ clay) µm**	**FRSP (no clay) (μm^2)**	**FRSP (w/clay) (μm^2)**	**MAP (no clay) (μm^2)**	**MAP (w/clay) (μm^2)**
Ave.	2.1	1.15	0.58	0.4	19.52	7.07	1.62	1.29
STDEV	1.37	0.98	0.42	0.52	37.72	15.95	2.31	5.24
Sum	92.0	50.5	45.5	62.1	858.9	311.3	126.6	216.3

Table 10. Volumes and Numbers and Sizes of the Pores with and without Clay in Polymers with Free Radical Solution Polymerization and Microwave-Assisted Polymerization

						Volume= $4/3*\pi*r^3$		
Pore #	**FRSP (no clay) µm**	**FRSP (w/clay) µm**	**MAP (no clay) µm**	**MAP (w/clay) µm**	**FRSP (no clay) (μm^3)**	**FRSP (w/ clay) (μm^3)**	**MAP (no clay) (μm^3)**	**MAP (w/ clay) (μm^3)**
Ave.	2.1	1.15	0.58	0.4	14.7	3.74E+00	3.12E-01	4.85E-01
STDEV	1.37	0.98	0.42	0.52	55.49	1.42E+01	6.48E-01	3.27E+00
Sum	92.0	50.5	45.5	62.1	645.4	1.64E+02	2.43E+01	8.15E+01

The average surface area to average volume ratios (SA/V) is calculated and summarized in TABLE 11. For FRSP, SA/V ratio increased to 1.89 for the clay containing samples. The ratio was 1.33 for the control. For the MAP, the ratio for the control was 5.23, but it decreased to 2.63 for the clay containing samples. It is interesting

that the ratio increases as clay is introduced to the polymer in FRSP, but it decreases in the case of the MAP. So, the improved properties of the polymers in the MAP is not necessarily related to the surface area.

Table 11. The Ratio of Surface Area to Volume with and without Clay in Polymers with Free Radical Solution Polymerization and Microwave-Assisted Polymerization. Note: FRSP Reaction Conditions: T=10C, [AA]=31% and [H_2O_2]=[AsA]=[APS]=150 ppm; MAP Reaction Conditions: T=10C, [AA]=31% and [APS]=5 ppm.

	FRSP (No Clay)	FRSP (w/Clay)	MAP (No Clay)	MAP (w/Clay)
(Ave. Surface Area / Ave. Volume) Ratio (SA / V)	1.33	1.89	5.23	2.63

Could the improved properties of the polymer in the MAP be due to the increased surface area of the polymer? The surface area of the voids in the polymer calculated based on the assumption that the particles are spherical. These results are summarized in Table 12. The total surface area of the voids in the control sample made with FRSP was 858.88 ± 6.27 μm^2, and its total volume was 645.36 ± 4.58 μm^3. The surface area and volume of the voids decreased to 311.28 ± 8.64 μm^2 and 164.46 ± 5.99 μm^3 respectively, for the samples with clay in the polymers. For the control produced with the MAP, the total surface area was 126.64 ± 3.07 μm^2, while the total volume was 24.31 ± 1.78 μm^3. These number increased to 216.29 ± 2.81 μm^2 and 81.54 ±1.17 μm^3 for the surface area and volume, respectively, with clay in the polymer samples.

Table 12. Total Volume and Surface Area of Pores with and without Clay in Polymers with Free Radical Solution Polymerization and Microwave-Assisted Polymerization. Note: FRSP Reaction Conditions: T=10C, [AA]=31% and [H_2O_2] = [AsA] = [APS] = 150 ppm; MAP Reaction Conditions: T=10C, [AA]=31% and [APS]=5 ppm.

			Surface area (μm^2)	Volume (μm^3)	SA_{Total}	V_{Total}
Samples	Diameter (μm)	#of Pores	$4*\pi*r^2$	$4/3*\pi*r^3$		
FRSP-Control	2.09	44	19.52	14.67	858.88	645.36
FSRP-W/Clay	1.15	44	7.07	3.74	311.28	164.46
MAP-Control	0.58	78	1.62	0.31	126.64	24.31
MAP-Clay	0.37	168	1.29	0.49	216.29	81.54

Percolation Theory

Despite the increase in the number of pores in the polymers with microwave-assisted polymerization, the surface areas are much smaller than the polymers produced with FRSP. So, the increased surface area cannot be the reason for improved properties. Hence, the initial hypothesis cannot be correct. But the observed behavior could be explained by percolation theory. David Austin in his article, “Percolation: Slipping through the Crack,” [9] writes that Geoffrey Grimmett begins his book, Percolation, with the question: "Suppose we immerse a large porous stone in a bucket of water. What is the probability that the center of the stone is wetted?"[10] In the case of superabsorbent polymer with clay, the proximity of the channels and voids facilitate the movement of liquid in the polymer network. On the other hand, voids and channels for the polymers without clay are further apart, and liquid movement is restricted.

Dr. Kim Christensen describes the percolation as a theory that "deals with the numbers and properties of the clusters formed when sites are occupied with probability p."[11] In Figure 32. There are 4 clusters; one with size 8, one with size 5, and 2 with size one. The percolation channels in red and green clusters facilitate liquid movement between the pores due to their proximity to each other. The clusters in blue have no connectivity and liquid cannot flow in that part of the lattice. In Figure 33, there are 7 clusters with size one with no connectivity between the pores, and therefore, the liquid will not flow between the pores. The lattice in Figure 32 represents a polymer with permeability. There are no empty spaces in clusters represented in red and green, so the liquid is free to move from one region to another. But the lattice in Fig. 33 represent a polymer without permeability. There are empty spaces between blue squares and liquid has no chance of penetrating these empty spaces.

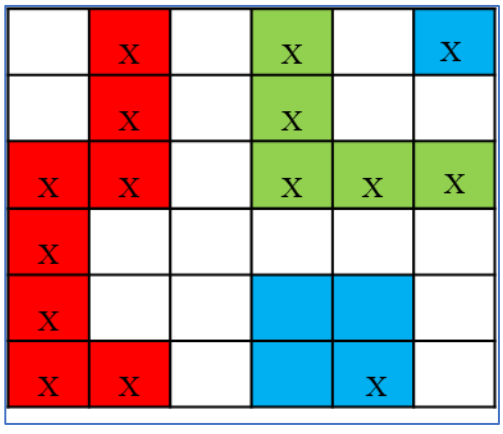

Figure 32. Percolation Channel in a Linear 2d Square Lattice of Size L = 6.

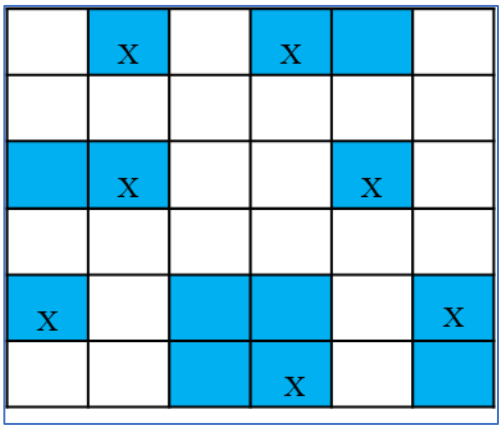

Figure 33. Percolation Blockage in a Linear 2d Square Lattice of Size L = 6.

So, our new hypothesis is that when the number of pores increases, they create channels by decreasing the distances between voids, which increases the probability of liquid penetrating through the polymer network. Improved polymer properties could be a direct result of this phenomena.

Conclusion

The average surface area to average volume ratio is larger in the polymers produced with MAP than those produced with FRSP, since the surface areas are larger for the polymers produced with FRSP, i.e., 19.52 vs 1.62 μm^2 for the controls and 7.07 vs 1.29 μm^2 for the clay containing samples, as is the volume, i.e., 14.67 vs 0.31 μm^3 for the control samples and 3.74 vs 0.49 μm^3. The ratio differences in the polymer samples with two different polymerization techniques, opens up a new set of questions, which need to be studied. Is it possible to resolve the lack of homogeneity which exists for the clay in free radical solution polymerization? Will the uniform distribution of the clay in the FRSP be enough to bridge the gap in properties between FRSP and MAP? Will another polymerization technique, such as UV polymerization, which has a short reaction time, produce a polymer that matches the properties of those produced with MAP? These questions will be addressed in a future study.

PAA SAP permeability tends to correlate well with the increasing number of voids created by introducing clay into the reaction mixture. This correlation is more pronounced in the case of MAP synthesis, as the clay appears to remain uniformly suspended in the mixture during synthesis. However, the results tend to be more variable

in the FRSP process, as the clay tends to settle out of solution over the longer reaction times for FRSP versus MAP syntheses. In general, percolation theory may provide an appropriate theoretical framework for understanding how additive void creation improves permeability through the PAA SAP systems.

References

1. Cook, J. P.; Goodall, G. W.; Khutoryanskaya, O. V.; Khutoryanskiy, V. V. *Macromol. Rapid Commun.* **2012**, *33*, *322*.
2. Buchholz, F. L.; Peppas, N. A. Modern Superabsorbent Polymers Science and Technology; ACS Symposium Series 573; American Chemical Society; Washington, DC, 1991; p *3-112.*
3. Azad, M. M.; Sandros, M. G. *J. Appl. Polym. Sci.* 2016, *133*, *43325.*
4. European Disposables and Nonwovens Association. Test Method No. 441.2-02 "Centrifuge Retention Capacity".
5. European Disposables and Nonwovens Association. Test Method No. 442.2-02 "Absorption Under Pressure".
6. European Disposables and Nonwovens Association. Test Method No. 470.2-02 "Extractable".
7. European Disposables and Nonwovens Association. Test Method No. 410.2-02 "Residual Monomers".
8. Losch, D.; Seidel, V.; Weismantel, M. US Patent 0256757 A1, 2005.
9. www.ams.org/publicoutreach/feature-column/fcarc-percolation.
10. Grimmett, G.; Percolation, Second Edition. Springer. 1999
11. Christensen, K.; Percolation Theory, Imperial College London. 2002

Graphical Abstract

MICROSCOPIC STUDIES OF THE IMPACT OF CLAY ON VOIDS AND PERMEABILITY IN SUPERABSORBENT POLYMERS

Michael M. Azad[1], Jianjun Wei[1], and Daniel J. C. Herr[1]
[1]Department of Nanoscience, University of North Carolina at Greensboro, 2907 East Gate City Boulevard, Greensboro, North Carolina 27401
Correspondence to: D. J. C. Herr (E- mail: djherr@uncg.edu)

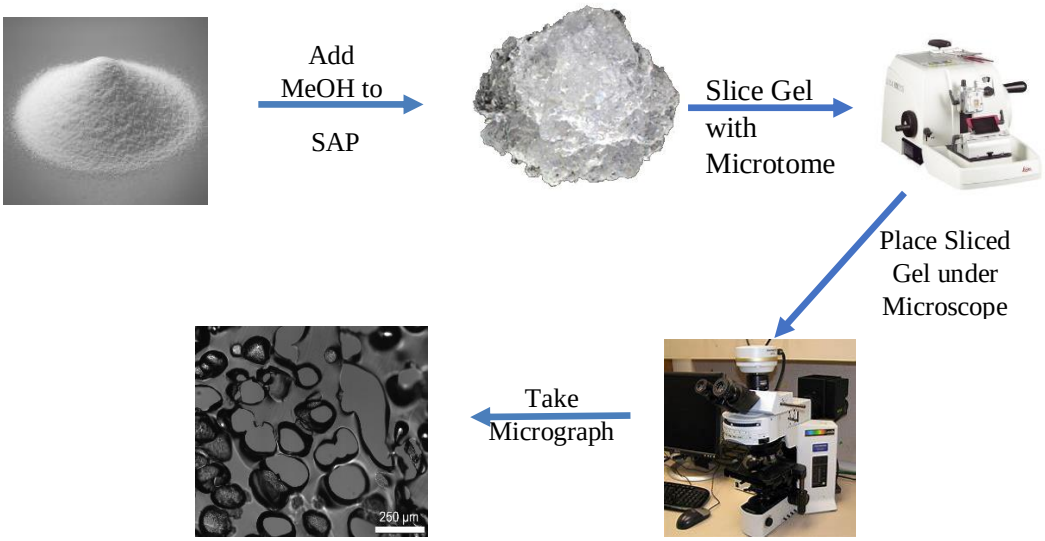

Schematic 5. A Schematic Representation of the Hydration of the Polymer and Studying the Pores Under Microscope

CHAPTER V

KINETIC STUDY OF SUPERABSORBENT POLYMERS

Michael M. Azad[1] and Daniel J. C. Herr[1]
[1]Department of Nanoscience, University of North Carolina at Greensboro, 2907 East Gate City Boulevard, Greensboro, North Carolina 27401
Correspondence to: D. J. C. Herr (E- mail: djherr@uncg.edu)

Abstract

This section studies and compares the formation kinetics of two approaches to synthesizing crosslinked polyacrylic acid (x-PAA) superabsorbent polymers (SAP). Specifically, it tests the applicability of the reported general rate expression for free radical solution polymerization to the synthesis of x-PAA SAPs via Microwave-Assisted Polymerization (MAP) and Free Radical Solution Polymerization (FRSP). This study of FRSP and MAP formation kinetics of x-PAA superabsorbent materials provides predictive models and new foundational insights into the rate-limiting steps for these three-dimensional polymerization reactions. These foundational models, based on the observed results from these designed kinetic studies, may help to guide and enable the design of new networked polymers with enhanced functional properties.

The published complex mechanism of PAA polymerization, which was assumed to explain the kinetics of superabsorbent polymerization, does not seem to be valid in FRSP

and MAP synthesis of PAA SAPs. In fact, for these kinetic studies, the data supported none of the initial hypotheses for all the data in a given reaction. For the FRSP, only a sequential kinetic model, i.e., zero-order followed by the first order in monomer model explains the observed data. For the MAP PAA SAP syntheses, several sequential kinetic models may explain the observed data. A first-order model supports the first-half-reaction, and a zero-order model explains the second-half-reaction. So overall, the key findings show that one cannot conclude with 99% confidence (2σ) the existence of a single zero or first-order kinetic process over the entire reaction for each type polymerization, i.e., MAP or FRSP. However, there are regions of sequential zero-order and/or first-order kinetics that explain the dominant mechanistic modes for both types of polymerizations.

Background

This section represents the third-part series of studies on polyacrylic acid (PAA) based superabsorbent polymers (SAPs). The first section described SAP via microwave-assisted polymerization (MAP) and compares this method via free radical solution polymerization (FRSP) approach traditionally used in manufacturing these materials.[1] The second section examines the impact of additives, such as clay, on permeability, for MAP and FRSP synthesized SAPs.[2] This final section focuses on the kinetics of SAPs formed via MAP or FRSP. It also provides insight into why clay additives enhance SAP permeability.

Dimer of Acrylic Acid

Acrylic acid was the monomer of choice in these studies. Since acrylic acid tends to self-polymerize, it is stabilized by the addition of MEHQ (mono methylether of hydroquinone) and oxygen to prevent polymerization during transport and storage. Despite all of these, there is a certain amount of dimer in the monomer. [3] Acrylic Acid forms a dimer by Michael addition and the reaction dependent on time, temperature and water content.[4,5] "The Michael reaction or Michael addition is the nucleophilic addition of a carbanion or another nucleophile to an α,β-unsaturated carbonyl compound."[6]

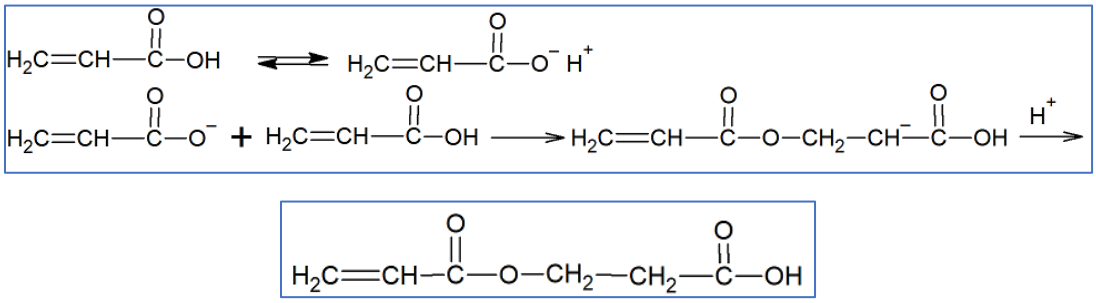

Schematic 6. A Schematic Representation of Dimer Formation by Michael Addition.

Or it could be written as:

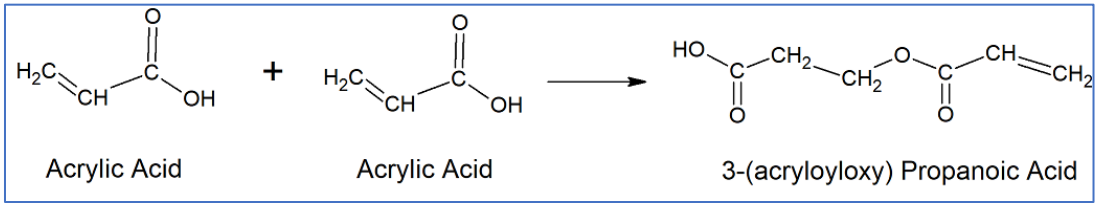

Schematic 7. A Schematic Representation of Dimer Formation by Michael Addition.

The dimer could be incorporated in the polymer chain, but it also could be thermally degraded by a reverse Michael reaction to regenerate acrylic acid. The dimer under basic conditions and high temperature could be cleaved, yielding an acrylic acid and β-hydroxypropionic acid.

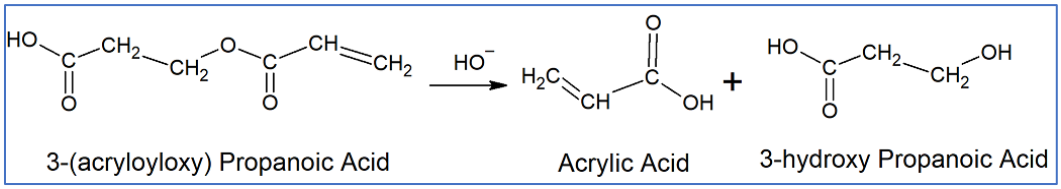

Schematic 8. A Schematic Representation Cleavage of Dimer Formation.

Polymerization of Acrylic Acid

Polymerization of acrylic acid with free radical solution polymerization follows the following schematic 9 (redrawn from a description by F. L. Buchholz).

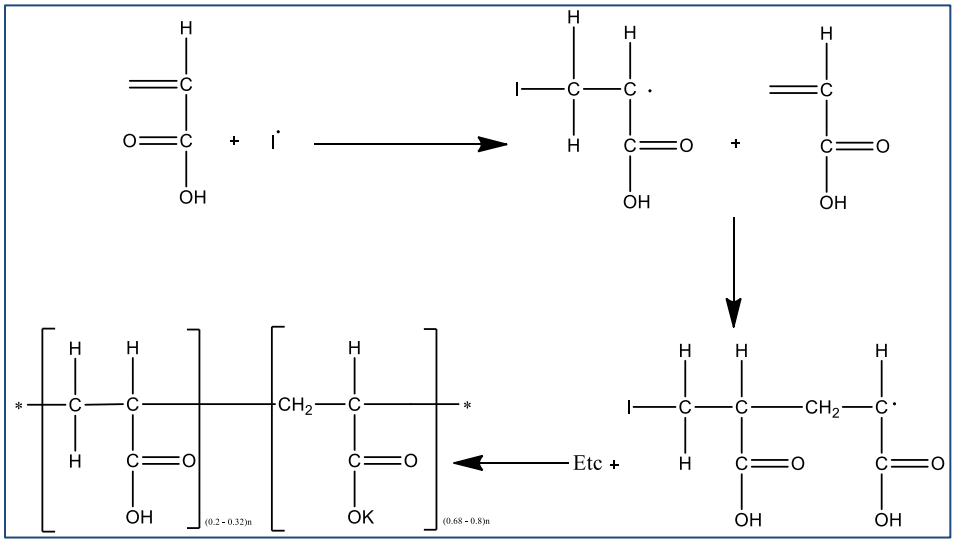

Schematic 9. Schematic Representation of the Polymerization of Acrylic Acid.

In this reaction, acrylic acid adds to an existing PAA chain via free radical addition.

Crosslinker

For use as a SAP, the PAA is partially ionized to form sodium polyacrylate, which is highly water-soluble. Consequently, a small amount of crosslinker, i.e., 0.1 – 0.5% based on acrylic acid, is added to the monomer solution to form a very lightly cross-linked PAA gel network, which exhibits low solubility in water. The crosslinker is a co-monomer with higher functionality, i.e., two or more double bonds, and its attachment to the polymer network is depicted in Scheme 10, below. Specifically, cross-linking in the polymerization stage forms a "network in which a cross-linking agent is a co-monomer with a higher functionality than the main monomer (reproduced from a description by F. L. Buchholz)."[7]

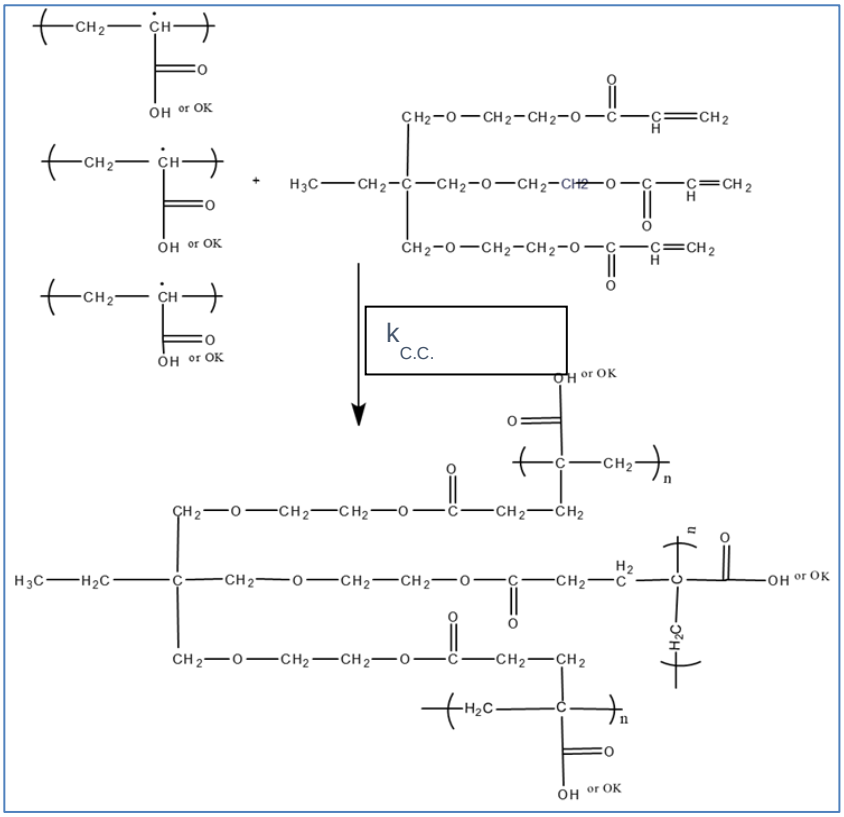

Schematic 10. Schematic Representation of the Crosslinking of Acrylic Acid

The reactivity ratio of the crosslinker versus the monomer determines "the distribution of the crosslinks in the network. If the reactivity ratio of the crosslinker is higher than that of the monomer, it will react at low monomer conversion. On the other hand, if the reactivity ratio of the crosslinker is lower than that of the monomer, it will react at a high monomer conversion."[8] Ethoxylate trimethylolpropane triacrylate (ETMPTA) has higher functionality, but its reactivity ratio is lower than the reactivity ratio for the acrylic acid.

Molecular Weight of Polymer

The resulting polymers have specific molecular weight distribution and molecular weight. The quality of the polymer is the direct result of these phenomena and the polymers with different molecular weight distributions, but identical molecular weight could have different properties. “Although crosslinked superabsorbent polymers are networks of essentially infinite molecular weight and are, therefore, impossible to analyze directly by chromatography.”[9] The only way of analyzing the molecular weight is through indirect methods which are not accurate. People have tried to get the molecular weight by “hydrolysis under heat and high pH.”[8] The heat and pH could break the ester bonds (only on those crosslinkers which form ester bonds) formed during the crosslinking stage. The reported results ranged from 5,000,000 to over 10,000,000 g/mol. This is not a reliable method and could not be used to determine the molecular weight of the polymer.

General Model for Free Radical Polymerization Kinetics for PAA Polymerization

Our first assumption is that SAP synthesis is dominated by traditional PAA polymerization kinetics. For this study, we initially assume that the cross-linking reaction has little impact on the overall rate of SAP synthesis, as the cross-linker concentration is 2-3 orders of magnitude less than that of the acrylic acid monomer.

The following scheme and rate expressions summarize the traditional understanding of free radical polymerization kinetics, such as for PAA, reported in the literature:[10, 11, 12]

Complex Order Kinetic of Acrylic Acid

1) Decomposition Step:

$$I_2 \xrightarrow{k_d} 2\,R^{\bullet} \quad (\text{e.g., } H_2O_2 \xrightarrow{k_d} 2HO^{\bullet}) \qquad 1.00$$

[Assumption: Equation 2.1 is the rate limiting step, i.e., the slow step.]

I = Initiator, M = Monomer Solution, $R^{\bullet}$ = Free Radical

k_i = Initiation Constant, k_d = Disassociation Constant, k_p = Propagation Constant

k_{tc} = Termination Through Combination, k_{dc} = Termination Through Disproportionation

$$\text{Addition: } R^{\bullet} + M \xrightarrow{k_i} M_1^{\bullet} \text{ (Fast Step)} \qquad 1.01$$

$$r_d = -2d[I] / dt \text{ and } r_i = d[M_i] / dt \qquad 1.02$$

Since $k_i >> k_d$. We only have to consider k_d.

$$-d[I] / dt = \tfrac{1}{2} [d\,M_i] / dt = k_d[I] \qquad 1.03$$

But, only a fraction (f) of radicals initiate chain growth

$$r_i = d[M_1^{\bullet}] /dt = 2fKd[I] \qquad 1.04$$

2) Propagation step: [Assumption: Reactivity is independent of chain length]

$$M_1^{\bullet} + M \xrightarrow{k_p} M_2^{\bullet} \qquad 1.05$$

$$M_2^{\bullet} + M \xrightarrow{k_p} M_3^{\bullet} \qquad 1.06$$

In general,

$$M_x^{\bullet} + M \xrightarrow{k_p} M_{x+1}^{\bullet} \qquad 1.07$$

And,

$$r_p = - d[M] / dt = kp[M][M^{\bullet}] \qquad 1.08$$

3) Termination Step:

There are two types of terminations:

1) Combination:

$$M_x^{\bullet} + M_y^{\bullet} \xrightarrow{k_{tc}} M_{x+y} \qquad 1.09$$

$$R_{tc} = - d[M^{\bullet}] / dt = k_{tc}[M^{\bullet}] \qquad 1.10$$

2) Disproportionation:

$$M_x^{\bullet} + M_y^{\bullet} \xrightarrow{k_{td}} M_{x+y} \qquad 1.11$$

$$R_{td} = - d[M^{\bullet}] / dt = k_{td}[M^{\bullet}] \qquad 1.12$$

Overall, the termination rate constant will be:

$$k_t = k_{tc} + k_{td} \qquad 1.13$$

$$r_t = - d[M^{\bullet}] / dt = k_{tc} + k_{td} \qquad 1.14$$

If one assumes that $[M^{\bullet}]$ is an unknown transient in a steady state concentration, i. e., that radicals are consumed at the same rate as they are generated, or $r_i = r_t$, then

$$2 f k_d [I] = 2 k_t [M^{\bullet}] [M^{\bullet}] \qquad 1.15$$

$$[M^{\bullet}] = [f k_d [I] / k_t]^{1/2} \qquad 1.16$$

Since the rate of propagation = Rate of polymerization, i. e.,

$$r_p = R_p, \qquad 1.17$$

Then plug 1.16 into 1.08

$$r_p = k_p \{[f k_d [I]] / k_t\}^{1/2} [M] \qquad 1.18$$

But [I] is not constant and from equation 1.03, $- d[I] / dt = k_d [I]$

Take log of both side and then solve for [I]

$$[I] = [I_0] e^{- k_d t} \qquad 1.19$$

$$r_p = \{k_p [f k_d / k_t]^{1/2} [M][I_0]^{1/2}\} \{e^{- k_d t / 2}\} \qquad 1.20$$

If our initial assumption is valid, then the traditionally published rate expression for PAA polymerization, i.e., equation 1.20, should be sufficient to describe the rate of formation of PAA superabsorbent polymers. Based on this published rate law, the rate of SAP polymerization should vary linearly with the time-dependent monomer

concentration, [M], and the square root of the initial initiator concentration, $[I_0]^{1/2}$. Please note that, in its published form, this complex rate expression exhibits an exponential dependence on the reaction time, t.

Other Potential Types of Kinetic Regimes

Diffusion Controlled Vs. Activation Controlled Chemical Reactions

This section provides a foundation for considering other options for explaining the kinetics of PAA superabsorbent polymer synthesis, i.e., diffusion vs. activation energy-controlled reactions. For example, consider a reaction that involves two reactants, A and B. Under certain conditions, A and B react directly, in a bimolecular fashion, to form a product, P, as shown below.[13-14]

$$A + B \xrightarrow{k_1} P \qquad 2.00$$

The rate, r_1, of this activation energy controlled bimolecular reaction may be expressed as follows:

$$r_1 = k_1[A][B] \qquad 2.01$$

However, suppose this reaction proceeds via an intermediate, AB, as shown below:

$$A + B \underset{k_{d'}}{\overset{k_d}{\rightleftharpoons}} AB \qquad 2.02$$

$$AB \xrightarrow{k_\alpha} P \qquad 2.03$$

In this example, reactants A and B may first diffuse together to form the intermediate, AB, which then goes on to form the product, P. For PAA synthesis, there may be some initial weak interaction between the PAA monomer, A, and the growing polymeric chain, B, which form intermediate AB that reacts to yield P, the next iteration in the polymerization.

One explanation for the interaction between A and B could be that A and B are surrounded by a solvent that, in turn, creates a single solvation sphere around A and B, as shown in equation 2.04. Since reaction is happening in a salvation sphere, there is no activation energy.

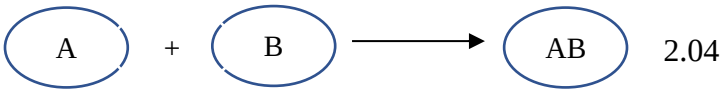

2.04

The next step will be writing the rate late for reaction 2.03.

$$r = K_{\alpha} [AB] \qquad 2.05$$

But this is not an easily quantifiable rate law, since [AB] is an intermediate product, and one has to calculate that. To calculate [AB], one assumes that intermediate [AB] reaches a “steady state” approximation. The “steady state” approximation assumes that for some induction period, the concentration of [AB] does not change.

$$d[AB] / dt = 0 \qquad 2.06$$

This means that the rate formation of [AB] is equal to the rate of its removal from the reaction mixture.

$$k_d[A][B] = k_\alpha[AB] + k_{d'}[AB] \qquad 2.07$$

$k_\alpha[AB]$ is the rate of the forming [AB] and $k_d[A][B]$ is rate the of the removing [AB].

From equation 1.07, [AB], the concentration of intermediate, could be calculated as shown in 2.08.

$$[AB] = (k_d[A][B]) / (k_\alpha + k_{d'}) \qquad 2.08$$

Inserting equation 2.08 in equation 2.05 yields the rate equation.

$$R = (k_\alpha\, k_d[A][B]) / (k_\alpha + k_{d'}) \qquad 2.09$$

One can set two types of limits to equation 2.09.

1) $k_\alpha >> k_{d'}$ Equation 2.09 could be re-written as:

$$R = (k_\alpha\, k_d[A][B]) / k_\alpha \qquad 2.10$$

$$R = k_\alpha\, [A][B] \qquad 2.11$$

Equation 2.11 is a diffusion-controlled reaction, and it is controlled by the diffusion of A and B through the solvent, and the properties of the solvent will control this type of process.[13-14]

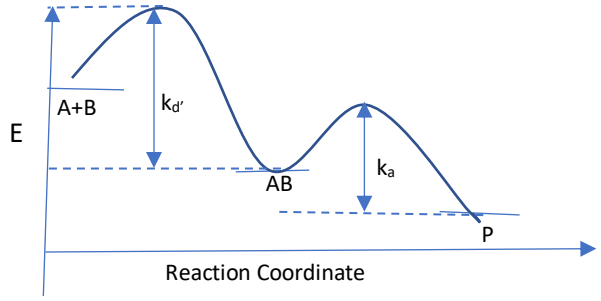

Schematic 11. A Schematic Representation of Diffusion-Controlled Reaction.

2) $k_\alpha << k_{d'}$ Equation 1.08 could be re-written as:

$$R = (k_\alpha k_d[A][B]) / k_{d'} \qquad 2.12$$

Equation 2.12 is a second-order activation-controlled reaction.[13]

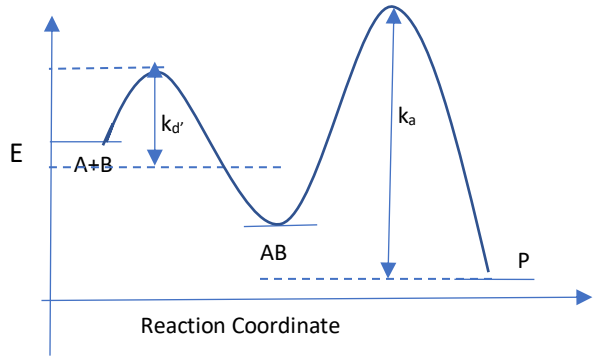

Schematic 12. A Schematic Representation of Activation-Controlled Reaction.

Experimental Design (DOE) and Response Surface Methodology (RSM)

Experimental designs and response surface methodologies can serve as useful tools for modeling and visualizing the properties of a system, as functions of key input factors. We used standard experimental design and response surface techniques, to efficiently probe the SAP experimental parameter and property space.

Experimental Design

Typically, experimental designs are used to generate empirical models and assume that the behavior of a given property may be approximated by a Taylor series. Usually second-order suffices, and fit the data as one would apply a French curve to interpolate between data. For example, consider the three-factor parameter space, as shown in figure 34.

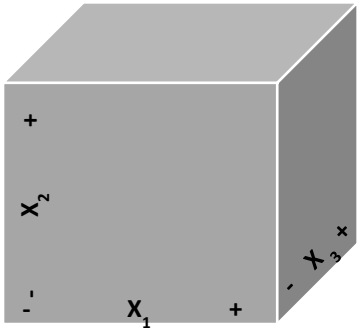

Figure 34. A Three-Factor Parameter Space, with Factors X_1, X_2 and X_3.

Experimental design studies typically follow a hierarchical approach to building a knowledge base, beginning with a screening study. For the three-factor parameter space, shown above, a screening study represents an efficient way to assess which factors are most significant. For this example, each factor is assigned two levels, i.e., -1 (low) and +1 (high). The 2^3 experimental design, i.e., 2-levels for all 3-factors, shown in Table 13 1 below, provides a set of 8 trials that would suffice to estimate a first-order Taylor series model of the Response, R, including interaction terms, shown in equation 1.1 below.

Table 13. A Typical 2^3 Factorial Design with Five Replicates

Trial	X_1 Level	X_2 Level	X_3 Level	Response, R
1	-1	-1	-1	R1
2	-1	-1	+1	R2
3	-1	+1	-1	R3
4	-1	+1	+1	R4
5	+1	-1	-1	R5
6	+1	-1	+1	R6
7	+1	+1	-1	R7
8	+1	+1	+1	R8
1	-1	-1	-1	R1
3	-1	+1	-1	R3
5	+1	-1	-1	R5
6	+1	-1	+1	R6
8	+1	+1	+1	R8

$$\text{Response} = a_0 + a_1X_1 + a_2X_2 + a_3X_3 + a_4X_1{*}X_2 + a_5X_1{*}X_3 + a_6X_2{*}X_3 + a_7X_1X_2X_3$$

Equation (1.1)

Each experimental design should include a number of replicate trials, which enables an estimation of replication error and helps to identify significant model parameters. In fact, increasing the number of replicates can help to increase the model's resolving power. For higher order designs and models, a comparison between the replication error and the lack of fit between the model and the data helps to assess the model's predictive value. Well conceived experimental designs offer an efficient

framework for probing and for testing hypotheses in multifactor experimental spaces. In some cases, these models can provide insight into the kinetic behavior of chemical reactions over significant domains of reaction concentrations, times, temperatures, etc.

Response Surfaces

A response surface graphically displays how selected properties change as a function of experimental factors. For example, the response surface, shown below, conveys how a reaction yield may vary as a function of three reaction factors, X_1, X_2, and X_3, where X3 represents an off-axis variable. These factors may correspond to reactant concentrations, reaction time, reaction temperature, etc.

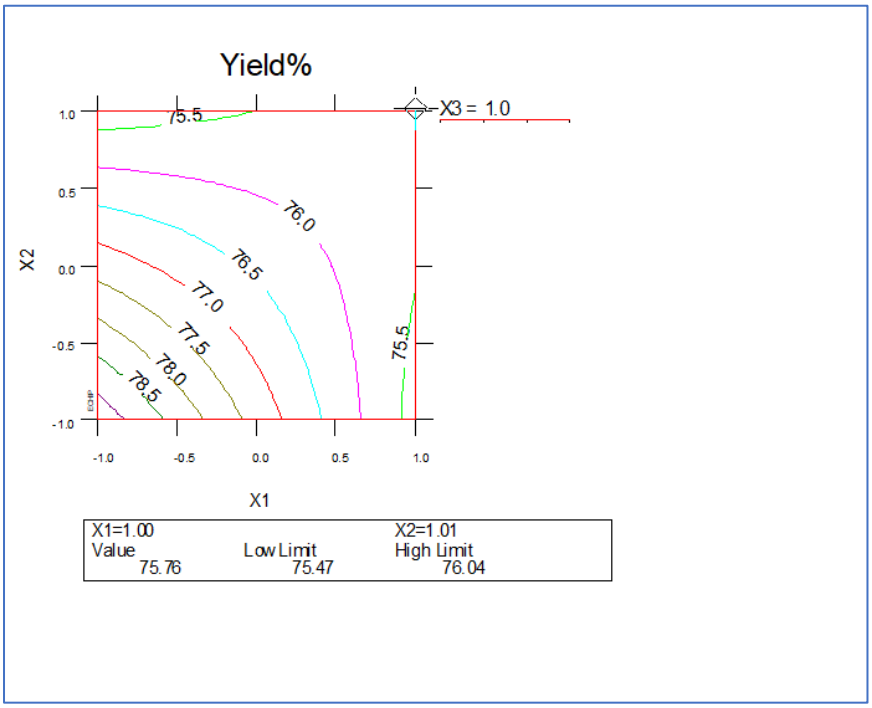

Figure 35. An Example of a Response Surface for the Percent Yield of a Reaction, as a Function of Three Reaction Factors, X_1, X_2, and X_3.

> It provides a topographical map of an empirical polynomial model and generates an approximation of the response's behavior over a factor region. Response surfaces help to visually identify interesting or optimal factor settings, with which one can maximize, minimize, or stabilize the responses of interest. [www.statease.com/webinar.html]

Reproducibility, Significance, and Model Testing

The following information describes the significance thresholds used in this study.[15-22]

Empirical Model Testing

The replicate standard deviation provides a metric for assessing the reproducibility and significance of a given experiment. For most empirical models, a $p < 0.05$ implies that the proposed model sufficiently fits the experimental data and/or that a given factor has a significant effect on the observed response. It is not necessarily crucial for an empirical model to fit well in the experimental design. However, an empirical model whose lack of fit is comparable to the replication error has a significant predictive capability within the probed experimental space. The correlation coefficient, R^2, is another metric that helps to assess the 'goodness-of-fit,' and is used to determine how well distributed the data points are around the fitted regression line.

> For the same data set, higher R^2 values represent smaller differences between the observed data and the fitted values. When a regression model accounts for more of the variance, the data points are closer to the regression line. Linear regression identifies the equation that produces the smallest difference between all of the observed values and their fitted values. To be precise, linear regression finds the smallest sum of squared residuals that is possible for the dataset. [http://statisticsbyjim.com/regression/interpret-r-squared-regression/]

Kinetic Model Testing

R^2 thresholds testing models may vary for different scenarios. For example, when testing for toxicity or pharmaceutical efficacy in living systems an R^2 threshold of 0.85 may suffice. However, when testing mechanistic hypotheses involving homogeneous chemical reaction kinetics, with sufficient experimental resolving power, one expects an R^2 threshold of ≥ 0.999, which would account for at least 97% of the observed standard deviation. [Reference: https://people.duke.edu/~rnau/rsquared.htm] For the purposes of this study, only kinetic models that satisfy an R^2 threshold of ≥ 0.999 will be considered as valid candidate kinetic models for explaining the observed data. The reproducibility and significance of a given experiment could be assessed by the standard deviation of the replica. Additionally, when considering two candidate models, we will assert an Occam's razor approach for selecting the best model. Specifically, if two models explain the data, preference will be given to the simpler model, i.e., the one with the fewest factors or assumption.

Hypotheses

Hypothesis 1: The published linearized integrated rate expression, equation 1.20, which proposes complex kinetics for PAA synthesis and assumes slow initiator decomposition, also explains the behavior of PAA SAP polymerization kinetics.
The following derivation is our linearized version of the published rate expression that can be used to test the validity of Hypothesis I for explaining PAA SAP polymerization kinetics.

Assumptions:

1) This published model for PAA polymerization assumes that initiator decomposition is the rate determining step, i.e., $I2 \xrightarrow{k_d} 2I^{\bullet}$ is slow.

2) The variable f is an unknown fraction of radicals that initiate chain growth.

Starting with equation 1.20:

$$r_p = \{k_p [f\, k_d / k_t]^{1/2} [M][I_0]^{1/2}\} \{e^{-k_d t/2}\} \qquad 1.20$$

Since $k_p [f\, k_d / k_t]^{1/2}$ and $^{-k_d 1/2}$ are constant in equation 1.20, then let

$$\alpha = k_p [f\, k_d / k_t]^{1/2} \qquad 3.00$$

$$\beta = (-k_d 1 / 2) \qquad 3.01$$

Substituting α and β into equation 1.20 yields

$$r_p = \alpha[M][I_0]^{1/2} * e^{\beta t} \qquad 3.02$$

From equations 3.02 and 1.08, replace r_p with d[M] / dt

$$d[M] / dt = \alpha[M][I_0]^{1/2} * e^{\beta t} \qquad 3.03$$

Where $[M_t]$ = The acrylic acid concentration at the time, t.

Rearranging yields 3.4.

$$d[M] / [M]_t = \alpha [I_0]^{1/2} * e^{\beta t} dt \qquad 3.04$$

For a given set of reactions, the initial initiator concentration, $[I_0]$, is constant.

Let,

$$\rho = \alpha[I_0]^{1/2} \qquad 3.05$$

$$d[M] / [M] = \rho\, e^{\beta t} dt \qquad 3.06$$

$$\int_{[M]_0}^{[M]_t} d[M] / [M] = \rho \int_{t_0}^{t_t} e^{\beta t} dt \qquad 3.07$$

Since

$$\int_{t_t}^{t_0} dx / x = \ln x_t - \ln x_0 \qquad 3.08$$

And

$$\int_{t_t}^{t_0} e^{\alpha x} dx / x = 1/\alpha\, e^{\alpha x}, \text{ then} \qquad 3.09$$

$$\ln [M]_t - \ln [M]_0 = \rho / \beta\, (e^{\beta}) \qquad 3.10$$

Rearranging yields,

$$\ln [M]_t = = \rho / \beta\, (e^{\beta}) + \ln [M]_0 \qquad 3.11$$

Substituting equations 2.23, 2.24 into 2.28, such that

$$\rho / \beta = - k_p [f\, k_d / k_t]^{1/2} [I_0]^{1/2} / -k_d / 2 \qquad 3.12$$

Rearranging equation 3.12 yields

$$\rho / \beta = 2kp\ [(f[I_0]) / (k_t\, k_d)]^{1/2} \qquad 3.13$$

Let:

$$S = \rho / \beta \qquad 3.14$$

And

$$\tau = e^{\beta t} \qquad 3.15$$

Substituting 3.14 and 3.15 into 3.11 yields the following linearized integrated rate expression:

$$Ln\ [M]_t = s\ \tau + \ln\ [M]_0 \qquad 3.16$$

A plot of $\ln[M]_t$ vs. τ should yield a straight line with slope *s*. However, τ represents an exponential function, with β as an unknown constant, which must be estimated. If the published expression is correct, then equation 3.16 must be a straight line with $R^2 \geq 0.999$.

Hypothesis 1 – Prediction 1: A plot of $\ln[M]_t$ vs. τ should yield a straight line with slope *s*. However, τ represents an exponential function, with β as an unknown constant, which must be estimated. If the published complex kinetic rate expression for PAA polymerization also explains PAA SAP synthesis kinetics, then a β should exist for equation 3.16 that yields a straight line through the data with an $R^2 \geq 0.999 \pm 2\sigma$.

Hypothesis 2: The published rate expression for PAA synthesis applies to the superabsorbent polymer synthesis reaction, if one assumes that the initiator decomposition is fast.

The following derivation linearizes the rate expression when initiator decomposition is fast, relative to other processes.

Assumption 1: $I_2 \xrightarrow{k_d} 2\ I^{\bullet}$ (Fast)

Definitions:

I = Initiator 4.00

I• = Initiator radical 4.01

M = Acrylic acid monomer 4.02

I-M• = Initial initiator-acrylic acid monomer radical 4.03

M• = Propagating polyacrylic acid radical 4.04

Assumption 2:

Initiator (I) $\rightarrow$ I• [Assumption: Fast] 4.05

I• + Acrylic Acid (M) $\rightarrow$ I-M• [Assumption: Fast] 4.06

$M^{\bullet} + M \xrightarrow{k_p} M^{\bullet}$ [Assumption: Slow] 4.07

$$I_2 \xrightarrow{k_1} 2\, I^{\bullet} \qquad 4.08$$

$$r_{I2} = K_1[I_2] \qquad 4.09$$

$$I^{\bullet} + M \xrightarrow{k_2} I - M^{\bullet} = M_1^{\bullet} \qquad 4.10$$

$$r_{1M} = k_2[I^{\bullet}]\,[M] \qquad 4.11$$

$$M^{\bullet} + M \xrightarrow{k_3} M^{\bullet} \qquad 4.12$$

$$r_{mm\bullet} = k_3[M^{\bullet}]\,[M] \qquad 4.13$$

$$[M\bullet] \approx 2[I_2]_0 \qquad 4.14$$

$$r_{mm\bullet} = 2k_3[I_2]_0\,[M] \qquad 4.15$$

$$d[M] / dt = 2k_3[I_2]_0\,[M] \qquad 4.16$$

Rearranging the equation yields

$$d[M] / [M]_t = 2k_3[I_2]_0\, dt \qquad 4.17$$

$$\int_{[M]_t}^{[M]_0} d[M] / [M] = \rho \int_{t_0}^{t_t} 2K_3\,[I_2]_0 dt \qquad 4.18$$

$$Ln\,[M]_t - \ln\,[M]_0 = 2\,k_3\,[I_2]_0 t \qquad 4.19$$

$$Ln\,[M]_t = 2\,k_3\,[I_2]_0\, t - \ln\,[M]_0 \qquad 4.20$$

Hypothesis 2 – Prediction 1: If hypothesis 2 is valid and explains PAA SAP synthesis kinetics, then a plot of ln [M_t] Vs. time should yield a straight line that demonstrates first-order kinetics, with an $R^2 \geq 0.999 \pm 2\sigma$. Unlike Hypothesis 1, Hypothesis 2 assumes that the rate-limiting step is the polymerization step.

Hypothesis 2 – Prediction 2: Additionally, from equation 4.20, the slope, $2k_3[I_2]_0$, should vary linearly with the initial initiator concentration. If this prediction is valid, the one can estimate the value of k_3, since

$$k_3 = (0.5*\text{Slope}) / [I_2]_0 = \alpha \text{ constant}, k_3 \pm 2\sigma \qquad 4.21$$

Hypothesis 3: The synthesis of SAP proceeds via zero order or pseudo zero order kinetics, i.e., diffusion controlled, with respect to monomer concentration.

Hypothesis 3 – Prediction 1: A plot of [M_t] Vs. time should be linear, with an $R^2 \geq 0.999 \pm 2\sigma$, over all data points for a given trial. If the observed data supports this prediction, then this type of reaction may represent a diffusion-controlled reaction. The rate-limiting step of a full zero-order reaction is independent of activation energy.

Hypothesis 4: Percolation theory can explain why the introduction of a clay additive to SAP enhances the polymer's permeability index.

Hypothesis 4 – Prediction 1: The role of inert materials as a spacer and increased surface area can explain why the introduction of a clay additive to SAP enhances the polymer's permeability index.

Hypothesis 4 – Prediction 2: The permeability increases with the surface area or volume of the voids created by the addition of the clay particles to the SAP, if the voids are large enough to be interconnected.

Materials

Purchased chemicals included: Glacial acrylic acid from BASF, potassium hydroxide, sodium chloride, hydrogen peroxide (H_2O_2), ascorbic acid ($C_6H_8O_6$), hydrochloric acid, 85% O-phosphoric acid, high performance liquid chromatography (HPLC)-grade methanol, ultrapure water, ethylene glycol diglycidyl ether, and ammonium persulfate [$(NH_4)_2S_2O_4$] from Aldrich, Laptonite clay (Synthetic Hectorite-like clay, diameter = 25 nm and thickness = 1 nm) from Southern clay, and ethoxylated trimethylolpropane triacrylate (ETMPTA) from Sartomer. All chemicals were used as received.

Equipment

The following equipment were used for polymerization and characterization: An HPLC instrument with UV detector from Water, a Dionex IonPac AS20 column, a Nucleosil column (C8, 120 A°, 5 mm, 250 X 4.6 mm, with a mobile phase of 0.2 mL 85% O-phosphoric acid, 5.0mL of HPLC-grade methanol, and 0.9948 L of ultrapure water) for residual acrylic acid analysis, a Retsch ZM1000 for milling, a RO-TAP model RX-29 equipped with USA Standard Test Sieve for sieving, a Heraeus Instrument

Labofuge 400 for centrifuge retention capacity (CRC), a Thermoscientific Lindberg Blue M lab oven for the drying of the polymer, a stereo microscope from Olympus (model SXZ 16), a Brinkman 816 titration system for extractables, and a Microwave from CEM for polymerization.

Monomer Solution

Monomer solutions were prepared as reported in our previous work.[2]

Microwave-Assisted Polymerization

Polymerizations were performed as reported in our previous work.[2]

Free-Radical Solution Polymerization

Polymerizations were performed as reported in our previous work.[2]

Surface Crosslinking Procedure

Surface crosslinking was performed as reported in our previous work.[2]

Water Content (WC) Measurement

The test was performed as reported in our previous work.[2]

Centrifuge Retention Capacity (CRC) Measurement

The centrifuge retention capacity of the superabsorbent polymer particles is measured by the EDANA recommended test method No. 441.2-02 “Centrifuge Retention Capacity”.[23]

Absorbency Under Load (AUL) Measurement

The absorbency under load of the superabsorbent polymer particles was measured by the EDANA recommended test method No. 442.2-02 “Absorption Under Pressure”, using a weight of 0.7 psi (49 g/cm^2) instead of a weight of 0.3 psi (21 g/cm^2) 0.9 psi (63 g/cm^2) 0.6 psi (42 g/cm^2) 0.01 psi (0.7 g/cm^2).[24]

Extractables Measurement

The percent extractables of the superabsorbent polymer particles was measured by the EDANA recommended test method No. 470.2-02 “Extractable”.[25]

Residual Acrylic Acid (RAA) Measurement

The residual monomers content in the superabsorbent polymer particles was measured according to EDANA recommended test method No. 410.2-02 “Residual Monomers”.[26]

All EDANA test methods are obtainable from the European Disposables and Nonwovens Association, Avenue Eugène Plasky 157, B-1030 Brussels, Belgium.

Permeability Index (PI) [Using Gel Bed Permeability (GBP) Test Measurement]

The method for Free Swell Gel Bed Permeability is described in US patent application no. US 2005/0256757 A1, paragraphs 61 through 75.[27]

Data Section

Experimental Studies to Test Hypotheses 1 – 3

To achieve the required resolution for testing these predictions over the large experimental space, over 5000 Free Radical Solution Polymerization (FRSP) reactions and 2200 Microwave Assisted Polymerization (MAP) reactions were performed. These numbers include three replicates for each trial condition. Additional sample data set may be found in the Appendix A and B. A complete set of data is available upon request.

A full factorial design was used to the experiments. To gather synthesis information on the entire synthetic space, there were 3024 experiments, 1008 unique trials with three replicates for FRSP. There was a total of 7 factors: %Acrylic Acid (7 levels, 31-60%), hydrogen peroxide, ascorbic acid, ammonium persulfate (16 levels, 50-200ppm), Temperature (7 levels, 273-303K), Time (5 levels, 1-40 mins).

For the MAP there were 1323 experiments, 441 unique trials with three replicates for the MAP. There was a total of 7 factors: %Acrylic Acid (7 levels, 31-60%), ammonium persulfate (7 levels, 2-20ppm), Temperature (7 levels, 273-303K), Time (5 levels, 1-5 mins). Tables 14 and 15 are selected sample data for FRSP and MAP. The rest of the data could be found in Appendix A.

$[M]_0$ = *The acrylic acid concentration at time = 0*

$[M]_t$ = *The acrylic acid concentration at time = t*

Table 14. Selected Data for FRSP

Trial 125, 20% AA, 273K **H2O2=150ppm, AsA=150ppm, APS=150 ppm**										
M0	Time(Sec.)	Ln Mt1	Yield1 [Mt]	1/[Mt]1	Ln Mt2	yield2 [Mt]	1/[Mt]2	Ln Mt3	Yield3 [Mt]	1/[Mt]3
2.7755	60.0000	1.0183	2.7685	0.3612	1.0196	2.7721	0.3607	1.0196	2.7721	0.3607
2.7755	600.0000	0.7263	2.0674	0.4837	0.7247	2.0641	0.4845	0.7216	2.0577	0.4860
2.7755	1200.0000	0.2030	1.2251	0.8163	0.2003	1.2218	0.8185	0.1951	1.2154	0.8228
2.7755	1800.0000	-0.4471	0.6395	1.5638	-0.4523	0.6361	1.5720	-0.4624	0.6298	1.5879
2.7755	2400.0000	-1.0287	0.3575	2.7974	-1.0380	0.3541	2.8237	-1.0562	0.3478	2.8755

Table 15. Selected Data for MAP

Trial 279, 45% AA, 293K **3 ppm Ini**										
M0	Time(Sec.)	Ln Mt1	Yield1 [Mt]	1/Yield 1[Mt]	Ln Mt2	Yield2 [Mt]	1/Yield 2[Mt]	Ln Mt3	Yield3 [Mt]	1/Yield 3[Mt]
6.2448	60.0000	1.8296	6.2316	0.1605	1.8277	6.2197	0.1608	1.8291	6.2285	0.1606
6.2448	120.0000	1.5220	4.5815	0.2183	1.5194	4.5696	0.2188	1.5213	4.5784	0.2184
6.2448	180.0000	1.2124	3.3616	0.2975	1.2089	3.3497	0.2985	1.2115	3.3585	0.2978
6.2448	240.0000	1.1930	3.2969	0.3033	1.1894	3.2851	0.3044	1.1920	3.2938	0.3036
6.2448	300.0000	1.1714	3.2264	0.3099	1.1677	3.2145	0.3111	1.1704	3.2233	0.3102

Results and Discussion

The following two tables provide an executive summary of the FRSP and MAP kinetic studies that tested Hypotheses 1-3.

Summary of Kinetic Study Results

FRSP Studies: Does the kinetic fit exhibit an $R^2 \geq 0.9990$?

Table 16. Summary of FRSP Synthesis Model Testing Results.

Model	Single Kinetic Model
	All data
Complex	No
Zero-Order	No
First-Order	No

MAP Studies: Does the kinetic fit exhibit an $R^2 \geq 0.9990$?

Table 17**.** Summary of MAP Synthesis Model Testing Results

Model	Single Kinetic Model
	All data
Complex	No
Zero-Order	No
First-Order	No

The data support none of the initial predictions of hypothesis 1-3, but there is good news.

Detailed Results for Free Radical Solution Polymerization (FRSP) Kinetic Studies

Test of Hypothesis #1: The value of the correlation coefficient, R^2, ranges from 0.6178-0.9966 as the value of the unknown variable ß was varied from 0.0002 to 0.0003 and 0.0045. The best R^2 of 0.9966 ± 0.0001 (2σ) was observed at a ß = 0.0002 and the

typical fit had R^2 of 0.6178 ± 0.0001 (2σ) which belonged to ß = 0.0045 as shown in Figures 36 and 37. These results fell short of the R^2 ≥0.999 threshold. Consequently, the observed data does not appear to support Hypothesis 1 prediction. This result implies that the traditional published complex kinetic behavior of PAA polymerization does not explain the observed PAA SAP synthesis kinetics.

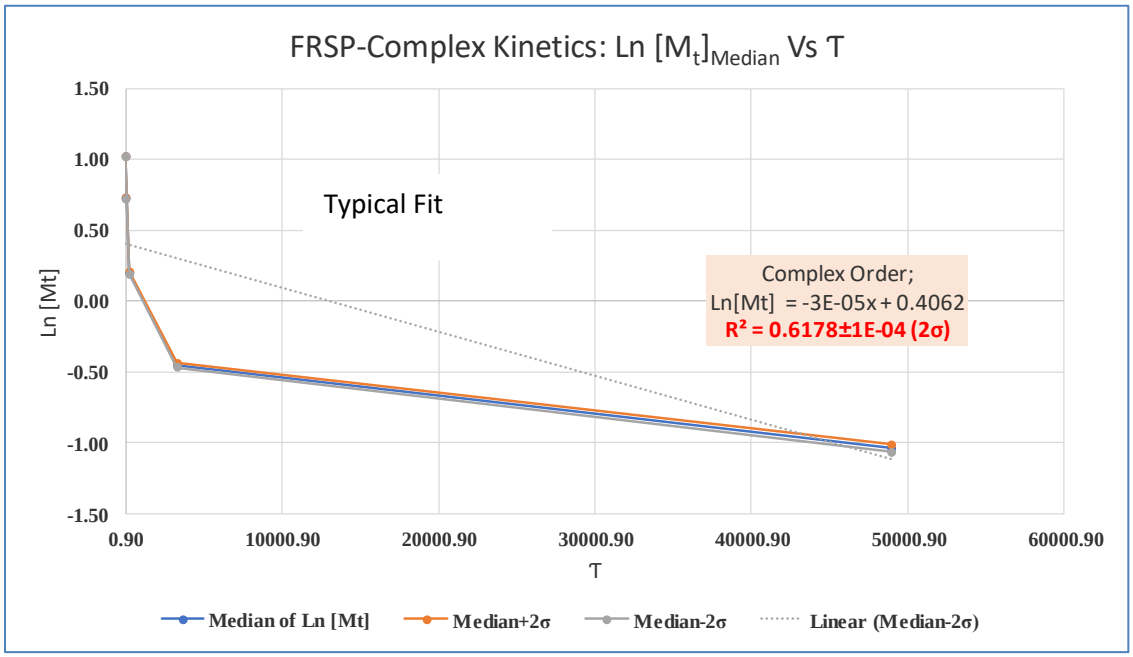

Figure 36. A Plot of the FRSP SAP Synthesis Reaction Data, Assuming Hypothesis 1 Kinetics, with **ß = 0.0045**. It Lists the Slope, Intercept, and R^2 for the Proposed Complex Kinetics, at a 150ppm Each Initiator (H_2O_2, AsA, APS) Made with 20% AA at a Polymerization Temperature of 273K.

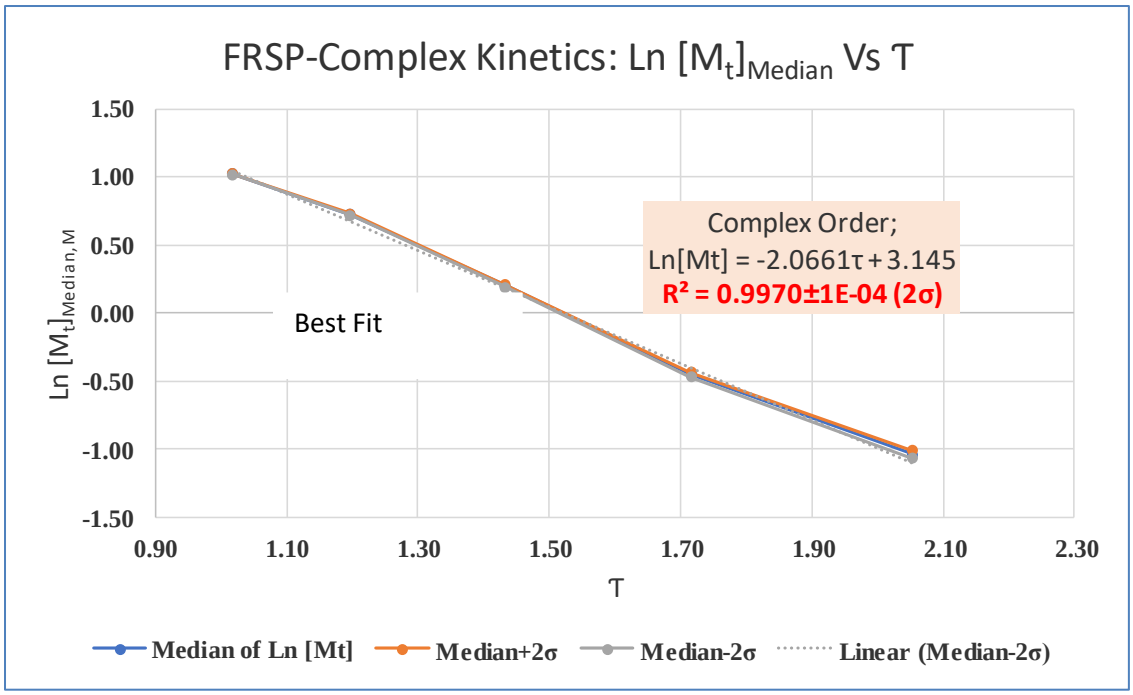

Figure 37. A Plot of the FRSP SAP Synthesis Reaction Data, Assuming Hypothesis 1 Kinetics, with **ß = 0.0002**. It Lists the Slope, Intercept, and R^2 for the Proposed Complex Kinetics, at a 150ppm Each Initiator (H_2O_2, AsA, APS) Made with 20% AA at a Polymerization Temperature of 273

First Order Reaction Kinetics in Acrylic Acid Monomer Concentration for FRSP

When first-order kinetics in monomer concentration is assumed over the entire reaction, the observed $R^2 = 0.9887 \pm 0.0001$ (2σ), as shown in Figure 38. This observation fails to support Hypothesis 2 over the entire reaction, as the observed R^2 fails to satisfy the $R^2 = 0.999$ threshold. Therefore, hypothesis 2 is not valid when all points are included.

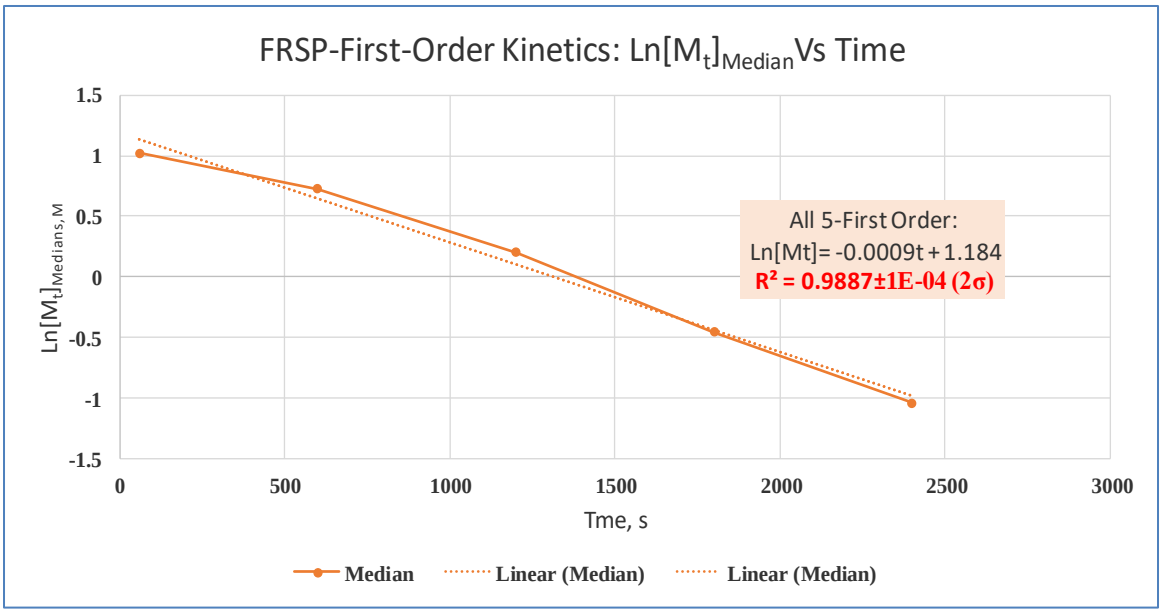

Figure 38. Observed Slope, Intercept, and R^2 for Kinetic Plot Over the Entire Reaction that Assumes Proposed Pseudo-Order Kinetic Behavior in Monomer Concentration, at a 150ppm Each Initiator (H_2O_2, AsA, APS) Made with 20% AA at a Polymerization Temperature of 273K

Zero Order or Pseudo-Zero Order Reaction Kinetics in Acrylic Acid Monomer Concentration for FRSP

When zero order or pseudo-zero order kinetics in monomer concentration is assumed over the entire reaction, the observed $R^2 = 0.9692 \pm 0.0006$ (2σ), as shown in Figure 39. This observation fails to support Hypothesis 3 over the entire reaction, as the observed R^2 fails to satisfy the $R^2 = 0.999$ threshold. Therefore, hypothesis 3 is not valid when all points are included.

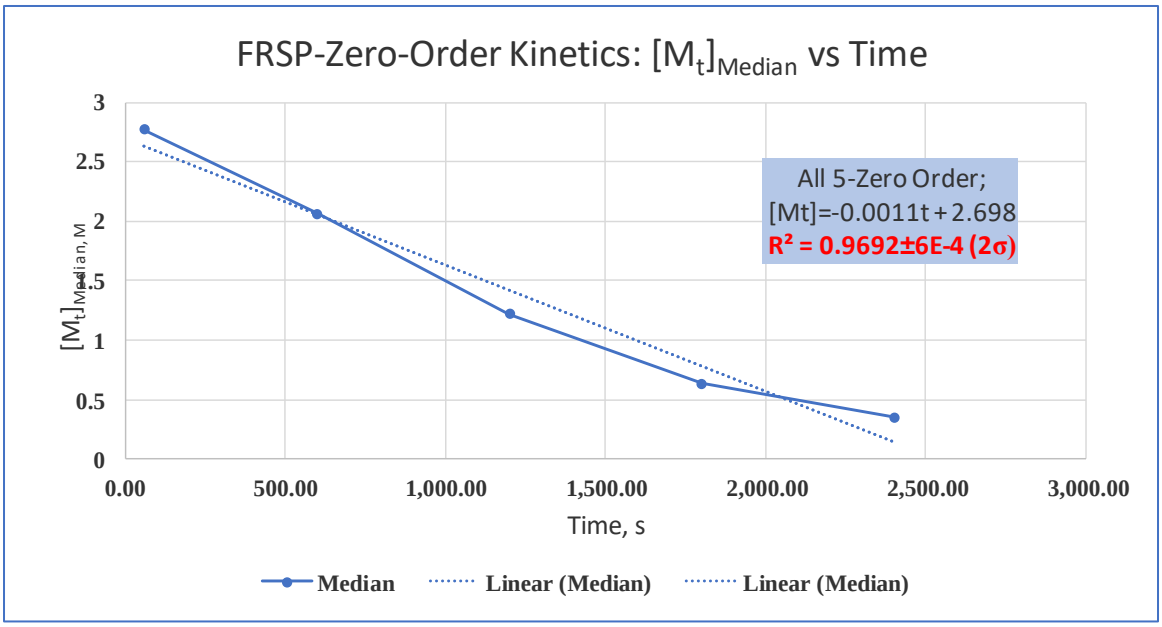

Figure 39. Observed Slope, Intercept, and R^2 for Kinetic Plot Over the Entire Reaction that Assumes Proposed Pseudo-Order Kinetic Behavior in Monomer Concentration, at a 150ppm Each Initiator (H_2O_2, AsA, APS) Made with 20% AA at a Polymerization Temperature of 273K.

Detailed Results for Microwave-Assisted Polymerization (MAP) Kinetic Studies

Test of Hypothesis #1: The value of the correlation coefficient, R^2, ranges from 0.6178-0.9966 as the value of the unknown variable ß was varied from 0.000002 to 0.002 and 0.0045. The best R^2 of 0.8237 ±0.0001 (2σ) was observed at a ß = 0.000002 and the typical fit for R^2 was 0.5327 ±0.0001 (2σ) which belonged to ß = 0.002 as shown in Figures 40 and 41. This result fell short of the $R^2 \geq 0.999$ threshold. Consequently, the observed data does not appear to support Hypothesis 1 prediction. This result implies that the traditional published complex kinetic behavior of PAA polymerization does not explain the observed PAA SAP synthesis kinetics.

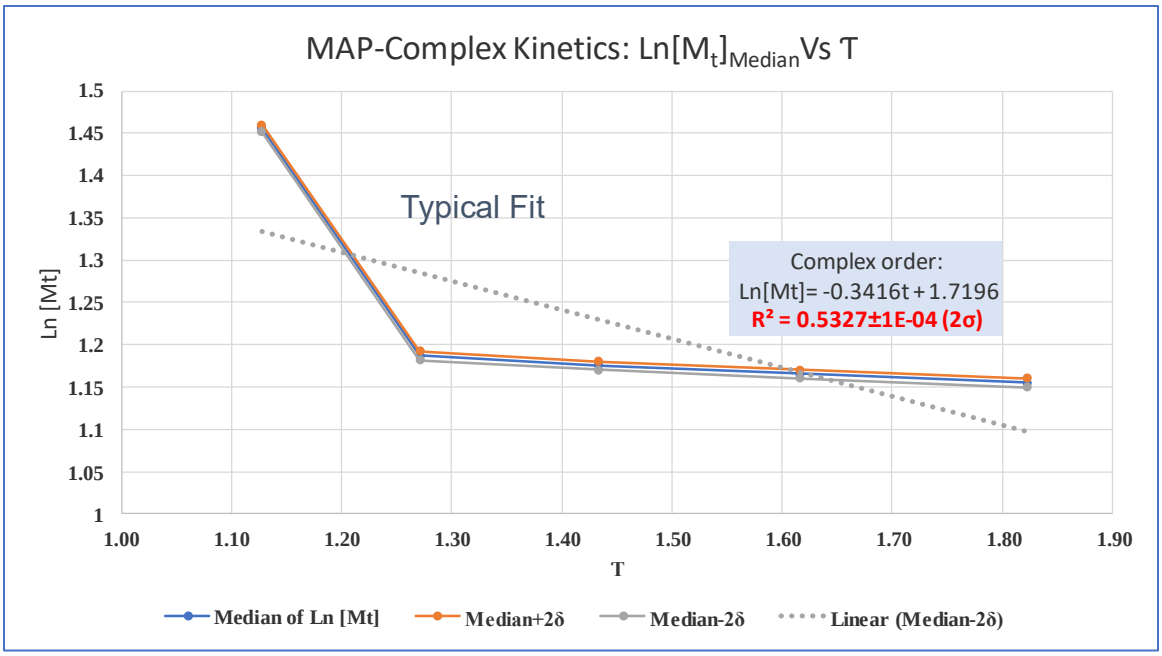

Figure 40. A Plot of the MAP SAP Synthesis Reaction Data, Assuming Hypothesis 1 Kinetics, with **ß = 0.002**. It Lists the Slope, Intercept, and R^2 for the Proposed Complex Kinetics, at a 3-ppm Made with 45% AA at a Polymerization Temperature of 293K.

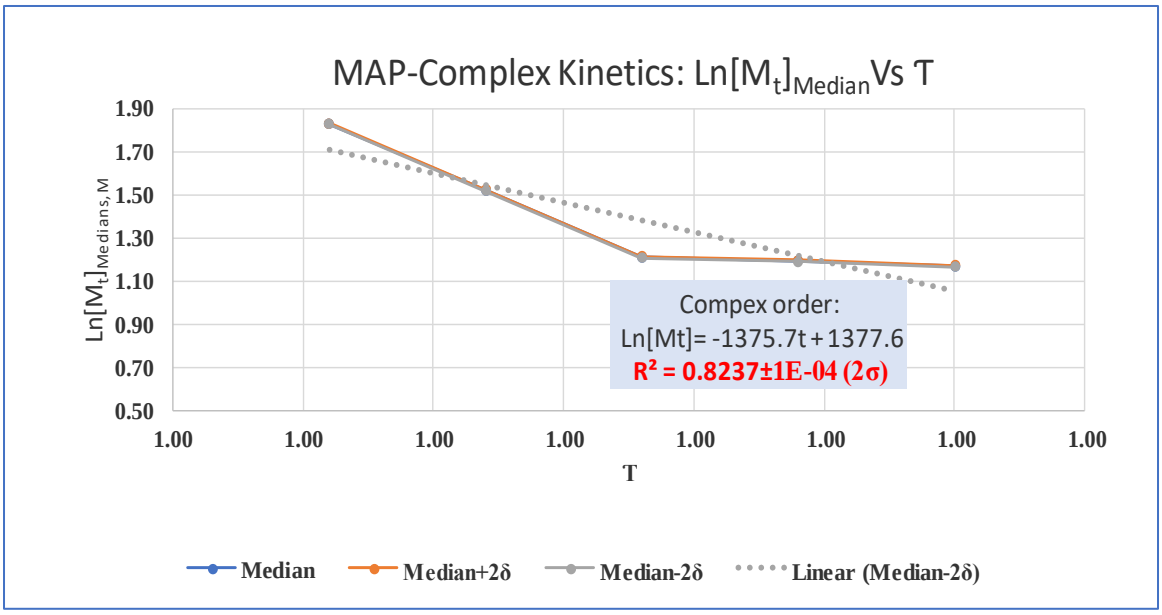

Figure 41. A Plot of the MAP SAP Synthesis Reaction Data, Assuming Hypothesis 1 Kinetics, with **ß = 0.000002**. It Lists the Slope, Intercept, and R^2 for the Proposed Complex Kinetics, at a 3-ppm Made with 45% AA at a Polymerization Temperature of 293K.

First-Order in Monomer Concentration MAP Synthesis Kinetic Studies

When first-order kinetics in monomer concentration is assumed over the entire reaction, the observed $R^2 = 0.8237 \pm 0.0001$ (2σ), as shown in Figure 42. This observation fails to support Hypothesis 2 over the entire reaction, as the observed R^2 fails to satisfy the $R^2 = 0.999$ threshold. Therefore, hypothesis 2 is not valid when all points are included.

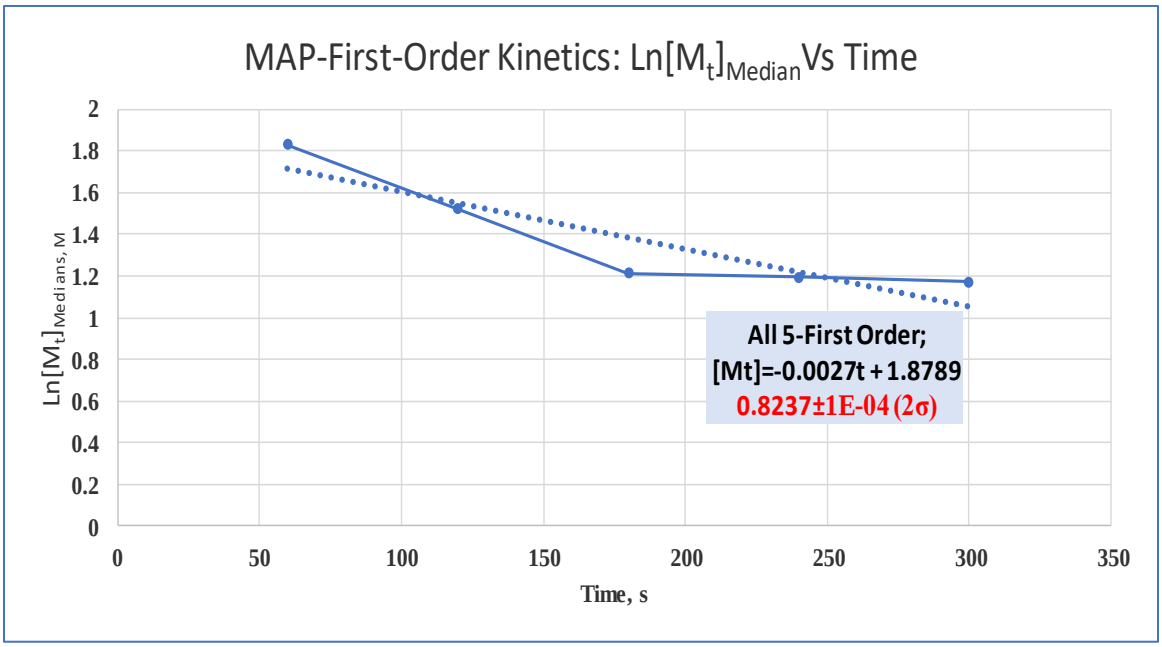

Figure 42. Observed Slope, Intercept, and R^2 for Kinetic Plot Over the Entire Reaction that Assumes Proposed Pseudo-Order Kinetic Behavior in Monomer Concentration, at a 3-ppm Initiator Made with 45% AA at a Polymerization Temperature of 293K.

Zero Order and Pseudo-Zero Order Reaction Kinetics in Monomer Concentration for MAP

When zero order and pseudo-zero order kinetics in monomer concentration is assumed over the entire reaction, the observed $R^2 = 0.7918 \pm 0.0006$ (2σ), as shown in Figure 43. This observation fails to support Hypothesis 3 over the entire reaction, as the observed R^2 fails to satisfy the $R^2 = 0.999$ threshold. Therefore, hypothesis 3 is not valid when all points are included.

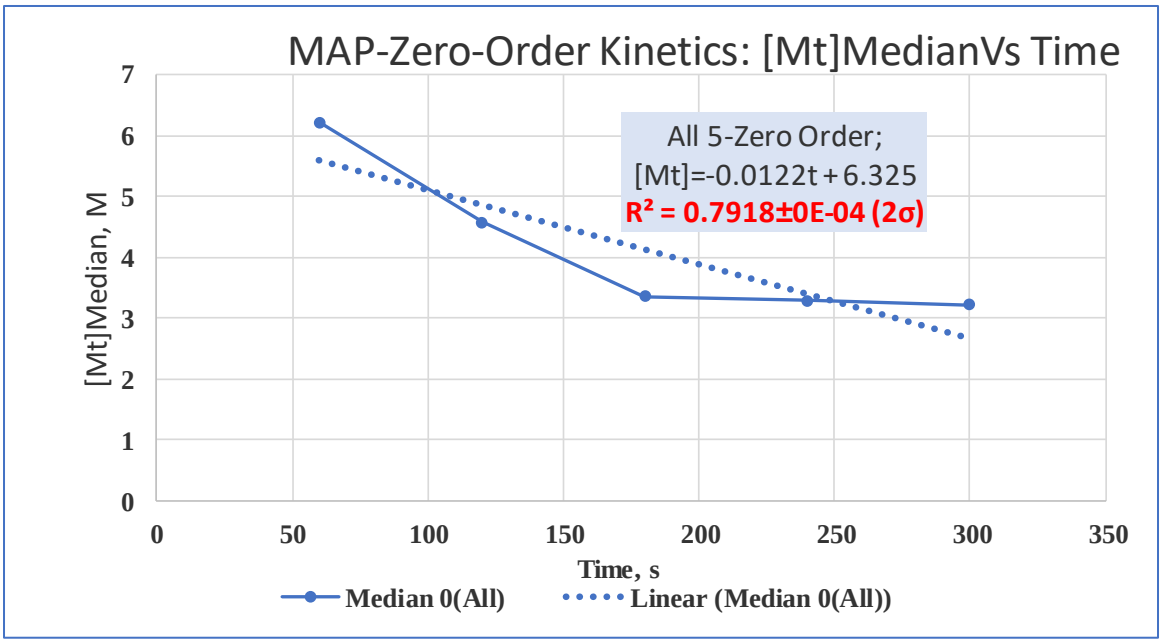

Figure 43. Observed Slope, Intercept, and R^2 for Kinetic Plot Over the Entire Reaction that Assumes Proposed Pseudo-Order Kinetic Behavior in Monomer Concentration, at a 3-ppm Initiator Made with 45% AA at a Polymerization Temperature of 293K.

Summary of Kinetic Study Observation

For the FRSP and MAP systems, throughout the PAA SAP synthesis, the system is undergoing a transition from a homogenous aqueous solution to a homogenous gel type phase, as shown below.

For the FRSP system, the polymerization is long, but volatile and probably diffusion controlled instead activation controlled for zero order. Since the SAP kinetic behavior over all time supports none of the proposed kinetic behavior, we consider two sequential processes. Over the course of the PAA SAP synthesis, the system is undergoing a transition from an aqueous solution to a homogenous gel type phase, as shown in Figures 44 and 45 below.

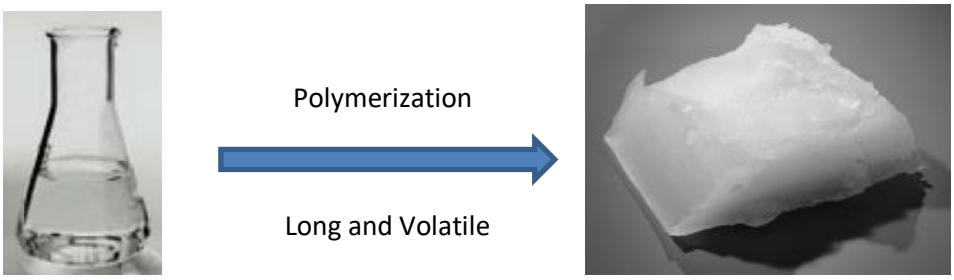

Figure 44. A Typical PAA SAP Gel Formed at FRSP Reaction Completion.

For the MAP, the polymerization is fast, but orderly and probably diffusion controlled instead activation controlled for zero order. Since the SAP kinetic behavior over all time supports none of the proposed kinetic behavior, we consider two sequential processes. Perhaps the system is undergoing a type of phase transition from an aqueous solution to a homogenous gel type phase.

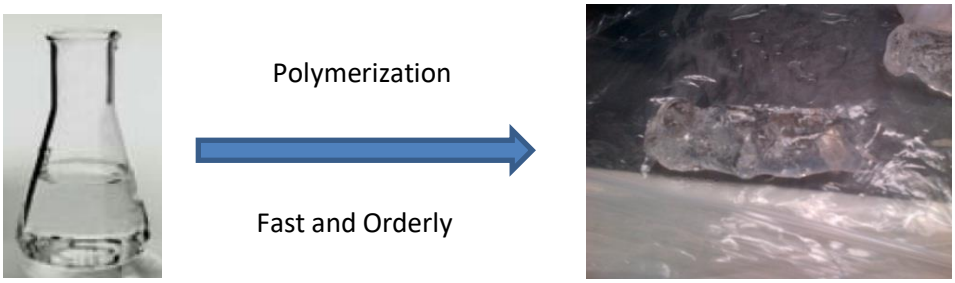

Figure 45. A Typical PAA SAP Gel Formed at MAP Reaction Completion.

New Hypothesis

The change in homogeneous medium composition drives sequential kinetics and rate changes, i.e., moving from a homogeneous aqueous solution to a homogenous gel. This explanation may be thought of as analogous to the property attributed to the

Hammett ρ parameter, which correlates observed changes in reaction rates with different solvents.

Potential Explanation**:** Sequential Kinetic and Hammett Parameter

Hammett equation can be written as log K / K0 = σ ρ, where σ = Substituent effect [H=1] and ρ = Substrate, solvent and system effect [H_2O=1], *K* and *K*o refer to the dissociation equilibrium constants of substituted and parent benzoic acids. The Hammett ρ parameter correlates observed changes in reaction rates with different chemical systems and/or solvent environments.[28]

Table 18. Hammett σs of Substituents

Substituent	CH_3	H	OCH_3	Cl	NO_2
σ_m	-0.07	0	0.12	0.37	0.71

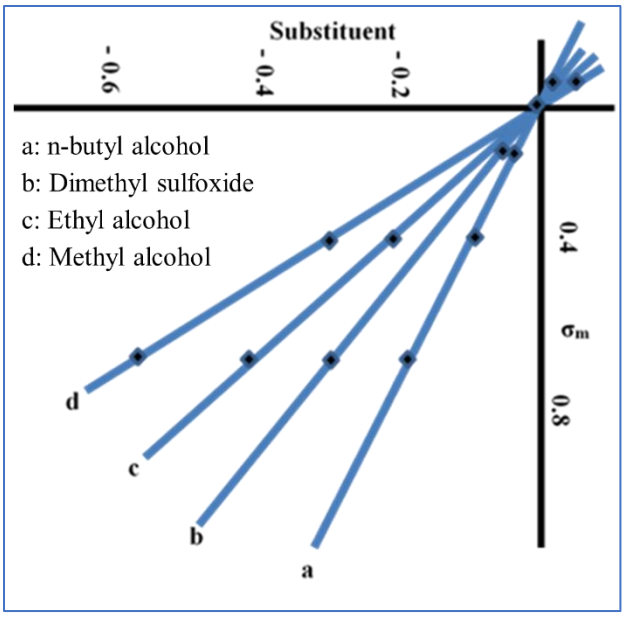

Figure 46. A Plot of Substituent Vs σ_m (reproduced from graph by Al-Nuri)

The ρ reflects a reaction's sensitivity to a given system or local environment.

Summary of Observed Kinetic Study

FRSP Studies: Does the kinetic fit exhibit an $R^2 \geq 0.9990$?

Table 19. Summary of FRSP Synthesis Model Testing Results.

Model	**Sequential Kinetic Model**	
Data Set	**Top Half**	**Bottom Half**
Complex	No	No
Zero-Order	**Yes**	No
First-Order	No	**Yes**

MAP Studies: Does the kinetic fit exhibit an $R^2 \geq 0.9990$?

Table 20. Summary of MAP Synthesis Model Testing Results.

Model	**Sequential Kinetic Model**	
Data Set	**Top Half**	**Bottom Half**
Complex	**Yes**	**Yes**
Zero-Order	No	**Yes**
First-Order	**Yes**	**Yes**

The following section provides detailed results for each of the models tested under FRSP and MAP reaction conditions.

We also considered sequentially plotting the first and second half of this reaction's data, for ß = 0.0002, as shown in Figure 47. Figure 47 shows R^2 values of 0.9934±0.0009 (2σ) and 0.9931 ±0.0001(2σ) for the first and second half sequential plots, respectively. As these observed R^2 values also fall short of the $R2 \geq 0.999$ threshold, a sequential application of Hypothesis 1 kinetics does not explain the observed data.

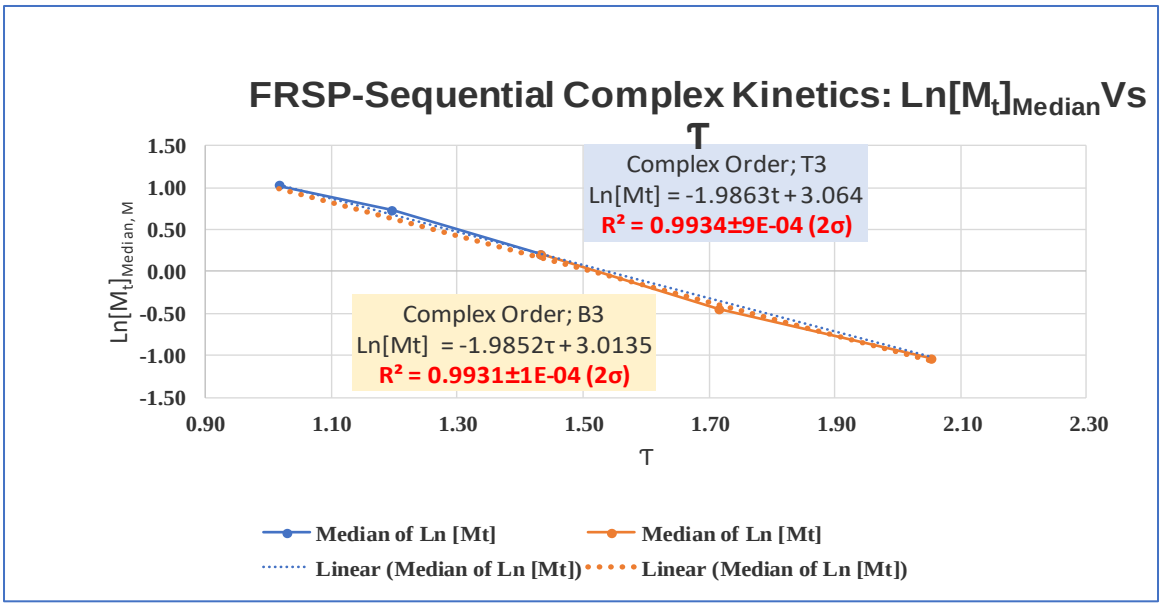

Figure 47. Sequential Plots of the FRSP SAP Synthesis Reaction Data, Assuming Hypothesis 1 Kinetics, with **ß = 0.0002**. It Lists the Slopes, Intercepts, and R^2 Values for the Proposed Complex Kinetics, at a 150ppm Each Initiator (H_2O_2, AsA, APS) Made with 20% AA at a Polymerization Temperature of 273K.

We also considered sequentially plotting the first and second half of this reaction's data as shown in Figure 48. Figure 48 shows R^2 values of 0.9832±0.0009 (2σ) and 0.9990 ±0.0001 (2σ) for the first and second half sequential plots, respectively. The first half of the reaction does not fall within the threshold of 0.999, but the second half does. Only observed R^2 value supports Hypothesis 2 for the second half of the reaction but falls short of the R2≥0.999 threshold for the second half of the reaction. So, a sequential application of Hypothesis 2 kinetics does not explain the whole set of observed data.

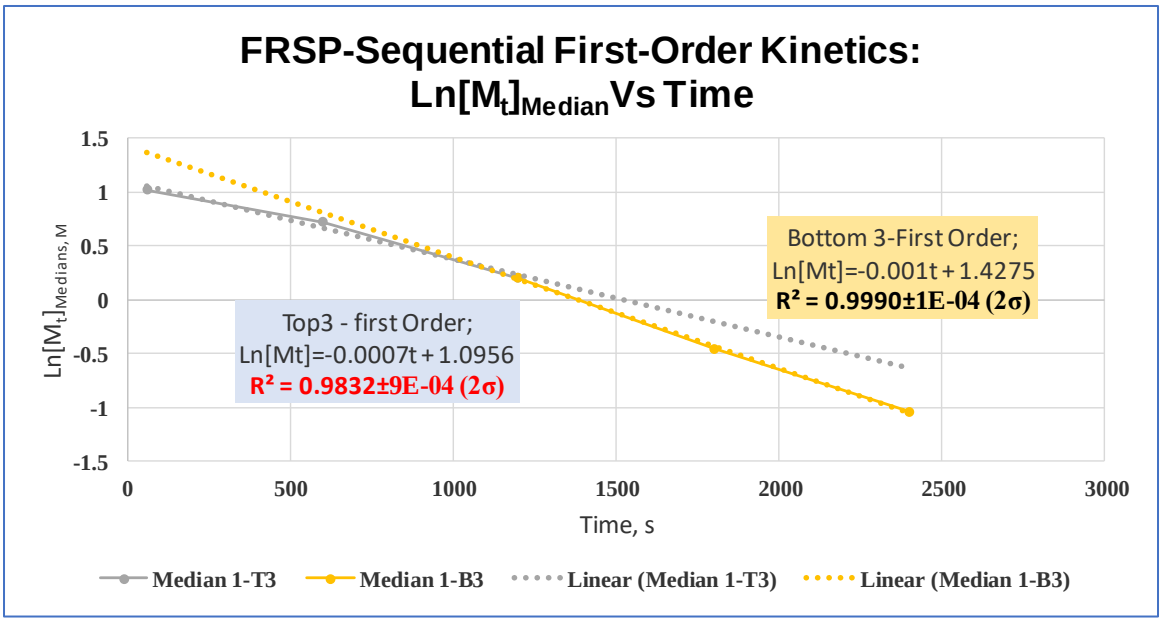

Figure 48. Observed Slope, Intercept, and R^2 for Kinetic Plot Over the Entire FRSP Reaction that Assumes Proposed Pseudo-Order Kinetic Behavior in Monomer Concentration, at a 150ppm Each Initiator (H_2O_2, AsA, APS) Made with 20% AA at a Polymerization Temperature of 273K.

We also considered sequentially plotting the first and second half of this reaction's data as shown in Figure 49. Figure 49 shows R^2 values of 0.9996±0.0002 (2σ) and 0.9608 ±0.0000(2σ) for the first and second half sequential plots, respectively. The first half of the reaction falls within the threshold of 0.999, but the second half does not. Only observed R^2 value supports Hypothesis 3 for the first half of the reaction but falls short of the R2≥0.999 threshold for the second half of the reaction. So, a sequential application of Hypothesis 3 kinetics does not explain the whole observed data.

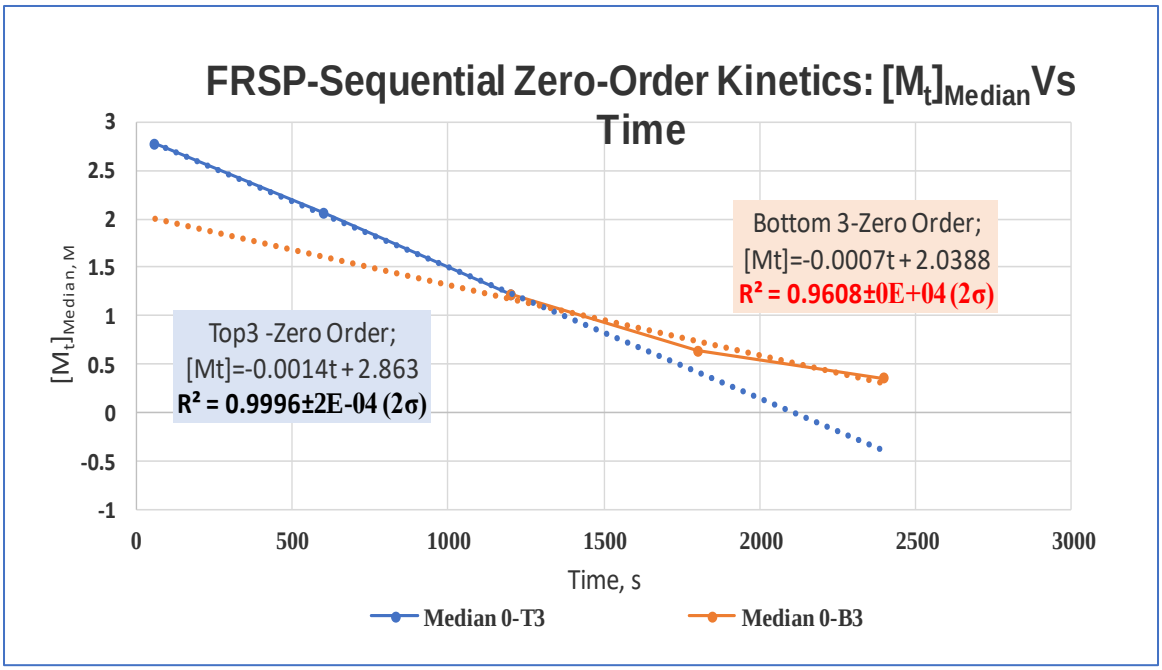

Figure 49. Sequential Plots of the FRSP SAP Synthesis Reaction Data, Assuming Hypothesis 3 Kinetics. It Lists the Slopes, Intercepts, and R^2 Values for the Proposed Pseudo-Order Kinetics in Monomer Concentration, at a 150ppm Each Initiator (H_2O_2, AsA, APS) Made with 20% AA at a Polymerization Temperature of 273K.

Since the observed FRSP SAP kinetics over all time supports none of the proposed kinetic models, we consider 2 sequential processes. As mentioned above, perhaps the system during the synthesis undergoes a type of phase transition from an aqueous solution to a homogenous gel type phase.

Sequential Zero Order and First Order Reactions

This scenario asserts a polymerization reaction that begins as a zero-order reaction, with an $R^2 = 0.9996$, that transitions to a reaction that is first-order in monomer

concentration, with an R^2 = 0.9990, for the second half of the reaction, as shown in Figure 50.

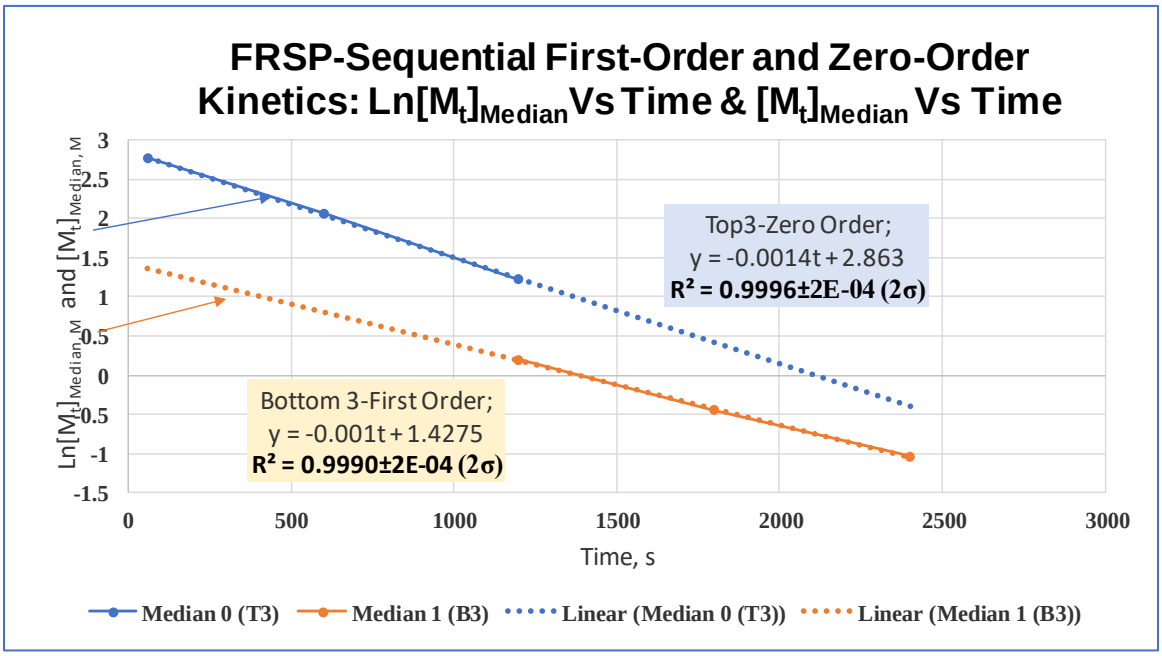

Figure 50. Observed Slope, Intercept, and R^2 for Kinetic Plot Over the Entire Reaction that Assumes Proposed Pseudo-Order Kinetic Behavior in Monomer Concentration, at a 150ppm each Initiator (H_2O_2, AsA, APS) Made with 20% AA at a Polymerization Temperature of 273K.

Overall, the data for the synthesis of PAA SAP via a FRSP process supports a sequential kinetic model, which begins as a zero-order or pseudo-zero-order process that transitions to a first order process, with respect to monomer concentration.

Detailed Results for Microwave-Assisted Polymerization (MAP) Kinetic Studies

Test of Hypothesis #1: The value of correlation coefficient, R^2, ranges from 0.6178-0.9966 as the value of the unknown variable ß was varied from 0.000002 to 0.002 and 0.0045. The best R^2 of 0.8237 ±0.0001 (2σ) was observed at a ß = 0.000002, as shown in Figure 51. This result fell short of the $R^2 \geq 0.999$ threshold. Consequently, the observed data does not appear to support the Hypothesis 1 prediction. This result implies that the traditional published complex kinetic behavior of PAA polymerization does not explain the observed PAA SAP synthesis kinetics.

Sequential Complex Order Reactions

We also considered sequentially plotting the first and second half of this MAP reaction's data, for ß = 0.000002, as shown in Figure 51. Figure 51 shows R^2 values of 1.0000±0.0001 (2σ) and 0.9990 ±0.0001(2σ) for the first and second half sequential plots, respectively. As these observed R^2 values satisfy the $R^2 \geq 0.999$ threshold, a sequential application of Hypothesis 1 kinetics can explain the observed data. Therefore, one may initially assert that these results support a sequential form of Hypothesis 1, implying that a sequential PAA SAP polymerization reaction may account for the proposed complex kinetic behavior.

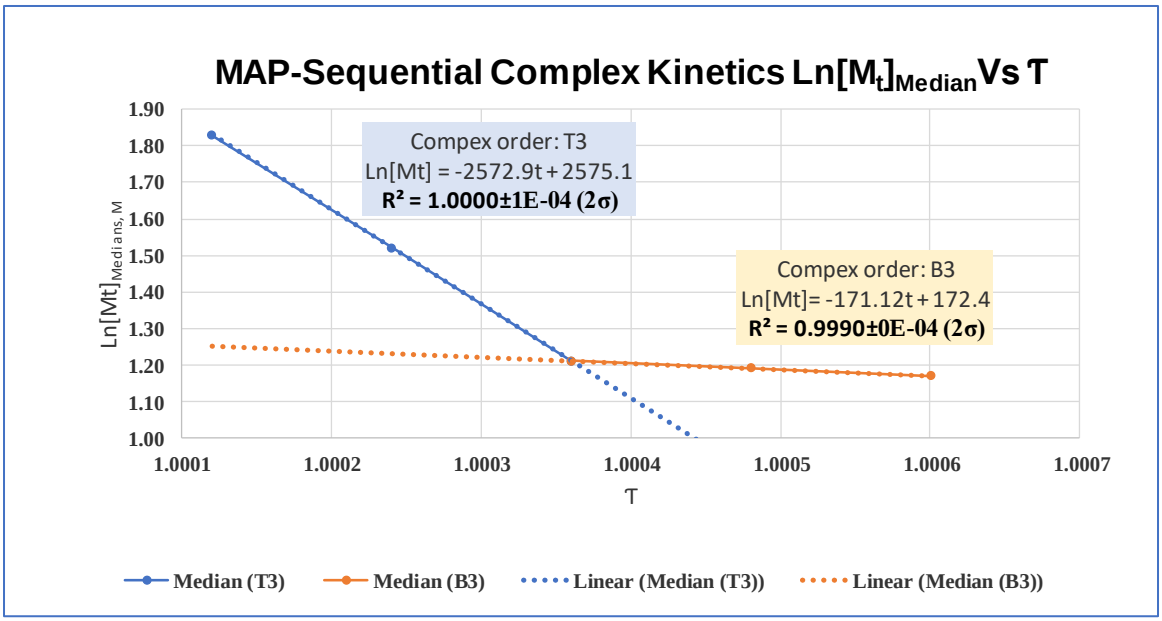

Figure 51. A Plot of the MAP SAP Synthesis Reaction Data, Assuming Hypothesis 1 Kinetics, with **ß = 0.000002**. It Lists the Slope, Intercept, and R^2 for the Proposed Complex Kinetics, at a 3-ppm Made with 20% AA at a Polymerization Temperature of 273K.

Sequential Zero Order Reactions

We also considered plotting the first and second half of this reaction's data assuming sequential zero-order kinetics in monomer concentration, as shown in Figure 52. Figure 52 shows R^2 values of 0.9926±0.0000 (2σ) and 0.9994 ±0.0000(2σ) for the first and second half sequential plots, respectively. As the observed R^2 values for the first half of the reaction falls short of the boundary of the R2 ≥ 0.999 threshold, a sequential application of the Hypothesis 2 kinetics model does not explain the all the observed reaction data. Please note that the second half of the PAA SAP type of MAP reaction can be explained by zero-order kinetic behavior, but not the first half of this reaction.

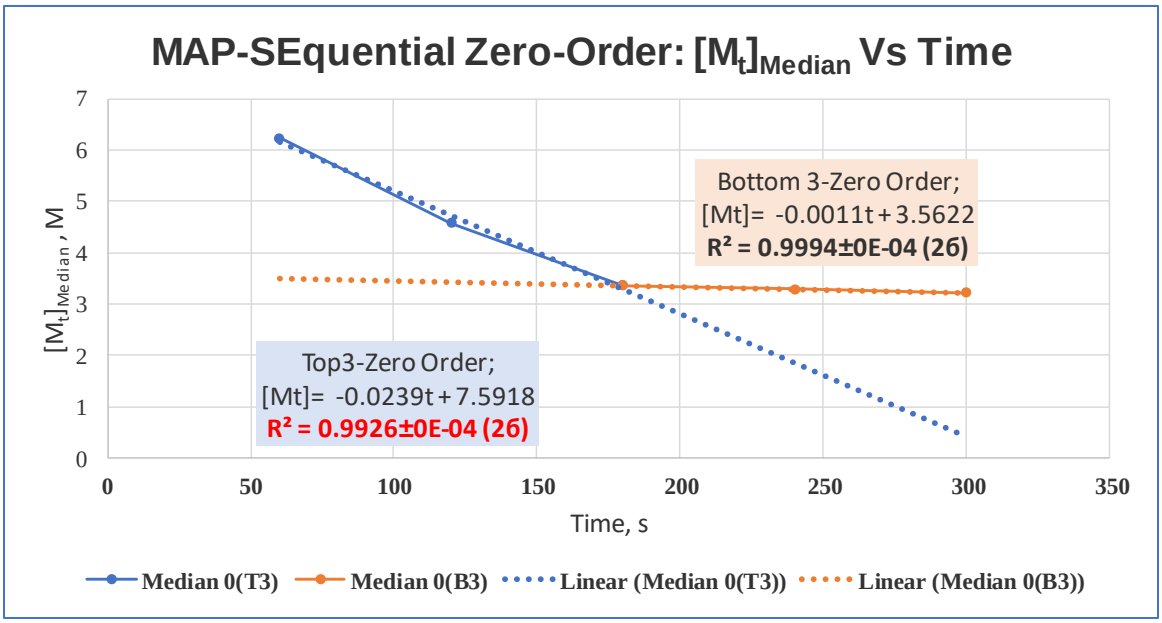

Figure 52. Observed Slope, Intercept, and R^2 for Kinetic Plot Over the Entire Reaction that Assumes Proposed Pseudo-Order Kinetic Behavior in Monomer Concentration, at a 3-ppm Initiator Made with 45% AA at a Polymerization Temperature of 293K.

Sequential First Order Reactions

When the first and second halves of the reaction are plotted as sequential first order reactions, as shown in Figure 53 1, R^2 values of 1.0000±0.0001(2σ) and 0.9990±0.0000(2σ), are respectively observed. These results support a sequential application of Hypothesis 2 over the entire reaction, as the observed R^2s satisfy the R^2 = 0.9990 threshold. Therefore, we may assert that sequential first-order models in monomer concentration can also explain the MAP synthesis of PAA SAP.

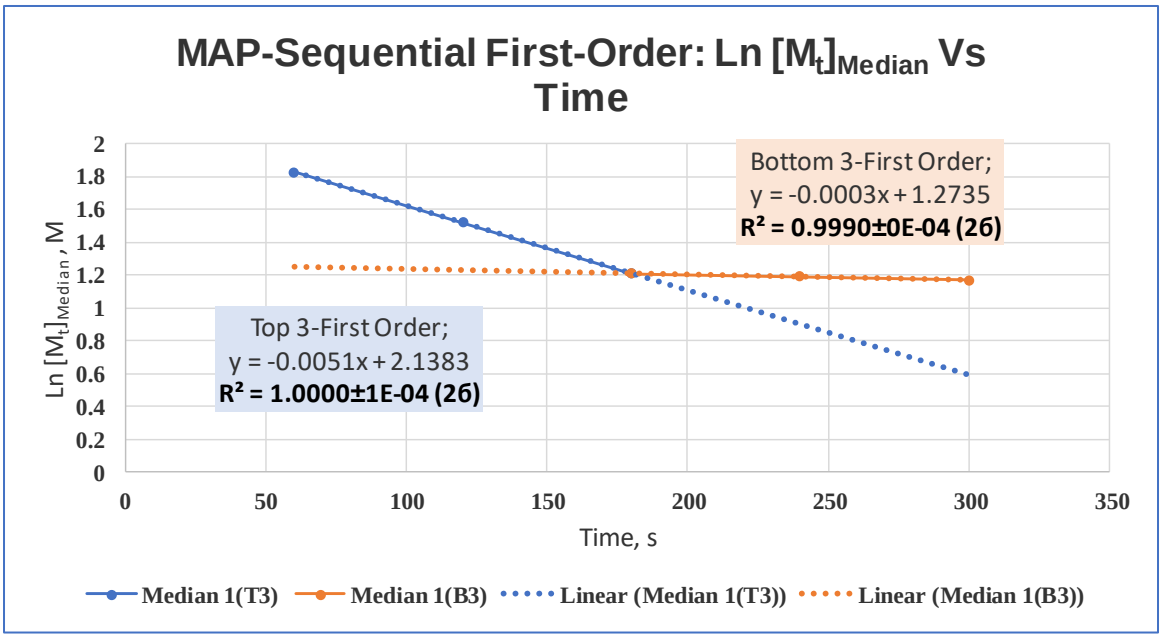

Figure 53. Observed Slope, Intercept, and R^2 for Kinetic Plot Over the Entire Reaction that Assumes Proposed Pseudo-Order Kinetic Behavior in Monomer Concentration, at a 3-ppm Initiator Made with 45% AA at a Polymerization Temperature of 293K.

Again, one would have to conclude that these results do not support Hypothesis 1, implying that the PAA SAP type of polymerization reaction does not follow the proposed complex kinetic behavior.

For MAP: Since the SAP kinetic behavior over all time supports none of the proposed kinetic behavior, we consider 2 sequential processes. Perhaps the system is undergoing a type of phase transition from an aqueous solution to a homogenous gel type phase.

Two sequential models can account for the observed behavior of the MAP synthesis of PAA SAPs, i.e., a sequential complex model and a sequential first order model. The former model assumes a slow initiator decomposition, while the latter model

assumes a rapid initiator decomposition and that the reaction is dominated by a simple first order process. We assert that the sequential first-order kinetics model best accounts for the data. The sequential complex model is more complex and requires the empirical fit of an unknown factor.

Arrhenius Plots

The classic Arrhenius equation, shown in equation 2.66, describes the dependency of a rate constant, k, on reaction temperature, T, and activation energy, E_a.

$$k = Ae^{-E_a/RT} \qquad 2.66$$

For a given reaction that proceeds via a single mechanism, a plot of ln(k) vs T^{-1} yields a straight line, with a slope, m, that corresponds to - E_a / R. For zero-order reactions, e.g., diffusion controlled, this slope equals zero.

Recap Summary of Kinetic Study Results

FRSP Studies: Does the kinetic fit exhibit an $R^2 \geq 0.9990$?

Table 21. Summary of FRSP Synthesis Model Testing Results.

Model	**Sequential Kinetic Model**	
Data Set	**Top Half**	**Bottom Half**
Complex	No	No
Zero-Order	**Yes**	No
First-Order	No	**Yes**

FRSP Studies: Does the kinetic fit exhibit an $R^2 \geq 0.9990$?

Table 22. Summary of MAP Synthesis Model Testing Results.

Model	**Sequential Kinetic Model**	
Data Set	**Top Half**	**Bottom Half**
Complex	**Yes**	**Yes**
Zero-Order	No	**Yes**
First-Order	**Yes**	**Yes**

Figure 54 shows a typical Arrhenius plot for Zero Order, first half reaction, which is highlighted in red in table 21.

Factors: 20% AA, 150ppm Hydrogen Peroxide, 150ppmAscorbic Acid, 150ppm Ammonium Persulfate

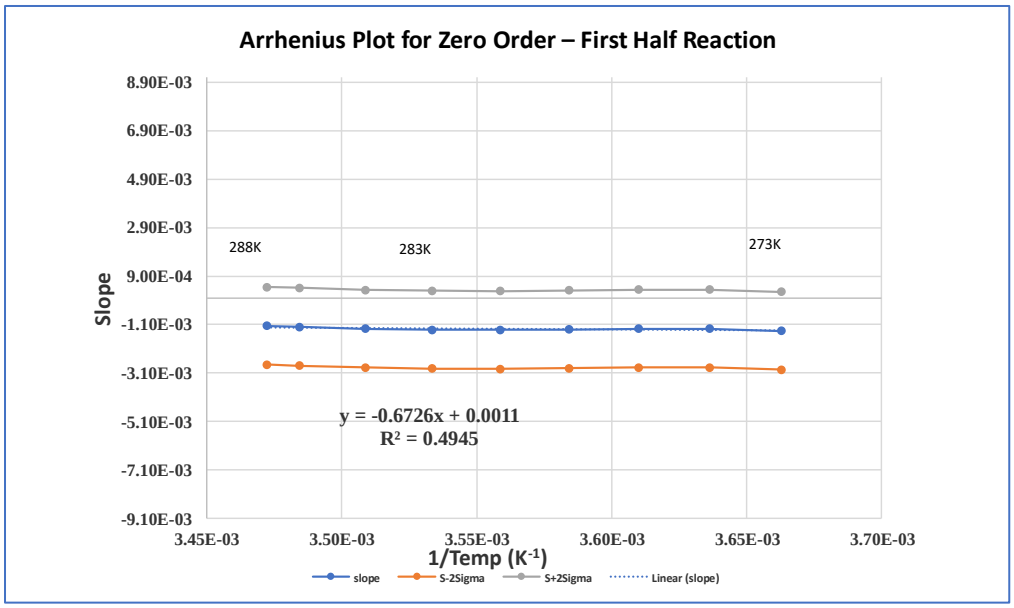

Figure 54. Typical Arrhenius Plot for a FRSP that is Consistent with Zero-Order Behavior. [Note: Given the 2σ Uncertainty, as Shown by the Grey and Orange Lines, the Slope Could be Slightly Non-Zero.]

As the slope of this Arrhenius plot is very close to zero, the reaction appears to be relatively independent of the reaction temperature. Additionally, this type of behavior implies that the activation barrier for this reaction is zero, or very close to zero.

The Kinetic Landscape

ECHIP, a statistical software package developed at the DuPont Experimental Station, is a tool for creating efficient experimental designs, generating predictive models, and visualizing response surfaces of desired system properties. For the purpose of this dissertation, it serves as a tool for visualizing trends in reaction rates over the studied reaction space, and for helping to clarify when changes in reaction kinetics become significant.

FRSP Zero-Order Slope Landscape for the First Half of the Reaction

Response Surface Method (RSM)-10-60% AA: Figure 55, shown below, was generated from 3024 experimental observations. The model's residual and trial replicate slope standard deviations are $\sigma_{residual} = 0.000767$, and $\sigma_{replicate} = 0.000616$, respectively. Since the magnitudes of the replicate and residual standard deviations are similar, most of the model's lack of fit can be accounted for by the replication error.

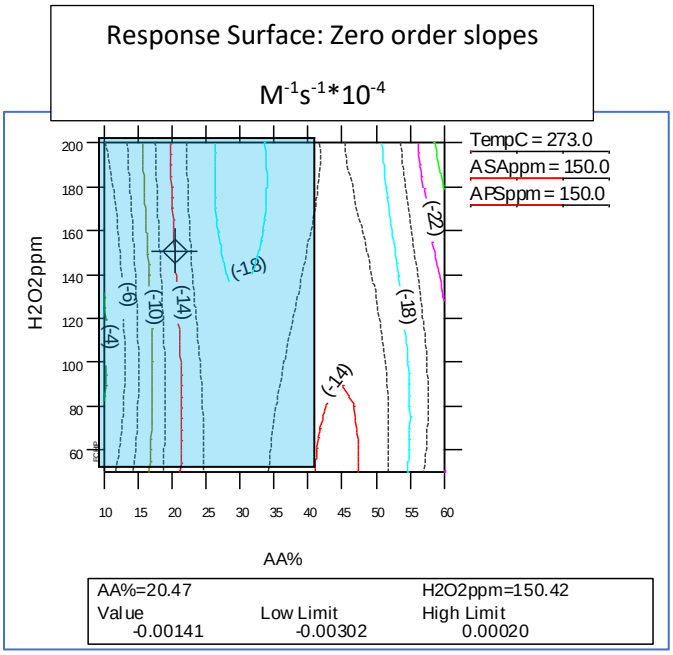

Figure 55. FRSP Response Surface for the Slopes, i.e., Zero Order Reaction Rates ($M^{-1} \cdot s^{-1}$), for the First Half of the Reaction with Top 3-Time Periods for 10-60% Initial Acrylic Acid and 60-200 ppm Initial H_2O_2 Initiator Concentrations.

This response surface is statistically flat over the study domains of initial initiator and acrylic acid concentrations, i.e., the light blue region (The useable manufacturing region). These rates tend to be independent of the initial initiator and acrylic acid concentrations over the region presented.

FRSP First-Order Slope Landscape for the Second Half of the Reaction

Response Surface Method (RSM)-10-60% AA: Figure 56, shown below, was generated from 3024 experimental observations. The model's residual and trial replicate slope standard deviations are $\sigma_{residual} = 0.000343$, and $\sigma_{replicate} = 0.000248$, respectively.

Since the magnitudes of the replicate and residual standard deviations are similar, most of the model's lack of fit can be accounted for by the replication error.

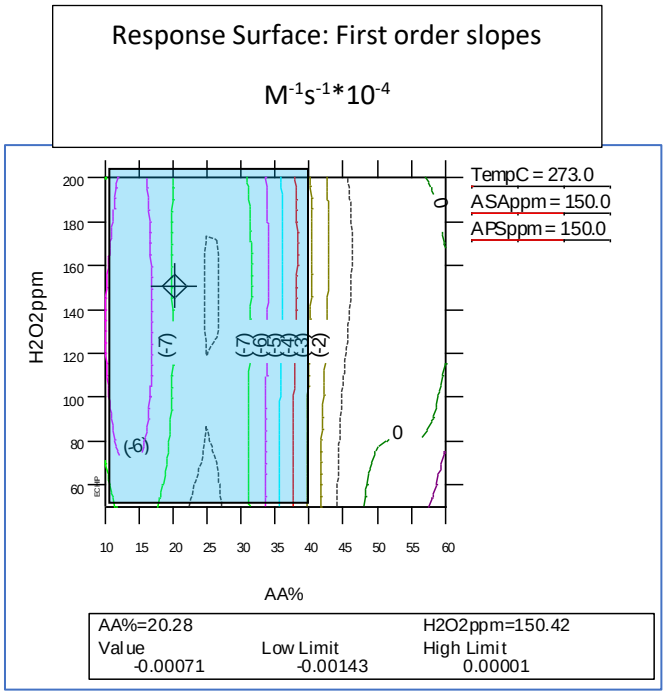

Figure 56. FRSP Response Surface for the Slopes, i.e., First-Order Reaction Rates ($M^{-1} \cdot s^{-1}$), for the Second Half of the Reaction, i.e., the Second-Half of the Reaction for 10-60% Initial Acrylic Acid and 60-200 ppm Initial H_2O_2 Initiator Concentrations.

This response surface is statistically flat over the study domains of initial initiator and acrylic acid concentrations, i.e., the light blue region (the useable region). These rates tend to be independent of the initial initiator and acrylic acid concentrations over the region presented.

MAP First-Order Slope Landscape for the First Half of the Reaction

Response Surface Method (RSM)-10-60% AA: Figure 57, shown below, was generated from 1323 experimental observations. The model's residual and trial replicate slope standard deviations are $\sigma_{residual}$ = 0.000434, and $\sigma_{replicate}$ = 0.000205, respectively. Since the magnitudes of the replicate and residual standard deviations are similar, most of the model's lack of fit can be accounted for by the replication error.

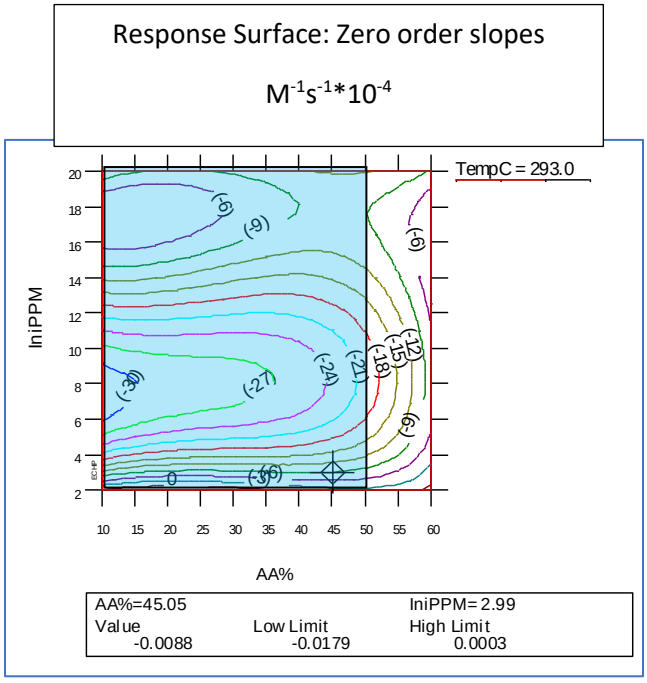

Figure 57. FRSP Response Surface for the Slopes, i.e., First-Order Reaction Rates ($M^{-1}\cdot s^{-1}$), for the First Half of the Reaction, i.e., the First Three Time Periods for 10-60% Initial Acrylic Acid and 2-20 ppm Initial APS Initiator Concentrations.

This response surface is statistically flat over the study domains of initial initiator and acrylic acid concentrations, i.e., the light blue region (the useable region). These

rates tend to be independent of the initial initiator and acrylic acid concentrations over the region presented.

MAP First-Order Slope Landscape for the Second Half of the Reaction

Response Surface Method (RSM)-10-60% AA: Figure 58, shown below, was generated from 1323 experimental observations. The model's residual and trial replicate slope standard deviations are $\sigma_{residual} = 0.000527$, and $\sigma_{replicate} = 0.000402$, respectively. Since the magnitudes of the replicate and residual standard deviations are similar, most of the model's lack of fit can be accounted for by the replication error.

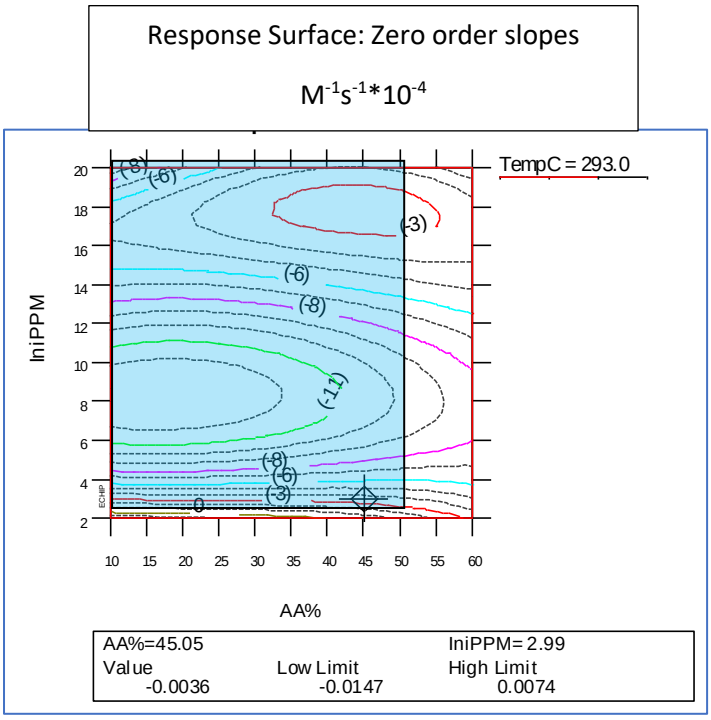

Figure 58. FRSP Response Surface for the Slopes, i.e., First-Order Reaction Rates ($M^{-1} \cdot s^{-1}$), for the Second Half of the Reaction, i.e., the Last Three Time Periods for 10-60% Initial Acrylic Acid and 2-20 ppm Initial APS Initiator Concentrations.

Conclusion

The kinetics and mechanistic studies of two type of polymerization techniques were studies, i.e., FRSP and MAP. For these kinetic studies, the data supported **none** of the initial hypotheses, i.e., Hypotheses 1-3, for all of the data in a given reaction. The complex mechanism of PAA polymerization, which is assumed to be valid in the case of superabsorbent polymerization, does not seem to be valid in FRSP and MAP syntheses.

At first glance, for the FRSP PAA SAP syntheses considered in this study, only a sequential kinetic model, i.e., zero-order in monomer model followed by a first-order in monomer model explains the observed data, as summarized in Table 21.

For the MAP PAA SAP syntheses considered in this study, several sequential kinetic models may account for the observed data, i.e., a complex model and first-order model for the first half of the reaction and a complex, zero-order, and first-order model for the second half of the reaction, as summarized in Table 22. Upon closer examination, we exclude the complex models, as they require an empirical fitting parameter and they are more complex than the remaining zero-and first-order models. As for the remaining models, the data demonstrate that a first order model explains the first half-reaction and suggests a slight preference for the second half-reaction for a zero-order model over a first order model, as the R^2s are 0.9994 vs 0.9990, respectively.

The comprehensive experimental design and response surface plots suggest that the findings, listed above, may apply to a fairly large sector of the PAA SAP fabrication space, as the topographies of the response surfaces for FRSP and MAP reaction rates are statistically rather flat, as demonstrated in Figures 55 -58. However, the FRSP approach tends to be a bit less stable at high loadings of acrylic acid, $\geq 50\%$.

References

1. Azad, M. M.; Sandros, M. G. *J. Appl. Polym. Sci.* **2016**, *133, 43325.*
2. Azad, M. M.; Sandros, M. G. *J. Appl. Polym. Sci.* **2016**, *133, 43990.*
3. Buchholz, F. L.; Graham, A. T. Modern Superabsorbent Polymers Science and Technology; The United States of America, 1998; p 130-131.
4. www.dowac.custhelp.com/app/answers/detail/a_id/2464/~/acrylic-acid-dimerization.
5. Buchholz, F. L.; Graham, A. T. Modern Superabsorbent Polymers Science and Technology; The United States of America, 1998; p 25-26.
6. Michael reaction, Wikipedia
7. Kiatkamjornwong, S. J. Sci. Asia. 2007, 33, 39-43.
8. www.coursehero.com.
9. Buchholz, F. L.; Graham, A. T. Modern Superabsorbent Polymers Science and Technology; The United States of America, 1998; p 128-129.
10. www.clarkson.edu/~drasmuss/ES360 Spring 2016/Polymer lectures.
11. Buchholz, F. L.; Peppas, N. A. In Modern Superabsorbent Polymers Science and Technology; ACS Symposium Series 573, Washington, DC, 1994, p. 14-19.
12. Buchholz, F. L.; Graham, A. T. Modern Superabsorbent Polymers Science and Technology; The United States of America, 1998; p 30-34.
13. https://www.youtube.com/watch?time_continue=108&v=YXv4P8MxcxY
14. Modern Aspects of Diffusion-Controlled Reactions, Cooperative Phenomena in Bimolecular Processes (Comprehensive Chemical Kinetics) 1st Edition, Vol. 34, ISBN-13: 978-0444824721
15. www.statisticbyjim.com/regression/interpret-r-squared-regression
16. Walpole, R.; Meyers, R.; Meyers, S.; and Ye, K. Probability and statistics for engineers & scientists
17. www.sciencedirect.com/science/article/pii/S0069804008702528
18. www.physics.bu.edu/~redner/542/book/reactions.pdf
19. www.youtube.com/watch?time_continue=108&v=YXv4P8MxcxY
20. www.statisticsbyjim.com/regression/interpret-r-squared-regression/]
21. www.people.duke.edu/~rnau/rsquared.htm
22. www.www.cs.princeton.edu/courses/archive/fall09/cos597A/papers/MacKay2003-Ch28.pdf
23. Azad, M. M.; Sandros, M. G. *J. Appl. Polym. Sci.* 2016, *133, 43325.*
24. European Disposables and Nonwovens Association. Test Method No. 441.2-02 “Centrifuge Retention Capacity”.
25. European Disposables and Nonwovens Association. Test Method No. 442.2-02 “Absorption Under Pressure”.
26. European Disposables and Nonwovens Association. Test Method No. 470.2-02 “Extractable”.

27. European Disposables and Nonwovens Association. Test Method No. 410.2-02 “Residual Monomers”.
28. Al-Nuri, M. solvent effects on p values of the Hammett' equation for the hydrolysis of benzylidene benzoylhydrazones. J. Res. ,1989, Vol. 1.

CHAPTER VI

OVERALL CONCLUSIONS AND FUTURE STUDIES

Overall Conclusions

The microwave-assisted polymerization is much superior polymerization technique when is compared to the free radical solution polymerization. The properties of the polymers, AUL, CRC, extractable, yield, and permeability, are higher and higher percentage of acrylic acid (50% in MAP Vs less 40% in FRSP) could be used in monomer solution. The time of polymerization also favors the microwave-assisted polymerization.

The addition of clay into the monomer solution improves the permeability of the polymer in the MAP, while the clay settles in the bottom of the polymerization vessel in the FRSP and the resultant permeabilities are inconsistent due to the heterogeneous nature of the polymers. The percolation channels may explain the permeability improvement of the superabsorbent polymer.

The synthesis of super absorbent polymers can be understood as proceeding via rather simple first-order or zero-order kinetics. However, during the synthesis, the reaction solute transforms from a homogeneous aqueous system to another homogeneous

system that behaves more like a gel. We assert that this transformation accounts for the observed sequential kinetics as the reaction proceeds through completion.

Future Studies

This dissertation generates many questions that warrant further studies. Selected future directions and questions include:

1. A future study may consider varying the cross-linking chemistry, i.e., the type and size of the cross-linking agent, as well as the solute, to test the aqueous to gel solute transformation hypothesis.
2. Closer kinetic study of the entire synthesis space.
3. What are the kinetics that account for other polymerization techniques, e.g., UV polymerization, which has a short reaction time? Will these new understandings provide guiding principles for designing polymer syntheses that match or exceed the properties of those produced with MAP?
4. Is it possible to resolve the lack of homogeneity that exists for the clay in free radical solution polymerization? Will the uniform distribution of the clay in the FRSP be enough to bridge the gap in properties between FRSP and MAP?
5. Additional studies also may help to clarify the suggested correlation between percolation theory and permeability. Specifically, these studies would consider questions and fundamental reasons that explain how additives impact permeability, e.g., vary additive composition and size may provide additional insight into the mechanisms for enhancing the chemistry, design and properties of super absorbent polymers.

APPENDIX A

TABLES AND FIGURES-PAPER 3

Table 23. Time, Ln [M_t]s, Median, STDEV, and σ for Polymers at 150 ppm of Each H_2O_2, AsA, APS Initiator Levels for Polymers Made with FRSP for all 5 Times with 20% AA and @ 273K Polymerization Temperature **(ß=0.0002)**

β= 0.000200								
Time(Sec.)	Ln [Mt]1	Ln [Mt]2	Ln [Mt]3	T=EXP(β*t)	Median of Ln [Mt]	Median+2σ	Median-2σ	STDEV
60	1.01832	1.01962	1.01962	1.01207	1.01962	1.02112	1.01811	7.52E-04
600	0.72631	0.72470	0.72160	1.12750	0.72470	0.72949	0.71991	2.39E-03
1200	0.20301	0.20029	0.19505	1.27125	0.20029	0.20838	0.19220	4.05E-03
1800	-0.44712	-0.45234	-0.46243	1.43333	-0.45234	-0.43678	-0.46790	7.78E-03
2400	-1.02868	-1.03804	-1.05623	1.61607	-1.03804	-1.01002	-1.06605	1.40E-02

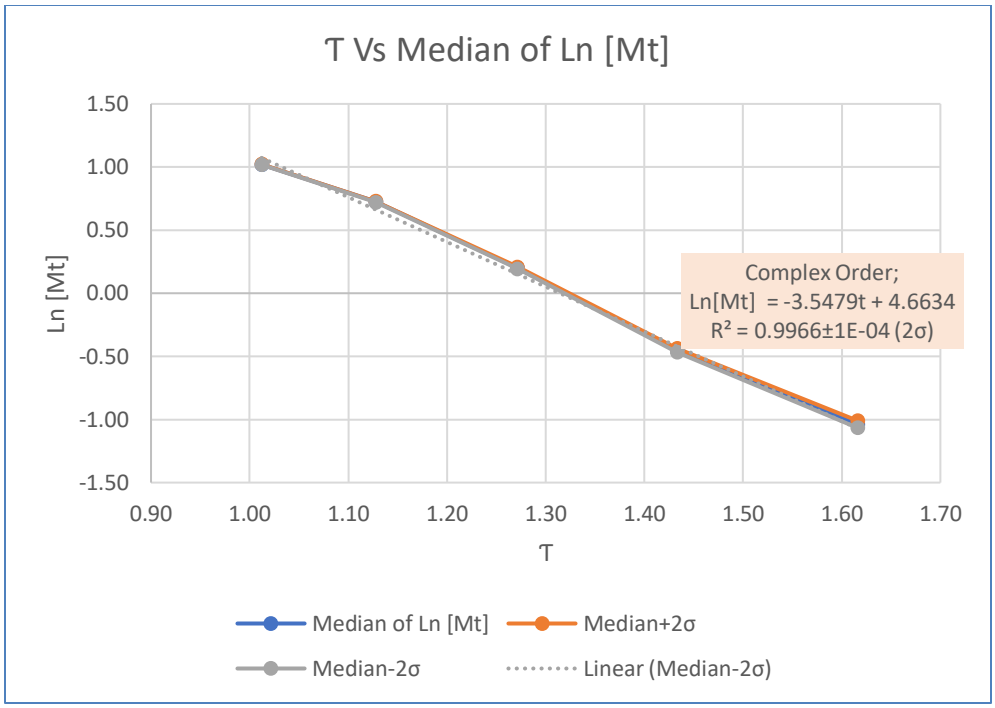

Figure 59. Slope, Intercept, and R^2 for Polymers with 150 ppm Each Initiator (H_2O_2, AsA, APS) Made with FRSP with 20% AA and @ 273K Polymerization Temperature

Table 24. Ln [M_t]s and Median of Top 3 and Bottom 3 Times at 150 ppm of Each H_2O_2, AsA, APS Initiator Levels for Polymers Made with FRSP with 20% AA and @ 273K Polymerization Temperature **(ß=0.0002)**

T=EXP(β*t)	Median of Ln [Mt]	Median of Ln [Mt]
1.012072289	1.019617541	
1.127496852	0.72470071	
1.27124915	0.200292151	0.200292151
1.433329415		-0.452342033
1.616074402		-1.038036647

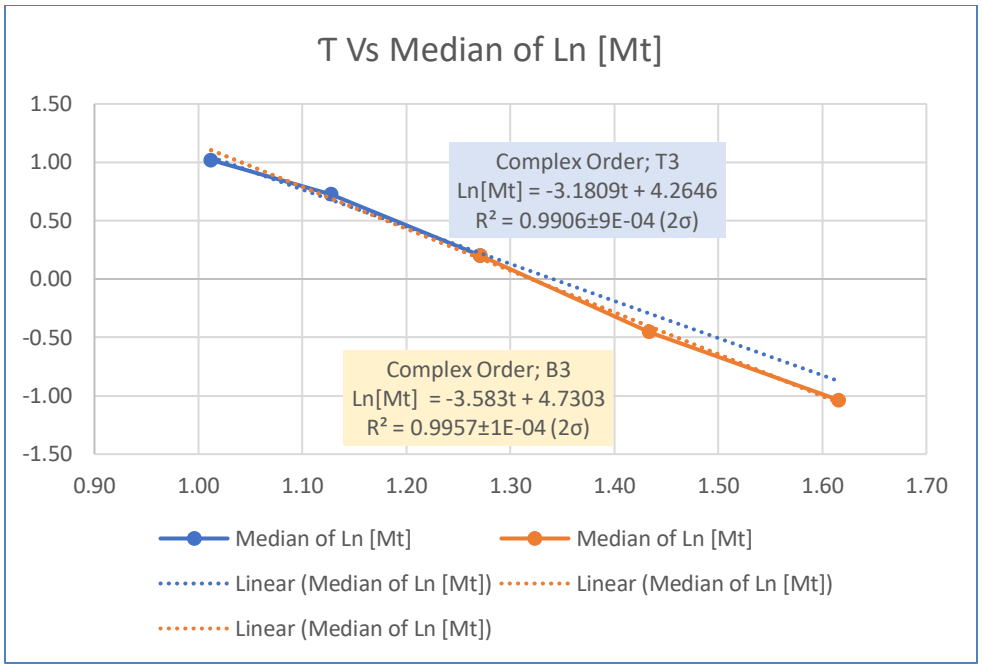

Figure 60. Slope, Intercept, and R^2 of Top 3 and Bottom 3 Times for Polymers with 150ppm Each Initiator (H_2O_2, AsA, APS) Made with FRSP with 20% AA and @ 273K Polymerization Temperature

Table 25. Time, Ln [Mt]s, Median, STDEV, and σ for Polymers with 150ppm Each Initiator (H_2O_2, AsA, APS) for Polymers Made with FRSP with 20% AA and @ 273K Polymerization Temperature **(ß=0.0003)**

β= 0.000300								
Time(Sec.)	Ln [Mt]1	Ln [Mt]2	Ln [Mt]3	T=EXP(β*t)	Median of Ln [Mt]	Median+2δ	Median-2δ	STDEV
60	1.01832	1.01962	1.01962	1.01816	1.01962	1.02112	1.01811	7.52E-04
600	0.72631	0.72470	0.72160	1.19722	0.72470	0.72949	0.71991	2.39E-03
1200	0.20301	0.20029	0.19505	1.43333	0.20029	0.20838	0.19220	4.05E-03
1800	-0.44712	-0.45234	-0.46243	1.71601	-0.45234	-0.43678	-0.46790	7.78E-03
2400	-1.02868	-1.03804	-1.05623	2.05443	-1.03804	-1.01002	-1.06605	1.40E-02

Table 26. Ln [M_t]s and Median of Top 3 and Bottom 3 Times at 150ppm of Each H_2O_2, AsA, APS Initiator Levels for Polymers Made with FRSP with 20% AA and @ 273K Polymerization Temperature **(ß=0.0002)**

T=EXP(β*t)	Median of Ln [Mt]	Median of Ln [Mt]
1.0182	1.0196	
1.1972	0.7247	
1.4333	0.2003	0.2003
1.7160		-0.4523
2.0544		-1.0380

Table 27. Time, Ln [Mt]s, Median, STDEV, and σ for Polymers with 150ppm Each Initiator (H_2O_2, AsA, APS) for Polymers Made with FRSP with 20% AA and @ 273K Polymerization Temperature **(ß=0.0045)**

β= 0.004500								
Time(Sec.)	Ln [Mt]1	Ln [Mt]2	Ln [Mt]3	T=EXP(β*t)	Median of Ln [Mt]	Median+2σ	Median-2σ	STDEV
60	1.01832	1.01962	1.01962	1.30996	1.01962	1.02112	1.01811	7.52E-04
600	0.72631	0.72470	0.72160	14.87973	0.72470	0.72949	0.71991	2.39E-03
1200	0.20301	0.20029	0.19505	221.40642	0.20029	0.20838	0.19220	4.05E-03
1800	-0.44712	-0.45234	-0.46243	3294.46808	-0.45234	-0.43678	-0.46790	7.78E-03
2400	-1.02868	-1.03804	-1.05623	49020.80114	-1.03804	-1.01002	-1.06605	1.40E-02

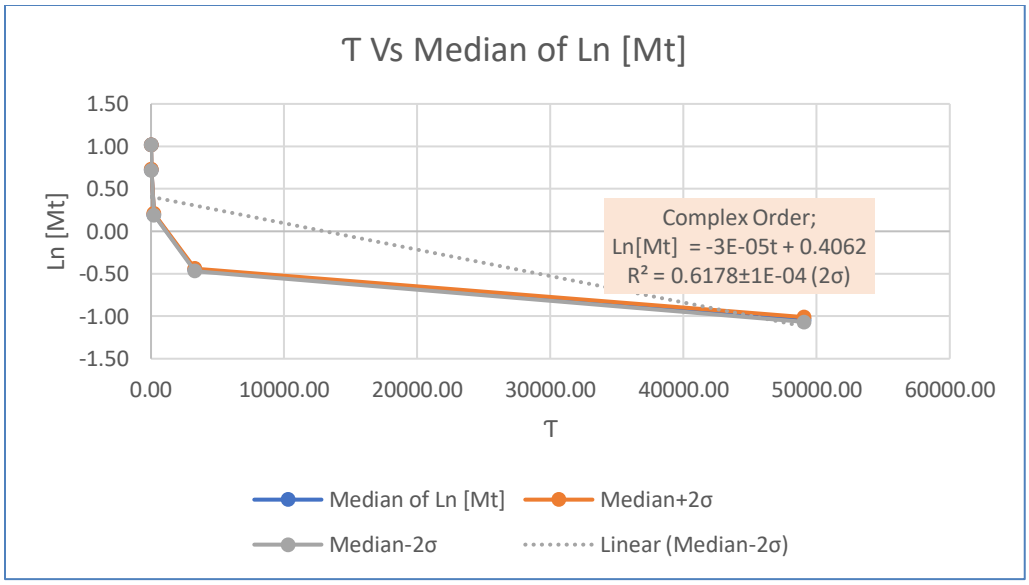

Figure 61. Slope, Intercept, and R^2 for Polymers with 150ppm Each Initiator (H_2O_2, AsA, APS) Made with FRSP with 20% AA and @ 273K Polymerization Temperature

Table 28. Ln [M_t]s and Median of Top 3 and Bottom 3 Times with 150ppm Each Initiator (H_2O_2, AsA, APS) for Polymers Made with FRSP with 20% AA and @ 273K Polymerization Temperature **(ß=0.0002)**

T=EXP(β*t)	Median of Ln [Mt]	Median of Ln [Mt]
1.3100	1.0196	
14.8797	0.7247	
221.4064	0.2003	0.2003
3294.4681		-0.4523
49020.8011		-1.0380

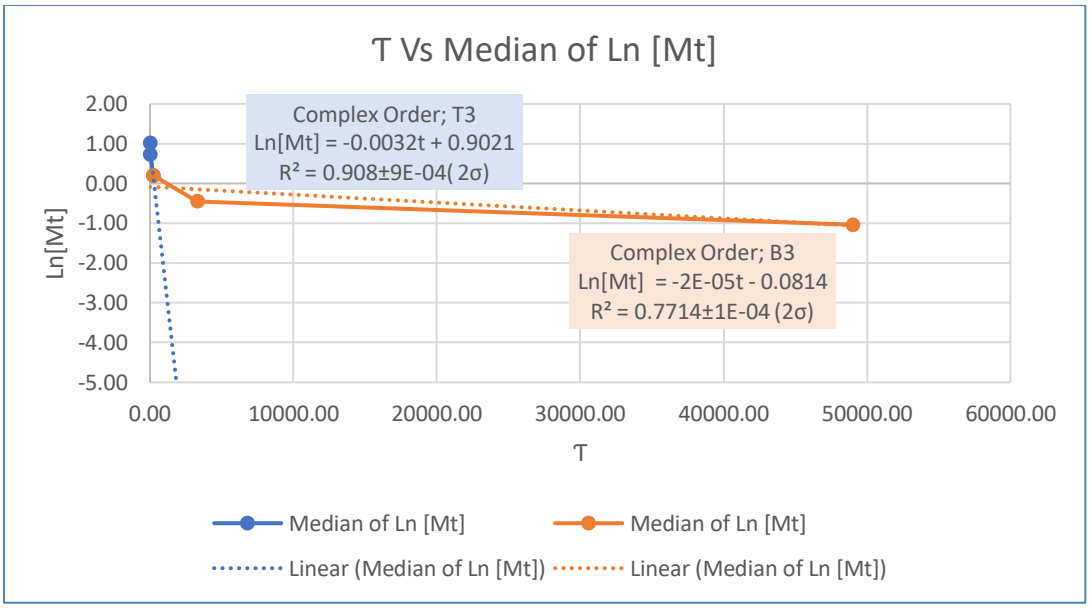

Figure 62. Slope, Intercept, and R^2 of Top 3 and Bottom 3 times for Polymers with 150ppm Each Initiator (H_2O_2, AsA, APS) Made with FRSP with 20% AA and @ 273K Polymerization Temperature

Table 29. Slopes, Intercepts, and R^2s in Triplicate for Polymers with 150ppm Each Initiator (H_2O_2, AsA, APS) for Polymers Made with FRSP with 20% AA and @ 273K Polymerization Temperature

Slope	Intercept	R2	Slope	Intercept	R2	Slope	Intercept	R2	
-0.00106	2.69710	0.96949	-0.00106	2.69796	0.96917	-0.00107	2.69543	0.96886	All 5(zero Order)
-0.00135	2.86034	0.99950	-0.00136	2.86302	0.99962	-0.00137	2.86218	0.99971	Top 3(zero Order)
-0.00072	2.04209	0.96078	-0.00072	2.03876	0.96078	-0.00072	2.03238	0.96078	Bottom 3(zero Order)
-0.00090	1.18237	0.98868	-0.00090	1.18399	0.98874	-0.00091	1.18563	0.98864	All 5(1st Order)
-0.00072	1.09442	0.98268	-0.00072	1.09558	0.98321	-0.00073	1.09564	0.98363	Top 3(1st Order)
-0.00103	1.42328	0.99897	-0.00103	1.42746	0.99903	-0.00104	1.43572	0.99914	Bottom 3(1st Order)

Table 30. Slopes, Intercepts, and R^2s in Triplicate for Polymers at Different Initiator Levels for Polymers Made with MAP with 45% AA, 3 ppm Initiator, and @ 293K Polymerization Temperature

Slope	Intercept	R2	Slope	Intercept	R2	Slope	Intercept	R2	
-0.01216	6.32809	0.79179	-0.01216	1.87766	0.79179	-0.01216	6.32497	0.79179	All (Zero Order
-0.02392	7.59490	0.99257	-0.02392	7.58303	0.99257	-0.02392	7.59178	0.99257	Top Three(Zero Order)
-0.00113	3.56536	0.99936	-0.00113	3.55350	0.99936	-0.00113	3.56224	0.99936	Bottom Three(Zero Order)
-0.00274	-0.00274	0.82366	-0.00275	-0.00275	0.82374	-0.00274	-0.00274	0.82368	All (First Order)
-0.00514	2.13858	1.00000	-0.00516	2.13753	1.00000	-0.00515	2.13830	1.00000	Top Three(First Order)
-0.00034	1.27436	0.99902	-0.00034	1.27104	0.99902	-0.00034	1.27348	0.99902	Bottom Three(First Order)

Table 31. Time, [M_t]s, and Median for Polymers with 150ppm Each Initiator (H_2O_2, AsA, APS) for Polymers Made with FRSP with 20% AA and @ 273K Polymerization Temperature

Time (Sec.)	Yield1 [Mt]	Yield 2 [Mt]	Yield3 [Mt]	Median
60.00000	2.76853	2.77213	2.77213	2.77213
600.00000	2.06744	2.06411	2.05773	2.06411
1200.00000	1.22509	1.22176	1.21538	1.22176
1800.00000	0.63947	0.63614	0.62975	0.63614
2400.00000	0.35748	0.35415	0.34777	0.35415

Table 32. Median of Top Three for First Order Reactions and Bottom Three for First-Order Reactions for Polymers with 150ppm Each Initiator (H_2O_2, AsA, APS) for Polymers Made with FRSP with 20% AA and @ 273K Polymerization Temperature

Time (Sec.)	Ln Mt1	Ln Mt2	Ln Mt3	Median
60.00000	1.01832	1.01962	1.01962	1.01962
600.00000	0.72631	0.72470	0.72160	0.72470
1200.00000	0.20301	0.20029	0.19505	0.20029
1800.00000	-0.44712	-0.45234	-0.46243	-0.45234
2400.00000	-1.02868	-1.03804	-1.05623	-1.03804

Table 33. Median of Top Three (T3) and Bottom Three (B3) for Zero Order and First-Order Reactions for Polymers with 150ppm Each Initiator (H_2O_2, AsA, APS) for Polymers Made with FRSP with 20% AA and @ 273K Polymerization Temperature

Trial 125, 20% AA, 273K H2O2=150ppm, AsA=150ppm, APS=150 ppm			Trial 125, 20% AA, 273 K H2O2=150ppm, AsA=150ppm, APS=150 ppm	
Time (Sec.)	Median 0 (T3)	Median 1 (B3)	Median 1 (T3)	Median 1 (B3)
60	2.772134333		1.019617541	
600	2.064113239		0.72470071	
1200	1.221759645	1.221759645	0.200292151	0.200292151
1800		0.636136553		-0.452342033
2400		0.35414932		-1.038036647

Table 34. Median of Top Three for Zero Order and Bottom Three for First-Order Reactions for Polymers with 150ppm Each Initiator (H_2O_2, AsA, APS) for Polymers Made with FRSP with 20% AA and @ 273K Polymerization Temperature

Time (Sec.)	Median 0 (T3)	Median 1 (B3)
60	2.772134333	
600	2.064113239	
1200	1.221759645	0.200292151
1800		-0.452342033
2400		-1.038036647

Table 35. Time, Ln [M_t]s, Median, STDEV, and σ for Polymers at 3 ppm Initiator Level for Polymers Made with 45% AA and @ 293K Polymerization Temperature with MAP **(ß = 0.000002)**

β= 0.0000020								
Time(Sec.)	Ln Mt1	Ln Mt2	Ln Mt3	Tau=EXP(b*t)	Median	Median+2δ	Median-2δ	STDEV
60	1.829631	1.8277254	1.82913	1.00012	1.82913	1.83111	1.82715	0.00099
120	1.522025	1.51943212	1.52134	1.00024	1.52134	1.52403	1.51865	0.00134
180	1.212409	1.20887335	1.21148	1.00036	1.21148	1.21515	1.20781	0.00183
240	1.192995	1.18938946	1.19205	1.00048	1.19205	1.19579	1.18831	0.00187
300	1.171359	1.16767454	1.17039	1.00060	1.17039	1.17421	1.16657	0.00191

Table 36. Ln [M_t]s and Median of Top 3 and Bottom 3 Times at 3 ppm Initiator Level for Polymers Made with MAP with 45% AA and @ 293K Polymerization Temperature **(ß=0.000002)**

T=EXP(β*t)	Median (T3)	Median (B3)
1.0001	1.8291	
1.0002	1.5213	
1.0004	1.2115	1.2115
1.0005		1.1920
1.0006		1.1704

Table 37. Time, Ln [M_t]s, Median, STDEV, and σ for Polymers at 3 ppm Initiator Level for Polymers Made with 45% AA and @ 293K Polymerization Temperature with MAP **(ß = 0.002)**

β= 0.0020000								
Time(Sec.)	Ln Mt1	Ln Mt2	Ln Mt3	T=EXP(β*t)	Median	Median+2δ	Median-2δ	STDEV
60	1.829631	1.8277254	1.82913	1.12750	1.82913	1.83111	1.82715	0.00099
120	1.522025	1.51943212	1.52134	1.27125	1.52134	1.52403	1.51865	0.00134
180	1.212409	1.20887335	1.21148	1.43333	1.21148	1.21515	1.20781	0.00183
240	1.192995	1.18938946	1.19205	1.61607	1.19205	1.19579	1.18831	0.00187
300	1.171359	1.16767454	1.17039	1.82212	1.17039	1.17421	1.16657	0.00191

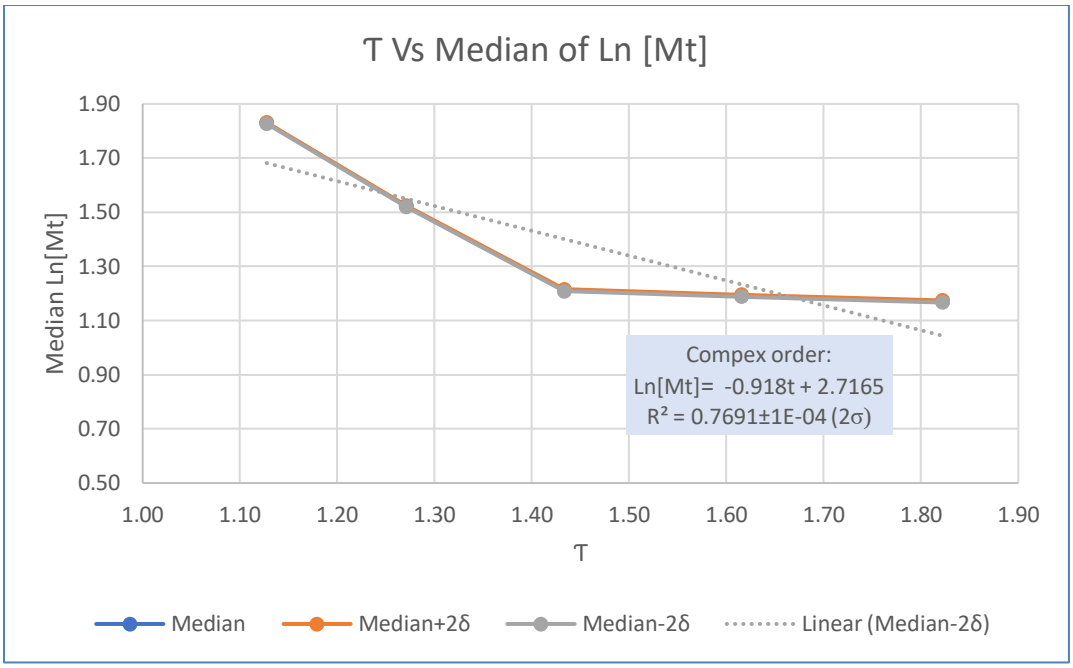

Figure 63. Slope, Intercept, and R^2 for Polymers at 3 ppm Initiator Level Made with MAP with 45% AA and @ 293K Polymerization Temperature **(ß = 0.002)**

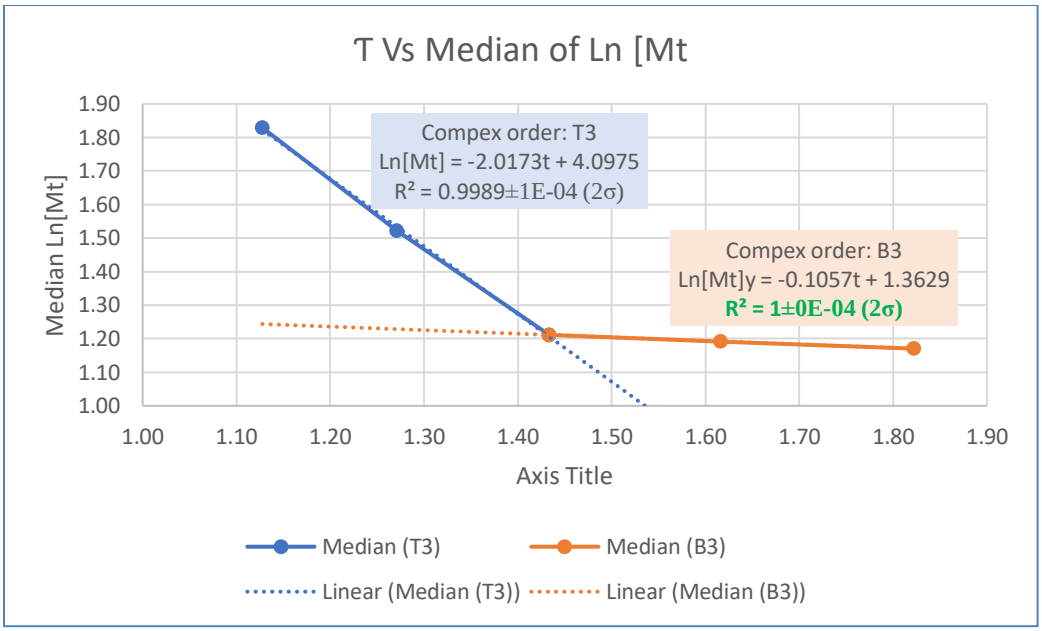

Figure 64. Slope, Intercept, and R^2 of Top 3 and Bottom 3 Times for Polymers at 3 ppm Initiator Level Made with MAP with 45% AA and @ 293K Polymerization Temperature **(ß = 0.002)**

Table 38. Ln [M_t]s and Median of Top 3 and Bottom 3 Times at 3 ppm Initiator Level for Polymers Made with MAP with 45% AA and @ 293K Polymerization Temperature **(ß=0.002)**

T=EXP(β*t)	Median (T3)	Median (B3)
1.1275	1.8291	
1.2712	1.5213	
1.4333	1.2115	1.2115
1.6161		1.1920
1.8221		1.1704

Table 39. Time, Ln [M_t]s, Median, STDEV, and σ for Polymers at 3 ppm Initiator Level for Polymers Made with 45% AA and @ 293K Polymerization Temperature with MAP **(ß = 0.0045)**

β= 0.0045000								
Time(Sec.)	Ln Mt1	Ln Mt2	Ln Mt3	T=EXP(β*t)	Median	Median+2δ	Median-2δ	STDEV
60	1.829631	1.8277254	1.82913	1.30996	1.82913	1.83111	1.82715	0.00099
120	1.522025	1.51943212	1.52134	1.71601	1.52134	1.52403	1.51865	0.00134
180	1.212409	1.20887335	1.21148	2.24791	1.21148	1.21515	1.20781	0.00183
240	1.192995	1.18938946	1.19205	2.94468	1.19205	1.19579	1.18831	0.00187
300	1.171359	1.16767454	1.17039	3.85743	1.17039	1.17421	1.16657	0.00191

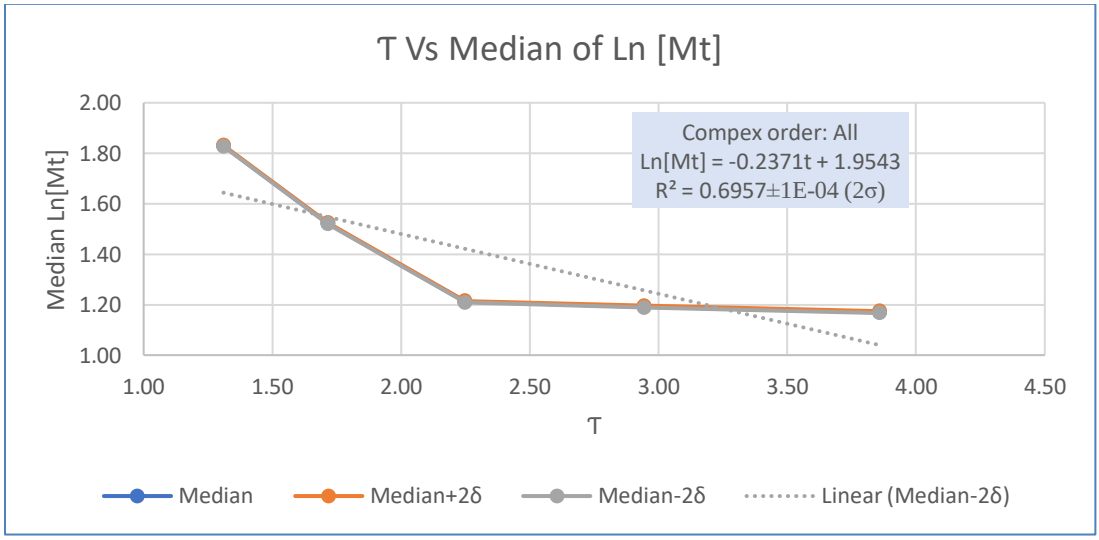

Figure 65. Slope, Intercept, and R^2 of Top 3 and Bottom 3 Times for Polymers at 3 ppm Initiator Level Made with MAP with 45% AA and @ 293K Polymerization Temperature **(ß = 0.0045)**

Table 40. Ln [Mt]s and Median of Top 3 and Bottom 3 Times at 3 ppm Initiator Level for Polymers Made with MAP with 45% AA and @ 293K Polymerization Temperature **(ß=0.0045)**

T=EXP(β*t)	Median (T3)	Median (B3)
1.309964451	1.82913005	
1.716006862	1.52134352	
2.247907987	1.21147994	1.211479942
2.944679551		1.192047273
3.857425531		1.170390619

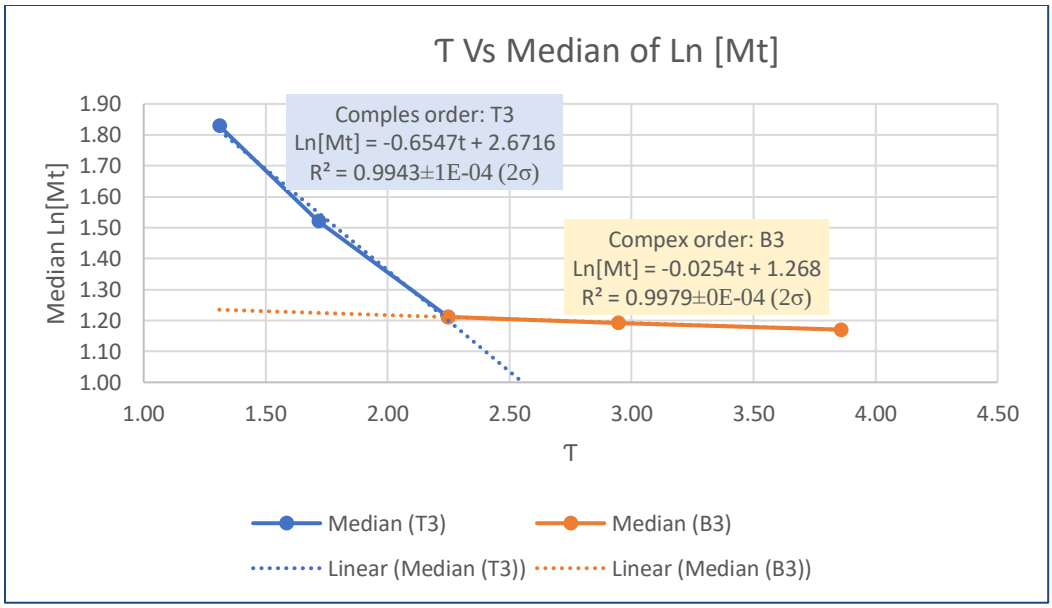

Figure 66. Slope, Intercept, and R^2 of Top 3 and Bottom 3 Times for Polymers at 3 ppm Initiator Level Made with MAP with 45% AA and @ 293K Polymerization Temperature **(ß = 0.0045)**

Table 41. Median of all 5 Points for Zero Order Reactions for Polymers with 45% AA, 3 ppm Initiator, and @ 293K Polymerization Temperature Made with MAP

Time (Sec.)	Yield1 [Mt]	Yield2 [Mt]	Yield3 [Mt]	Median
60	6.23158826	6.219723147	6.228465862	6.22846586
120	4.581494588	4.569629475	4.57837219	4.57837219
180	3.361573689	3.349708576	3.358451291	3.35845129
240	3.29694005	3.285074938	3.293817652	3.29381765
300	3.226373855	3.214508743	3.223251457	3.22325146

Table 42. Median of Top Three for Zero Order Reaction and Bottom Three for Zero Order Reactions for Polymers Made with MAP with 45% AA, 3 ppm Initiator, and @ 293K Polymerization Temperature

Time (Sec.)	Median Zero Order (T3)	Median Zero Order (B3)
60	6.228465862	
120	4.57837219	
180	3.358451291	3.358451291
240		3.293817652
300		3.223251457

Table 43. Time, Ln [M_t]s, and Median for Polymers Made with MAP with 45% AA, 3 ppm Initiator, and @ 293K Polymerization Temperature

Time (Sec.)	Ln Mt1	Ln Mt2	Ln Mt3	Median
60	1.829631238	1.827725396	1.829130052	1.82913005
120	1.522025274	1.519432124	1.521343518	1.52134352
180	1.212409224	1.20887335	1.211479942	1.21147994
240	1.192994781	1.189389464	1.192047273	1.19204727
300	1.171358861	1.167674544	1.170390619	1.17039062

Table 44. Median of Top Three for First Order Reaction and Top and Bottom Three for First Order Reactions for Polymers Made with MAP with 45% AA, 3 ppm Initiator, and @ 293K Polymerization Temperature

Time (Sec.)	Median First Order (T3)	Median First Order (B3)
60	1.829130052	
120	1.521343518	
180	1.211479942	1.211479942
240		1.192047273
300		1.170390619

Table 45. Median of Top Three for First Order Reaction and Top and Bottom Three for First Order Reactions for Polymers Made with MAP with 45% AA, 3 ppm Initiator, and @ 293K Polymerization Temperature

Trial 279, 45% AA, 293K 3 ppm Initiator, Zero Order			**Trial 279, 45% AA, 293 K 3 ppm Initiator, First order**		
Time (Sec.)	Median 0(T3)	Median 0(B3)	Time (Sec.)	Median 1(T3)	Median 1(B3)
60	6.228465862		60	1.829130052	
120	4.57837219		120	1.521343518	
180	3.358451291	3.358451291	180	1.211479942	1.211479942
240		3.293817652	240		1.192047273
300		3.223251457	300		1.170390619

Table 46. Median of Top Three for First Order Reaction and Top and Bottom Three for First Order Reactions for Polymers Made with MAP with 45% AA, 3 ppm Initiator, and @ 293K Polymerization Temperature

Time (Sec.)	Median 0 (T3)	Median 1(B3)
60	6.228465862	
120	4.57837219	
180	3.358451291	1.211479942
240		1.192047273
300		1.170390619

Table 47. Arrhenius Table for FRSP at Different Temperature and Constant Initiator (Zero Order, Top 3)

H2O2	ASA	APS		
100	100	100		
Temp.(K)	**1/Temp.(K^{-1})**	**Slope (S)**	**S-2Sigma**	**S+2Sigma**
273	3.66E-03	-7.53E-04	-1.07E-03	-4.31E-04
275	3.64E-03	-8.02E-04	-1.12E-03	-4.81E-04
277	3.61E-03	-8.44E-04	-1.16E-03	-5.25E-04
279	3.58E-03	-8.81E-04	-1.20E-03	-5.62E-04
281	3.56E-03	-9.12E-04	-1.23E-03	-5.92E-04
283	3.53E-03	-9.36E-04	-1.26E-03	-6.16E-04
285	3.51E-03	-9.54E-04	-1.27E-03	-6.34E-04
287	3.48E-03	-9.65E-04	-1.29E-03	-6.45E-04
288	3.47E-03	-9.69E-04	-1.29E-03	-6.47E-04

Table 48. Arrhenius Table for FRSP at Different Temperature and Constant Initiator (First Order, Top 3)

H2O2	ASA	APS		
150	150	150		
Temp.(K)	**1/Temp.(K^{-1})**	**Slope (S)**	**S-2Sigma**	**S+2Sigma**
273	3.66E-03	-8.54E-04	-1.17E-03	-5.34E-04
275	3.64E-03	-8.85E-04	-1.20E-03	-5.66E-04
277	3.61E-03	-9.10E-04	-1.23E-03	-5.91E-04
279	3.58E-03	-9.28E-04	-1.25E-03	-6.10E-04
281	3.56E-03	-9.41E-04	-1.26E-03	-6.11E-04
283	3.53E-03	-9.47E-04	-1.27E-03	-6.29E-04
285	3.51E-03	-9.47E-04	-1.27E-03	-6.29E-04
287	3.48E-03	-9.41E-04	-1.26E-03	-6.23E-04
288	3.47E-03	-9.36E-04	-1.25E-03	-6.17E-04

Table 49. Arrhenius Table for FRSP at Different Temperature and Constant Initiator (First Order, Bottom 3)

H_2O_2	ASA	APS		
200 ppm	200 ppm	200ppm		
Temp.(K)	**1/Temp.(K^{-1})**	**Slope (S)**	**S-2Sigma**	**S+2Sigma**
273	3.66E-03	-9.27E-04	-1.25E-03	-6.06E-04
275	3.64E-03	-9.41E-04	-1.26E-03	-6.20E-04
277	3.61E-03	-9.48E-04	-1.27E-03	-6.28E-04
279	3.58E-03	-9.49E-04	-1.27E-03	-6.29E-04
281	3.56E-03	-9.43E-04	-1.26E-03	-6.24E-04
283	3.53E-03	-9.32E-04	-1.25E-03	-6.12E-04
285	3.51E-03	-9.14E-04	-1.23E-03	-5.94E-04
287	3.48E-03	-8.90E-04	-1.21E-03	-5.69E-04
288	3.47E-03	-8.76E-04	-1.20E-03	-5.54E-04

Table 50. Arrhenius Table for MAP at Different Temperature and Constant Initiator (Zero Order, Top 3)

Initiator(ppm)	AA%			
2	40			
Temp.(K)	**1/Temp.(K^{-1})**	**Slope (S)**	**S-2Sigma**	**S+2Sigma**
273	3.66E-03	-2.80E-03	-1.37E-02	8.00E-03
275	3.64E-03	-3.00E-03	-1.39E-02	7.90E-03
277	3.61E-03	-3.10E-03	-1.40E-02	7.70E-03
279	3.58E-03	-3.20E-03	-1.41E-02	7.60E-03
281	3.56E-03	-3.30E-03	-1.42E-02	7.60E-03
283	3.53E-03	-3.30E-03	-1.42E-02	7.50E-03
285	3.51E-03	-3.40E-03	-1.43E-02	7.50E-03
287	3.48E-03	-3.40E-03	-1.43E-02	7.50E-03
289	3.46E-03	-3.40E-03	-1.42E-02	7.50E-03
291	3.44E-03	-3.30E-03	-1.42E-02	7.60E-03
293	3.41E-03	-3.20E-03	-1.41E-02	7.60E-03
295	3.39E-03	-3.10E-03	-1.40E-02	7.70E-03
297	3.37E-03	-3.00E-03	-1.39E-02	7.80E-03
299	3.34E-03	-2.90E-03	-1.38E-02	8.00E-03
301	3.32E-03	-2.70E-03	-1.36E-02	8.10E-03
303	3.30E-03	-2.50E-03	-1.34E-02	8.40E-03

Table 51. Arrhenius Table for MAP at Different Temperature and Constant Initiator (Zero Order, Bottom 3)

Initiator(ppm)	AA%			
0	40			
Temp.(K)	**1/Temp.(K^{-1})**	**Slope (S)**	**S-2Sigma**	**S+2Sigma**
273	3.66E-03	4.10E-03	-6.80E-03	1.51E-02
275	3.64E-03	4.00E-03	-6.90E-03	1.49E-02
277	3.61E-03	3.90E-03	-7.00E-03	1.48E-02
279	3.58E-03	3.90E-03	-7.00E-03	1.47E-02
281	3.56E-03	3.80E-03	-7.10E-03	1.47E-02
283	3.53E-03	3.80E-03	-7.10E-03	1.47E-02
285	3.51E-03	3.80E-03	-7.10E-03	1.47E-02
287	3.48E-03	3.80E-03	-7.10E-03	1.47E-02
289	3.46E-03	3.90E-03	-7.10E-03	1.48E-02
291	3.44E-03	3.90E-03	-7.00E-03	1.49E-02
293	3.41E-03	4.00E-03	-6.90E-03	1.49E-02
295	3.39E-03	4.10E-03	-6.80E-03	1.50E-02
297	3.37E-03	4.30E-03	-6.60E-03	1.52E-02
299	3.34E-03	4.40E-03	-6.40E-03	1.53E-02
301	3.32E-03	4.60E-03	-6.30E-03	1.55E-02
303	3.30E-03	4.80E-03	-6.10E-03	1.58E-02

Table 52. Arrhenius Table for MAP at Different Temperature and Constant Initiator (First Order, Top 3)

Initiator(ppm)	AA%			
20	40			
Temp.(K)	**1/Temp.(K^{-1})**	**Slope (S)**	**S-2Sigma**	**S+2Sigma**
273	3.66E-03	-4.30E-03	-1.53E-02	6.70E-03
275	3.64E-03	-4.80E-03	-1.57E-02	6.20E-03
277	3.61E-03	-5.20E-03	-1.61E-02	5.70E-03
279	3.58E-03	-5.50E-03	-1.64E-02	5.40E-03
281	3.56E-03	-5.70E-03	-1.66E-02	5.20E-03
283	3.53E-03	-5.70E-03	-1.66E-02	5.20E-03
285	3.51E-03	-5.70E-03	-1.66E-02	5.20E-03
287	3.48E-03	-5.60E-03	-1.65E-02	5.40E-03
289	3.46E-03	-5.30E-03	-1.62E-02	5.60E-03
291	3.44E-03	-4.90E-03	-1.58E-02	6.00E-03
293	3.41E-03	-4.50E-03	-1.54E-02	6.40E-03
295	3.39E-03	-3.90E-03	-1.48E-02	7.00E-03
297	3.37E-03	-3.20E-03	-1.41E-02	7.70E-03
299	3.34E-03	-2.40E-03	-1.33E-02	8.50E-03
301	3.32E-03	-1.40E-03	-1.24E-02	9.50E-03
303	3.30E-03	-4.00E-04	-1.14E-02	1.06E-02

APPENDIX B

TABLES AND FIGURES-PAPER 4

Table 53. Measured Polymer Properties at Different Acid Contents (Free Radical Solution Polymerization) AA-1: 1.5% Clay, AA-2: 3.5% Clay, AA-3: 5% Clay, 150ppm Each Initiator

Samples	CRC (g/g)	0.9AUL (g/g)	PI (Darcy)	RAA (ppm)	Yield (%)	PAI (g/g)
31%AA-1	22.5	5.4	2	39854	5.4	53.2
	18.2	6.7	4	19635	18.9	63.7
Mean	20.35	6.05	3	29744.5	12.15	58.45
STDEV	3.04	0.92	1.41	14296.99	9.55	7.42
31%AA-2	19.4	6.8	9	24689	6.9	44.4
	16.3	10.1	2	31265	21.1	75.1
Mean	17.85	8.45	5.50	27977.00	14.00	59.75
STDEV	2.19	2.33	4.95	4649.93	10.04	21.71
31%AA-3	34.1	12.3	35	12578	15.4	55.9
	18.6	6.7	4	36458	21.5	63.2
Mean	26.35	9.5	19.5	24518	18.45	59.55
STDEV	10.96	3.96	21.92	16885.71	4.31	5.16
35%AA-1	10.1	6.6	19	9524	24.9	63.4
	29.5	12.3	5	35698	15.9	43.2
Mean	19.8	9.45	12	22611	20.4	53.3
STDEV	13.72	4.03	9.90	18507.81	6.36	14.28
35%AA-2	19.4	5.8	5	34567	18.3	29.7
	15.43	4.9	17	3941	28.1	71.2
Mean	17.42	5.35	11.00	19254.00	23.20	50.45
STDEV	2.81	0.64	8.49	21655.85	6.93	29.34
35%AA-3	15.4	9.5	7	65489	15.8	49.7
	17.8	5.4	3	13256	25.9	63.2
Mean	16.6	7.45	5	39372.5	20.85	56.45
STDEV	1.70	2.90	2.83	36934.31	7.14	9.55
50%AA-1	35.1	4.6	1	65478	2.5	31.7
	12.3	8.5	6	23546	45.3	69.5
Mean	23.70	6.55	3.50	44512.00	23.90	50.60
STDEV	16.12	2.76	3.54	29650.40	30.26	26.73
50%AA-2	29	6.3	27	75243	4.9	39.8
	18.6	9.4	8	12654	35.8	42.3
Mean	23.80	7.85	17.50	43948.50	20.35	41.05
STDEV	7.35	2.19	13.44	44257.11	21.85	1.77
50%AA-3	11.4	10.2	3	39644	7.7	24.5
	25.4	10.2	19	36625	45.4	49.7

Mean	18.4	10.2	11	38134.5	26.55	37.1
STDEV	9.90	0.00	11.31	2134.76	26.66	17.82

Table 54. Measured Polymer Properties at Different Acid Contents (Microwave-Assisted Polymerization), AA-1: 1.5% Clay, AA-2: 3.5% Clay, AA-3: 5% Clay, 5 ppm of Initiator

Samples	CRC (g/g)	0.9AUL (g/g)	PI (Darcy)	RAA (g/g)	Yield (%)	PAI (g/g)
31%AA-1	33.5	21.8	15	765	97.5	129.8
	33.7	21.6	18	763	98.2	130.4
Mean	33.6	21.7	16.5	764	97.85	130.1
STDEV	0.14	0.14	2.12	1.41	0.49	0.42
31%AA-2	33.7	22	27	625	98.2	129.3
	33.6	24	29	543	98.4	128.7
Mean	33.65	23	28	584	98.3	129
STDEV	0.07	1.41	1.41	57.98	0.14	0.42
31%AA-3	33.6	23.1	39	530	97.9	130.9
	33.5	23.4	42	596	98.1	129.9
Mean	33.55	23.25	40.5	563	98	130.4
STDEV	0.07	0.21	2.12	46.67	0.14	0.71
35%AA-1	34.1	23.1	18	770	96.8	131.6
	33.9	22.8	21	765	97.2	131.1
Mean	34	22.95	19.5	767.5	97	131.35
STDEV	0.14	0.21	2.12	3.54	0.28	0.35
35%AA-2	33.4	23.4	31	632	97.1	131.8
	33.5	23.9	35	654	97.5	131.5
Mean	33.45	23.65	33	643	97.3	131.65
STDEV	0.07	0.35	2.83	15.56	0.28	0.21
35%AA-3	32.9	23.7	42	510	98.2	133.3
	33.1	24.1	49.6	498	98.5	133.7
Mean	33	23.9	45.8	504	98.35	133.5
STDEV	0.14	0.28	5.37	8.49	0.21	0.28
50%AA-1	33.6	23.5	23	740	96.7	131.9
	33.8	23.4	26	732	97.1	132.1
Mean	33.7	23.45	24.5	736	96.9	132
STDEV	0.14	0.07	2.12	5.66	0.28	0.14
50%AA-2	33.1	23.6	36	605	97.5	132.6
	33	23.7	38	598	97.8	133.2
Mean	33.05	23.65	37	601.5	97.65	132.9
STDEV	0.07	0.07	1.41	4.95	0.21	0.42
50%AA-3	33	23.9	44	430	97.9	134.9
	32.8	24.6	52	415	98.2	134.5
Mean	32.9	24.25	48	422.5	98.05	134.7
STDEV	0.14	0.49	5.66	10.61	0.21	0.28

Table 55. Percent of Clay in Fines and Polymers with Mass Balance and Ion Chromatography (Free Radical Solution Polymerization**)**, 31% AA, 150ppm of Each Initiator

% Clay & Fines with Mass Balance	Control (without Clay) %	1.5% Clay	3.5% Clay	5% Clay
% Fines & Clay - Sample 1	2.49	3.91	5.97	7.44
% Fines & Clay - Sample 2	2.38	2.83	5.88	6.48
% Fines & Clay - Sample 3	2.48	2.98	4.99	6.43
% Fines & Clay - Sample 4	2.37	3.96	5.82	5.35
% Fines & Clay - Sample 5	2.41	3.48	4.81	7.37
% Fines & Clay - Sample 6	2.41	3.88	3.77	7.49
Mean	2.42	3.51	5.21	6.76
STDEV	0.05	0.50	0.86	0.84
% Clay & Fines with Ion Chromatography	Control (with Clay) %	1.5% Clay	3.5% Clay	5% Clay
% Fines & Clay - Sample 1	0.01	1.2	1.2	2.5
% Fines & Clay - Sample 2	0.02	0.05	0.18	1.4
% Fines & Clay - Sample 3	0.00	0.03	3.2	0.07
% Fines & Clay - Sample 4	0.00	1.1	2.3	1.03
% Fines & Clay - Sample 5	0.03	1.3	1.1	4.89
% Fines & Clay - Sample 6	0.02	0.07	0.38	2.4
Mean	0.01	0.63	1.39	2.05
STDEV	0.01	0.63	1.16	1.66

Table 56. Percent of Clay in Fines and Polymers with Mass Balance and Ion Chromatography (Microwave Polymerization), 31% AA, 5ppm of Initiator

% Clay & Fines with Mass Balance	Control (without Clay) %	1.5% Clay	3.5% Clay	5% Clay
% Fines & Clay - Sample 1	2.4	2.41	2.47	2.44
% Fines & Clay - Sample 2	2.39	2.43	2.48	2.48
% Fines & Clay - Sample 3	2.41	2.38	2.39	2.4
% Fines & Clay - Sample 4	2.38	2.46	2.42	2.35
% Fines & Clay - Sample 5	2.39	2.48	2.41	2.37
% Fines & Clay - Sample 6	2.4	2.38	2.37	2.49
Mean	2.40	2.42	2.42	2.42
STDEV	0.01	0.04	0.04	0.06
% Clay & Fines with Ion Chromatography	Control (with Clay) %	1.5% Clay	3.5% Clay	5% Clay
% Fines & Clay - Sample 1	0	1.48	3.52	5.1
% Fines & Clay - Sample 2	0.01	1.48	3.47	5
% Fines & Clay - Sample 3	0.01	1.47	3.49	4.96
% Fines & Clay - Sample 4	0.02	1.51	3.49	4.95
% Fines & Clay - Sample 5	0.01	1.5	3.48	4.95
% Fines & Clay - Sample 6	0	1.49	3.47	4.99
Mean	0.01	1.49	3.49	4.99
STDEV	0.01	0.01	0.02	0.06

Table 57. Volume, Numbers, and Sizes of the Pores with and without Clay in Polymers with Free Radical Solution Polymerization and Microwave-Assisted Polymerization (31% AA, 150ppm of Each Initiator for FRSP and 5ppm Initiator for MAP)

					Volume= $4/3*\pi*r^3$			
Pore #	**FRSP (no clay) µm**	**FRSP (w/ clay) µm**	**MAP (no clay) µm**	**MAP (w/ clay) µm**	**FRSP (No Clay) (μm^3)**	**FRSP (w/ clay) (μm^3)**	**MAP (no Clay) (μm^3)**	**MAP (w/ clay) (μm^3)**
1.0	2.4	1.2	1.5	0.5	7.2	7.97E-01	1.77E+00	6.55E-02
2.0	2.3	1.1	0.7	0.1	6.4	6.97E-01	1.80E-01	5.24E-04
3.0	2.6	0.8	0.8	0.1	9.2	2.68E-01	2.68E-01	5.24E-04
4.0	2.6	0.8	0.3	0.1	9.2	2.21E-01	1.41E-02	5.24E-04
5.0	1.7	0.9	0.4	0.1	2.6	3.22E-01	3.35E-02	5.24E-04
6.0	1.8	2.2	1.1	0.1	3.1	5.58E+00	6.97E-01	5.24E-04
7.0	1.9	1.7	1.2	0.1	3.6	2.57E+00	9.05E-01	5.24E-04
8.0	1.4	5.6	0.7	0.1	1.4	9.20E+01	1.80E-01	5.24E-04
9.0	2.2	0.7	1.4	0.1	5.6	1.80E-01	1.44E+00	5.24E-04
10.0	2.4	0.5	0.4	0.1	7.2	6.55E-02	3.35E-02	5.24E-04
11.0	2.5	0.8	0.6	0.1	8.2	2.68E-01	1.13E-01	5.24E-04
12.0	1.2	0.6	0.5	0.1	0.9	1.13E-01	6.55E-02	5.24E-04

13.0	1.2	0.5	0.3	0.1	0.9	6.55E-02	1.41E-02	5.24E-04
14.0	1.2	0.5	0.8	0.1	0.9	6.55E-02	2.68E-01	5.24E-04
15.0	1.0	0.5	1.1	0.1	0.5	6.55E-02	6.97E-01	5.24E-04
16.0	2.6	0.7	0.6	0.1	9.2	1.80E-01	8.71E-02	5.24E-04
17.0	1.6	1.2	0.4	0.1	2.2	7.97E-01	3.35E-02	5.24E-04
18.0	1.9	1.1	1.1	0.1	3.6	6.97E-01	6.97E-01	5.24E-04
19.0	2.5	1.7	0.1	0.1	8.2	2.57E+00	5.24E-04	5.24E-04
20.0	1.1	0.4	0.1	0.1	0.7	3.35E-02	5.24E-04	5.24E-04
21.0	2.1	0.9	0.3	0.1	4.9	3.22E-01	1.41E-02	5.24E-04
22.0	0.9	1.2	0.7	0.1	0.4	9.05E-01	1.80E-01	5.24E-04
23.0	2.2	0.3	0.2	0.1	5.6	1.41E-02	4.19E-03	5.24E-04
24.0	0.6	2.8	0.2	0.1	0.1	1.15E+01	4.19E-03	5.24E-04
25.0	2.8	0.7	0.1	0.1	11.5	1.80E-01	5.24E-04	5.24E-04
26.0	2.9	0.6	0.5	0.1	12.8	1.13E-01	6.55E-02	5.24E-04
27.0	1.1	0.8	0.3	0.8	0.7	2.68E-01	1.41E-02	2.68E-01
28.0	2.0	1.6	1.6	0.1	4.2	2.15E+00	2.15E+00	5.24E-04
29.0	0.7	1.3	0.5	0.1	0.2	1.15E+00	6.55E-02	5.24E-04
30.0	0.8	1.3	0.3	0.1	0.3	1.15E+00	1.41E-02	5.24E-04
31.0	0.8	0.8	0.6	0.1	0.3	2.68E-01	1.13E-01	5.24E-04
32.0	2.1	0.8	0.3	0.1	4.9	2.68E-01	1.41E-02	5.24E-04
33.0	1.9	3.5	1.1	0.1	3.6	2.25E+01	6.97E-01	5.24E-04
34.0	4.6	1.8	0.2	1.5	51.0	3.05E+00	4.19E-03	1.77E+00
35.0	2.6	0.8	0.2	0.1	9.2	2.68E-01	4.19E-03	5.24E-04
36.0	1.9	2.7	0.2	0.1	3.6	1.03E+01	4.19E-03	5.24E-04
37.0	1.1	0.8	0.2	0.2	0.7	2.68E-01	4.19E-03	4.19E-03
38.0	8.9	0.9	0.2	0.3	369.3	3.82E-01	4.19E-03	1.41E-02
39.0	3.9	1.4	0.2	0.1	31.1	1.44E+00	4.19E-03	5.24E-04
40.0	3.7	0.2	0.2	0.3	26.5	4.19E-03	4.19E-03	1.41E-02
41.0	1.2	0.5	0.2	0.2	0.9	6.55E-02	4.19E-03	4.19E-03
42.0	1.1	0.6	1.9	0.1	0.7	1.13E-01	3.59E+00	5.24E-04
43.0	2.8	0.8	0.4	0.2	11.5	2.68E-01	3.35E-02	4.19E-03
44.0	1.2	0.1	0.8	0.1	0.9	5.24E-04	2.68E-01	5.24E-04
45.0			0.3	0.1			1.41E-02	5.24E-04
46.0			0.3	0.1			1.41E-02	5.24E-04
47.0			0.3	0.1			1.41E-02	5.24E-04
48.0			0.3	0.1			1.41E-02	5.24E-04
49.0			0.2	0.1			4.19E-03	5.24E-04
50.0			0.6	0.4			1.13E-01	3.35E-02
51.0			0.2	0.4			4.19E-03	3.35E-02
52.0			0.2	0.2			4.19E-03	4.19E-03
53.0			0.1	0.2			5.24E-04	4.19E-03
54.0			0.1	0.1			5.24E-04	5.24E-04
55.0			0.6	0.1			1.13E-01	5.24E-04
56.0			0.4	0.1			3.35E-02	5.24E-04
57.0			0.3	0.1			1.41E-02	5.24E-04
58.0			0.9	0.1			3.82E-01	5.24E-04

59.0			0.3	0.1			8.18E-03	5.24E-04
60.0			0.3	0.2			1.41E-02	4.19E-03
61.0			0.7	0.3			1.80E-01	1.41E-02
62.0			1.8	0.1			3.05E+00	5.24E-04
63.0			1.4	0.1			1.44E+00	5.24E-04
64.0			1.2	0.1			9.05E-01	5.24E-04
65.0			0.5	0.1			6.55E-02	5.24E-04
66.0			0.6	0.1			1.13E-01	5.24E-04
67.0			0.6	0.1			1.13E-01	5.24E-04
68.0			0.5	0.1			6.55E-02	5.24E-04
69.0			0.7	0.2			1.80E-01	4.19E-03
70.0			0.6	0.2			1.13E-01	4.19E-03
71.0			0.9	0.2			3.82E-01	4.19E-03
72.0			0.6	0.6			1.13E-01	1.13E-01
73.0			0.4	0.1			3.35E-02	5.24E-04
74.0			1.1	2.6			6.97E-01	9.21E+00
75.0			1.2	1.4			9.05E-01	1.44E+00
76.0			0.8	0.6			2.68E-01	1.13E-01
77.0			0.6	0.7			1.13E-01	1.80E-01
78.0			0.5	0.4			6.55E-02	3.35E-02
79.0				0.1				5.24E-04
80.0				0.1				5.24E-04
81.0				0.1				5.24E-04
82.0				0.1				5.24E-04
83.0				0.1				5.24E-04
84.0				0.1				5.24E-04
85.0				0.4				3.35E-02
86.0				0.2				4.19E-03
87.0				0.2				4.19E-03
88.0				0.2				4.19E-03
89.0				0.2				4.19E-03
90.0				0.2				4.19E-03
91.0				0.4				3.35E-02
92.0				0.6				1.13E-01
93.0				0.1				5.24E-04
94.0				0.1				5.24E-04
95.0				0.1				5.24E-04
96.0				0.1				5.24E-04
97.0				0.6				1.13E-01
98.0				0.9				3.82E-01
99.0				0.5				6.55E-02
100.0				0.8				2.68E-01
101.0				0.8				2.68E-01
102.0				0.1				5.24E-04
103.0				0.1				5.24E-04
104.0				0.1				5.24E-04

105.0				0.1				5.24E-04
106.0				0.1				5.24E-04
107.0				0.1				5.24E-04
108.0				0.1				5.24E-04
109.0				0.1				5.24E-04
110.0				0.1				5.24E-04
111.0				0.2				4.85E-03
112.0				0.9				3.82E-01
113.0				0.6				1.13E-01
114.0				1.0				4.49E-01
115.0				1.1				6.97E-01
116.0				0.8				2.21E-01
117.0				0.1				5.24E-04
118.0				0.1				5.24E-04
119.0				0.1				5.24E-04
120.0				0.1				5.24E-04
121.0				0.1				5.24E-04
122.0				0.1				5.24E-04
123.0				0.1				5.24E-04
124.0				0.4				3.35E-02
125.0				0.4				3.35E-02
126.0				0.8				2.68E-01
127.0				3.4				2.06E+01
128.0				1.2				9.05E-01
129.0				0.9				3.82E-01
130.0				1.0				4.49E-01
131.0				4.1				3.61E+01
132.0				0.1				5.24E-04
133.0				0.1				5.24E-04
134.0				0.1				5.24E-04
135.0				0.1				5.24E-04
136.0				0.1				5.24E-04
137.0				0.1				5.24E-04
138.0				0.1				5.24E-04
139.0				0.2				4.19E-03
140.0				0.2				4.19E-03
141.0				0.2				4.19E-03
142.0				0.7				1.80E-01
143.0				0.8				2.68E-01
144.0				0.2				4.19E-03
145.0				0.3				1.41E-02
146.0				0.4				3.35E-02
147.0				0.6				1.13E-01
148.0				0.8				2.68E-01
149.0				0.7				1.80E-01
150.0				0.8				2.21E-01

151.0				0.8				2.68E-01
152.0				1.1				6.06E-01
153.0				0.3				1.41E-02
154.0				0.3				1.41E-02
155.0				0.8				2.68E-01
156.0				1.1				6.97E-01
157.0				0.6				1.13E-01
158.0				0.9				3.82E-01
159.0				1.1				6.97E-01
160.0				0.4				3.35E-02
161.0				0.2				4.19E-03
162.0				1.1				6.97E-01
163.0				0.2				4.19E-03
164.0				1.0				5.24E-01
165.0				0.6				1.13E-01
166.0				0.2				4.19E-03
167.0				0.7				1.80E-01
168.0				0.9				3.22E-01
Ave.	**2.1**	**1.2**	**0.6**	**0.4**	**14.7**	**3.74E+00**	**3.12E-01**	**4.85E-01**
STDEV	**1.4**	**1.0**	**0.4**	**0.5**	**55.5**	**1.42E+01**	**6.48E-01**	**3.27E+00**
Sum	**92.0**	**50.5**	**45.5**	**62.1**	**645.4**	**1.64E+02**	**2.43E+01**	**8.15E+01**

Table 58. Surface Area, Numbers, and Sizes of the Pores with and without Clay in Polymers with Free Radical Solution Polymerization and Microwave-Assisted Polymerization (31% AA, 150ppm of Each Initiator for FRSP and 5ppm Initiator for MAP)

					Surface Area= $4*\pi*r^2$			
Pore #	**FRSP (no clay) µm**	**FRSP (w/ clay) µm**	**MAP (no clay) µm**	**MAP (w/ clay) µm**	**FRSP (no Clay) (μm^2)**	**FRSP (Clay) (μm^2)**	**MAP (no Clay) (μm^2)**	**MAP (clay) (μm^2)**
1.0	2.4	1.2	1.5	0.5	18.1	4.2	7.1	0.8
2.0	2.3	1.1	0.7	0.1	16.6	3.8	1.5	0.0
3.0	2.6	0.8	0.8	0.1	21.3	2.0	2.0	0.0
4.0	2.6	0.8	0.3	0.1	21.3	1.8	0.3	0.0
5.0	1.7	0.9	0.4	0.1	9.1	2.3	0.5	0.0
6.0	1.8	2.2	1.1	0.1	10.2	15.2	3.8	0.0
7.0	1.9	1.7	1.2	0.1	11.4	9.1	4.5	0.0
8.0	1.4	5.6	0.7	0.1	6.2	98.6	1.5	0.0
9.0	2.2	0.7	1.4	0.1	15.2	1.5	6.2	0.0
10.0	2.4	0.5	0.4	0.1	18.1	0.8	0.5	0.0
11.0	2.5	0.8	0.6	0.1	19.6	2.0	1.1	0.0
12.0	1.2	0.6	0.5	0.1	4.5	1.1	0.8	0.0

13.0	1.2	0.5	0.3	0.1	4.5	0.8	0.3	0.0
14.0	1.2	0.5	0.8	0.1	4.5	0.8	2.0	0.0
15.0	1.0	0.5	1.1	0.1	3.1	0.8	3.8	0.0
16.0	2.6	0.7	0.6	0.1	21.3	1.5	1.0	0.0
17.0	1.6	1.2	0.4	0.1	8.1	4.2	0.5	0.0
18.0	1.9	1.1	1.1	0.1	11.4	3.8	3.8	0.0
19.0	2.5	1.7	0.1	0.1	19.6	9.1	0.0	0.0
20.0	1.1	0.4	0.1	0.1	3.8	0.5	0.0	0.0
21.0	2.1	0.9	0.3	0.1	13.9	2.3	0.3	0.0
22.0	0.9	1.2	0.7	0.1	2.6	4.5	1.5	0.0
23.0	2.2	0.3	0.2	0.1	15.2	0.3	0.1	0.0
24.0	0.6	2.8	0.2	0.1	1.1	24.6	0.1	0.0
25.0	2.8	0.7	0.1	0.1	24.6	1.5	0.0	0.0
26.0	2.9	0.6	0.5	0.1	26.4	1.1	0.8	0.0
27.0	1.1	0.8	0.3	0.8	3.8	2.0	0.3	2.0
28.0	2.0	1.6	1.6	0.1	12.6	8.1	8.1	0.0
29.0	0.7	1.3	0.5	0.1	1.5	5.3	0.8	0.0
30.0	0.8	1.3	0.3	0.1	2.0	5.3	0.3	0.0
31.0	0.8	0.8	0.6	0.1	2.0	2.0	1.1	0.0
32.0	2.1	0.8	0.3	0.1	13.9	2.0	0.3	0.0
33.0	1.9	3.5	1.1	0.1	11.4	38.5	3.8	0.0
34.0	4.6	1.8	0.2	1.5	66.5	10.2	0.1	7.1
35.0	2.6	0.8	0.2	0.1	21.3	2.0	0.1	0.0
36.0	1.9	2.7	0.2	0.1	11.4	22.9	0.1	0.0
37.0	1.1	0.8	0.2	0.2	3.8	2.0	0.1	0.1
38.0	8.9	0.9	0.2	0.3	249.0	2.6	0.1	0.3
39.0	3.9	1.4	0.2	0.1	47.8	6.2	0.1	0.0
40.0	3.7	0.2	0.2	0.3	43.0	0.1	0.1	0.3
41.0	1.2	0.5	0.2	0.2	4.5	0.8	0.1	0.1
42.0	1.1	0.6	1.9	0.1	3.8	1.1	11.4	0.0
43.0	2.8	0.8	0.4	0.2	24.6	2.0	0.5	0.1
44.0	1.2	0.1	0.8	0.1	4.5	0.0	2.0	0.0
45.0			0.3	0.1			0.3	0.0
46.0			0.3	0.1			0.3	0.0
47.0			0.3	0.1			0.3	0.0
48.0			0.3	0.1			0.3	0.0
49.0			0.2	0.1			0.1	0.0
50.0			0.6	0.4			1.1	0.5
51.0			0.2	0.4			0.1	0.5
52.0			0.2	0.2			0.1	0.1
53.0			0.1	0.2			0.0	0.1
54.0			0.1	0.1			0.0	0.0
55.0			0.6	0.1			1.1	0.0
56.0			0.4	0.1			0.5	0.0
57.0			0.3	0.1			0.3	0.0
58.0			0.9	0.1			2.6	0.0

59.0			0.3	0.1			0.2	0.0
60.0			0.3	0.2			0.3	0.1
61.0			0.7	0.3			1.5	0.3
62.0			1.8	0.1			10.2	0.0
63.0			1.4	0.1			6.2	0.0
64.0			1.2	0.1			4.5	0.0
65.0			0.5	0.1			0.8	0.0
66.0			0.6	0.1			1.1	0.0
67.0			0.6	0.1			1.1	0.0
68.0			0.5	0.1			0.8	0.0
69.0			0.7	0.2			1.5	0.1
70.0			0.6	0.2			1.1	0.1
71.0			0.9	0.2			2.6	0.1
72.0			0.6	0.6			1.1	1.1
73.0			0.4	0.1			0.5	0.0
74.0			1.1	2.6			3.8	21.3
75.0			1.2	1.4			4.5	6.2
76.0			0.8	0.6			2.0	1.1
77.0			0.6	0.7			1.1	1.5
78.0			0.5	0.4			0.8	0.5
79.0				0.1				0.0
80.0				0.1				0.0
81.0				0.1				0.0
82.0				0.1				0.0
83.0				0.1				0.0
84.0				0.1				0.0
85.0				0.4				0.5
86.0				0.2				0.1
87.0				0.2				0.1
88.0				0.2				0.1
89.0				0.2				0.1
90.0				0.2				0.1
91.0				0.4				0.5
92.0				0.6				1.1
93.0				0.1				0.0
94.0				0.1				0.0
95.0				0.1				0.0
96.0				0.1				0.0
97.0				0.6				1.1
98.0				0.9				2.6
99.0				0.5				0.8
100.0				0.8				2.0
101.0				0.8				2.0
102.0				0.1				0.0
103.0				0.1				0.0
104.0				0.1				0.0

105.0				0.1				0.0
106.0				0.1				0.0
107.0				0.1				0.0
108.0				0.1				0.0
109.0				0.1				0.0
110.0				0.1				0.0
111.0				0.2				0.1
112.0				0.9				2.6
113.0				0.6				1.1
114.0				1.0				2.8
115.0				1.1				3.8
116.0				0.8				1.8
117.0				0.1				0.0
118.0				0.1				0.0
119.0				0.1				0.0
120.0				0.1				0.0
121.0				0.1				0.0
122.0				0.1				0.0
123.0				0.1				0.0
124.0				0.4				0.5
125.0				0.4				0.5
126.0				0.8				2.0
127.0				3.4				36.3
128.0				1.2				4.5
129.0				0.9				2.6
130.0				1.0				2.8
131.0				4.1				52.8
132.0				0.1				0.0
133.0				0.1				0.0
134.0				0.1				0.0
135.0				0.1				0.0
136.0				0.1				0.0
137.0				0.1				0.0
138.0				0.1				0.0
139.0				0.2				0.1
140.0				0.2				0.1
141.0				0.2				0.1
142.0				0.7				1.5
143.0				0.8				2.0
144.0				0.2				0.1
145.0				0.3				0.3
146.0				0.4				0.5
147.0				0.6				1.1
148.0				0.8				2.0
149.0				0.7				1.5
150.0				0.8				1.8

151.0				0.8				2.0
152.0				1.1				3.5
153.0				0.3				0.3
154.0				0.3				0.3
155.0				0.8				2.0
156.0				1.1				3.8
157.0				0.6				1.1
158.0				0.9				2.6
159.0				1.1				3.8
160.0				0.4				0.5
161.0				0.2				0.1
162.0				1.1				3.8
163.0				0.2				0.1
164.0				1.0				3.1
165.0				0.6				1.1
166.0				0.2				0.1
167.0				0.7				1.5
168.0				0.9				2.3
Ave.	**2.1**	**1.2**	**0.6**	**0.4**	**19.5**	**7.1**	**1.6**	**1.3**
STDEV	**1.4**	**1.0**	**0.4**	**0.5**	**37.7**	**16.0**	**2.3**	**5.2**
Sum	**92.0**	**50.5**	**45.5**	**62.1**	**858.9**	**311.3**	**126.6**	**216.3**